NATIONAL CENTER FOR EARTHQUAKE ENGINEERING RESEARCH

State University of New York at Buffalo

Shake Table Test of a 1/6 Scale Two-Story Lightly Reinforced Concrete Building

by

A-G. El-Attar, R. N. White and P. Gergely

Department of Structural Engineering
School of Civil and Environmental Engineering
Cornell University
Ithaca, New York 14853-3501

Technical Report NCEER-91-0017

February 28, 1991

This research was conducted at Cornell University and was partially supported by the National Science Foundation under Grant No. ECE 86-07591.

NOTICE

This report was prepared by Cornell University as a result of research sponsored by the National Center for Earthquake Engineering Research (NCEER). Neither NCEER, associates of NCEER, its sponsors, Cornell University, or any person acting on their behalf:

a. makes any warranty, express or implied, with respect to the use of any information, apparatus, method, or process disclosed in this report or that such use may not infringe upon privately owned rights; or

b. assumes any liabilities of whatsoever kind with respect to the use of, or the damage resulting from the use of, any information, apparatus, method or process disclosed in this report.

Shake Table Test of a 1/6 Scale
Two-Story Lightly Reinforced Concrete Building

by

A.G. El-Attar[1], R.N. White[2] and P. Gergely[3]

February 28, 1991

Technical Report NCEER-91-0017

NCEER Project Number 89-1001B

NSF Master Contract Number ECE 86-07591

1 Instructor, Cairo University, Cairo, Egypt; former Graduate Research Assistant, School of Civil and Environmental Engineering, Cornell University
2 James A. Friend Family Professor of Engineering, School of Civil and Environmental Engineering, Cornell University
3 Professor, School of Civil and Environmental Engineering, Cornell University

NATIONAL CENTER FOR EARTHQUAKE ENGINEERING RESEARCH
State University of New York at Buffalo
Red Jacket Quadrangle, Buffalo, NY 14261

PREFACE

The National Center for Earthquake Engineering Research (NCEER) is devoted to the expansion and dissemination of knowledge about earthquakes, the improvement of earthquake-resistant design, and the implementation of seismic hazard mitigation procedures to minimize loss of lives and property. The emphasis is on structures and lifelines that are found in zones of moderate to high seismicity throughout the United States.

NCEER's research is being carried out in an integrated and coordinated manner following a structured program. The current research program comprises four main areas:

- Existing and New Structures
- Secondary and Protective Systems
- Lifeline Systems
- Disaster Research and Planning

This technical report pertains to Program 1, Existing and New Structures, and more specifically to system response investigations.

The long term goal of research in Existing and New Structures is to develop seismic hazard mitigation procedures through rational probabilistic risk assessment for damage or collapse of structures, mainly existing buildings, in regions of moderate to high seismicity. The work relies on improved definitions of seismicity and site response, experimental and analytical evaluations of systems response, and more accurate assessment of risk factors. This technology will be incorporated in expert systems tools and improved code formats for existing and new structures. Methods of retrofit will also be developed. When this work is completed, it should be possible to characterize and quantify societal impact of seismic risk in various geographical regions and large municipalities. Toward this goal, the program has been divided into five components, as shown in the figure below:

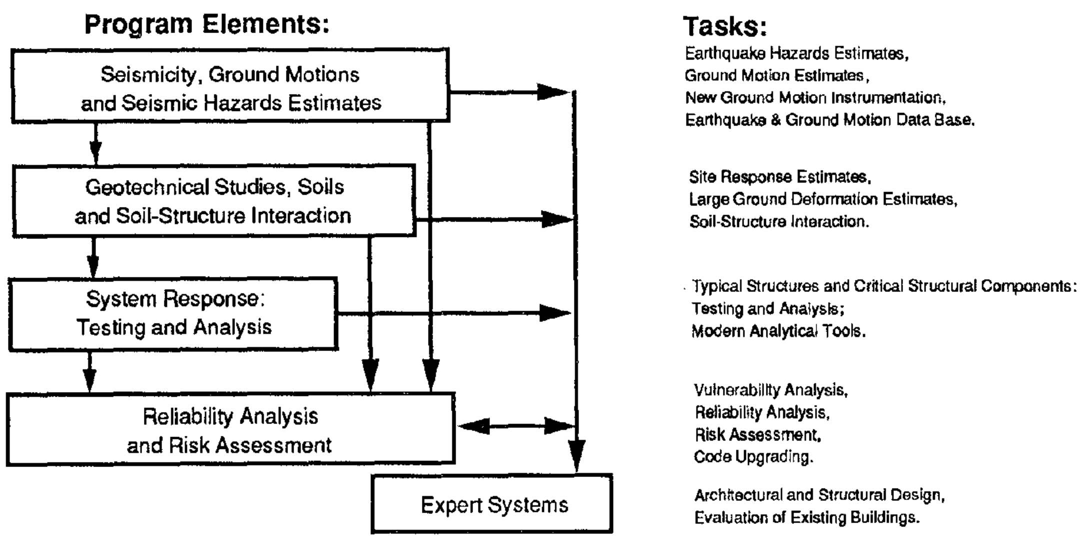

System response investigations constitute one of the important areas of research in Existing and New Structures. Current research activities include the following:

1. Testing and analysis of lightly reinforced concrete structures, and other structural components common in the eastern United States such as semi-rigid connections and flexible diaphragms.
2. Development of modern, dynamic analysis tools.
3. Investigation of innovative computing techniques that include the use of interactive computer graphics, advanced engineering workstations and supercomputing.

The ultimate goal of projects in this area is to provide an estimate of the seismic hazard of existing buildings which were not designed for earthquakes and to provide information on typical weak structural systems, such as lightly reinforced concrete elements and steel frames with semi-rigid connections. An additional goal of these projects is the development of modern analytical tools for the nonlinear dynamic analysis of complex structures.

The greatest effort in the Existing and New Structures area concentrated on the evaluation and response-prediction of existing "weak" buildings that are common in regions of low seismicity. Most of these lightly reinforced concrete buildings and steel buildings with semi-rigid connections were not designed for seismic forces and many not even for wind loading. The coordinated research program on concrete buildings has included full-scale tests of frame joint regions, flat-plate structures, and shake-table tests of frames at various scales. These tests were done at Cornell University, University at Buffalo, and Rice University. One of the main goals of this effort has been the development of analytical tools for the complete nonlinear analysis of such structures so that realistic estimates of their expected response can be made to aid practicing engineers and researchers in the risk/reliability research area.

This report summarizes the results of shake-table tests on a two-story building with weak design details. The results show that the structure did not collapse when subjected to increasing ground motion levels because the large flexibility reduced the energy input. However, the P-delta effect may become serious, especially for taller buildings.

ABSTRACT

A 1/6 scale 2-story one-bay by one-bay lightly reinforced concrete building was tested on the Cornell University shake table. The model structure was designed solely for gravity loads without regard to any kind of lateral loads (wind or earthquakes), and had no walls or partitions. The reinforcement details were based on typical reinforced concrete frame structures constructed in the Central and Eastern United States since the mid 1900's, and characterized by (a) low reinforcement ratio in the columns, (b) discontinuous positive moment beam reinforcement at the columns, (c) little or no joint confinement, and (d) lap splices located immediately above the floor level. The model was tested using the time-compressed Taft 1952 S69E at different amplitudes. Auxiliary tests (static loading and free-vibration) were performed before and after each seismic test to study the changes in the model building properties.

Test results indicated that this type of reinforced concrete frame will experience very large deformations associated with a considerable stiffness degradation during a moderate earthquake. Although the non-seismic reinforcement details may form a potential source of damage for lightly reinforced concrete buildings, it was found experimentally that they did not lead to collapse or a complete failure mechanism. The model failures occurred outside the joint region, indicating that the lack of joint confinement was not a potential source of damage. Also, the location and details of the column lap splices did not cause a serious problem to the model.

Both experimental and analytical results indicated that the inclusion of the slab contribution to the beam flexural strength is a vital step in the assessment of the performance of lightly reinforced concrete structures during earthquakes since it has the potential of altering the relatively ductile strong column-weak beam mechanism to the more brittle soft-story mechanism.

ACKNOWLEDGEMENTS

The authors would like to express their appreciation for the assistance provided by Tim Bond, Manager of the George Winter Laboratory, and extend thanks to Paul Jones and Glenn Darling of the Civil Engineering machine shop for their help.

Thanks are also extended to the many Civil Engineering students who helped with the experimental work. In particular, the authors acknowledge Adam Hoffman and Rebecca Frein for their invaluable help.

TABLE OF CONTENTS

SECTION TITLE PAGE

LIST OF ILLUSTRATIONS

FIGURE TITLE **PAGE**

LIST OF TABLES

CHAPTER 1
INTRODUCTION

1.1 Background information

There are many thousands of low-rise reinforced concrete frame buildings existing in the Central and Eastern U.S. that were designed for primarily gravity loads. These structures can be characterized as "lightly reinforced", which is defined as (a) low reinforcing ratios in columns, (b) lap splices in column reinforcement just above floor levels, (c) minimal column ties, (d) no confining ties in the beam-column joint regions, and (e) discontinuous positive moment beam steel at some (or all) of the columns. Very little is available in the literature on the performance of such buildings under seismic hazards. It is believed that, with a better understanding of the behavior of these structures, evaluation of their safety during earthquakes can be done on a much more reliable basis than that at the present time. In addition, improved code provisions and schemes for retrofitting can be developed, and analytical capabilities incorporating improved behavior models can be perfected.

The current work is part of a comprehensive research effort being carried out at Cornell University to investigate the behavior of lightly reinforced concrete frames, and frame components under dynamic loads at small scale.

In the first phase of the reduced scale model research, two prototype cantilever type specimens and four 1/6 scale model specimens were fabricated and tested under cyclic (quasi-static) loading [10]. It has been shown that the prototype concrete stress-strain curve can be accurately modeled by careful selection of aggregates, aggregate grading, and water/cement ratio. Also, by using properly heat-treated threaded rods as model reinforcement, the prototype cracking and hysteresis loops were successfully reproduced, even after severe loadings with ductility factors up to 6.

In the second phase of the model building study, which is described in this report, the improved modeling techniques are applied to a complete structure (2-story building), tested dynamically on a shake table. The prototype structure is designed, detailed, and constructed to reflect typical eastern United States design features. Test results are compared with those of a similar building but with modern seismic detailing tested at 70% scale at the U.C. Berkeley. Results from the full-scale frame component experiments are summarized in [19].

1.2 Objectives and scope

A 1/6 scale reinforced concrete two story office building was fabricated and tested on the Cornell University shake table to study the building performance at different levels of seismic excitation. The building design is similar to that of a building tested at 70% scale at the University of California at Berkeley, except that the current building was designed and detailed to support gravity loads only.

The experiment was designed to serve the following purposes;

1. To gain a better understanding of the behavior of lightly reinforced concrete buildings under earthquake hazards, and to provide preliminary answers to questions such as;
   - What magnitude of seismic excitation can this class of buildings resist without significant structural damage?
   - How does the response of the non-seismically detailed model compare to that of one with seismic details?
   - Is it possible to reproduce a specific seismic test at a different scale, and to what extent can results be compared?
2. To provide data for calibrating the available analytical tools for more accurate prediction of the response of such structures during earthquakes.
3. To gain experience with seismic testing, including shake table control, seismic qualification tests, application of small-scale modeling techniques [10], instrumentation, and data acquisition.

CHAPTER 2
CORNELL UNIVERSITY SHAKE TABLE

2.1 Table Configuration

The shake table (figure 2.1) is composed of a 4" thick aluminum plate with a working area of 60" x 84". The plate is uniformly supported by a massive, 7" thick, precision ground granite block. A thin oil film is used to minimize the friction between the aluminum plate and the granite block.

The table can move in one horizontal degree of freedom along the centerline of the long direction (84"). The motion is guided by two hydrostatic journal bearings, each with a maximum capacity of 10,000 lb.

A 6" stroke L.A.B. hydraulic actuator (model HV-21-6) with maximum capacities of 14,000 lb dynamic force and 21,000 lb static force is used to drive the shake table. The pressurized (3,000 psi) oil flow to the actuator is regulated by an electrically controlled servo-valve, which is sized to allow for high frequency operation of the system. The interface between the servo-valve and the hydraulic power supply is provided by a hydraulic manifold model L.A.B. HM-40. The manifold ensures clean, full-pressure oil flow to the servo-valve. It also has a special circuit to provide a soft start/stop function for the hydraulic actuator.

The reaction mass for the system (table and actuator) is composed of several concrete blocks, post-tensioned together to form a massive block of a total weight of approximately 100,000 lb. A 3/4" thick plywood sheet is used to separate the reaction mass from the laboratory floor.

2.2 Table Control

The table runs under closed loop displacement control using a L.A.B. servo-controller model 8830. The controller, acting as the link between the command signal and the hydraulic actuator, sums the command signal supplied by a DEC VAX II/GPX station and the measured actuator LVDT output, and generates an error signal which causes the servo-valve to port oil into the actuator and produce the required motion.

A L.A.B. automatic pump controller model 8837 is used to remotely monitor and control the hydraulic power supply. It has a logic interlock to protect the system by shutting down the

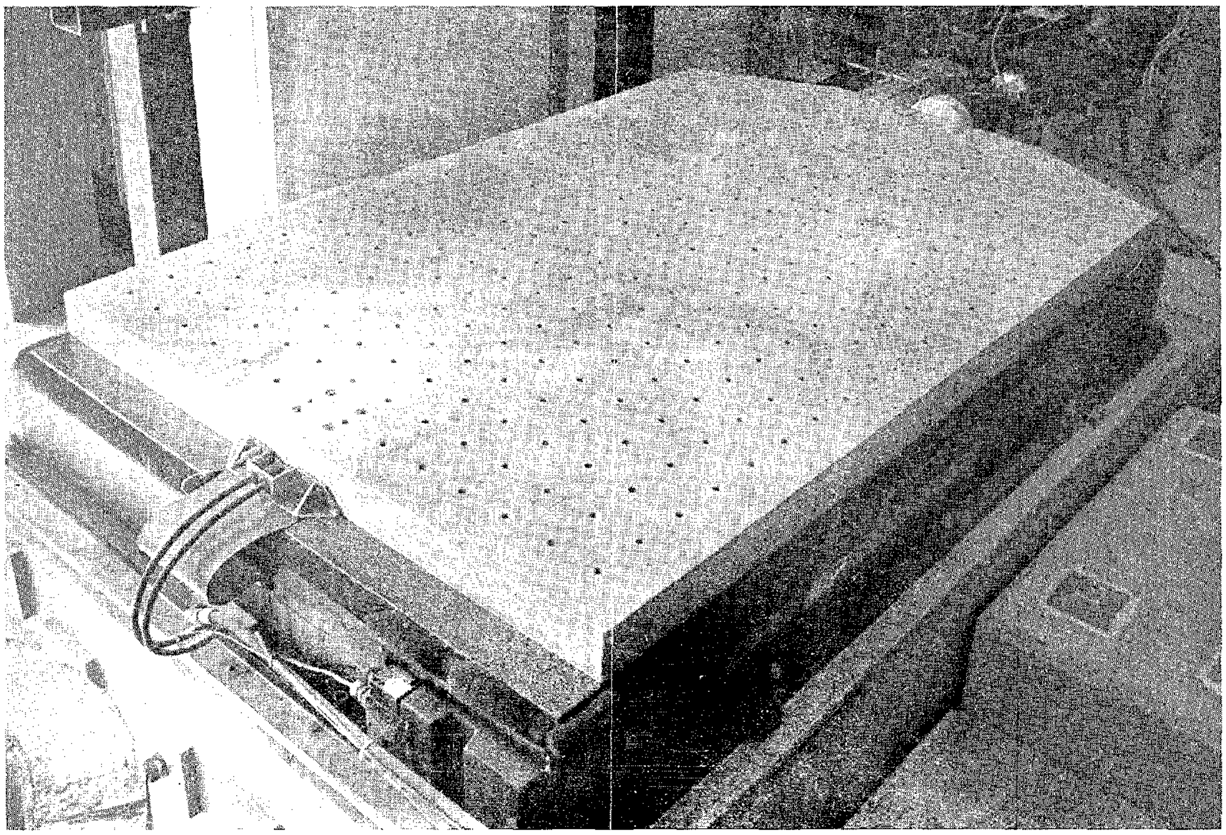

Figure 2.1: Cornell University Shake Table.

power supply during a fault condition. It also continuously monitors the oil temperature, pressure, oil level and filter condition alerting the operator for any problem by displaying an error message on its 20 digit vacuum fluorescent display.

The control system also includes a sine vibration monitor,an automatic frequency sweeper, and an automatic level control. These features are used for other kinds of applications and were not implemented in the present work.

2.3 Displacement Measurements and Reference Frame

Figure 2.2 shows the reference frame used to support the displacement measurement devices. The frame is attached to the reaction mass. The natural frequencies of the frame obtained from free vibration test were 12, 45, and 56 hz. Although the first fundamental frequency is close to the expected frequencies of the tested model buildings, the reference frame displacements obtained under equivalent load conditions were found to be very small (of the order of 0.005"). The frame can be adjusted to a maximum height of 10' above the table surface, and to a maximum width of 5'.

2.4 Data Acquisition System

The data acquisition system is composed of a NEFF 620 analog to digital converter, and 20 Vishay 2300 signal conditioners. The NEFF system does 15 bit analog to digital conversion (including sign). It can simultaneously sample and hold data for 20 different channels with a maximum conversion rate of 50 K samples/second. The VAX II/GPX station simultaneously controls the command signal and the data gathering functions.

The Vishay signal conditioners provides; (a) excitation for most transducers, (b) bridge completion, (c) amplification (from 1 to 11,000), and (d) anti-aliasing filtering.

2.5 System Limitation

The maximum specimen size is limited by the available working surface on the shake table (5'x7'), and the height of the reference frame (10'). The specimen weight, and its mass spatial distribution, are constrained by the following limitations as recommended by the table manufacturer;

1. Maximum vertical load on the shake table should not exceed the vertical capacity of

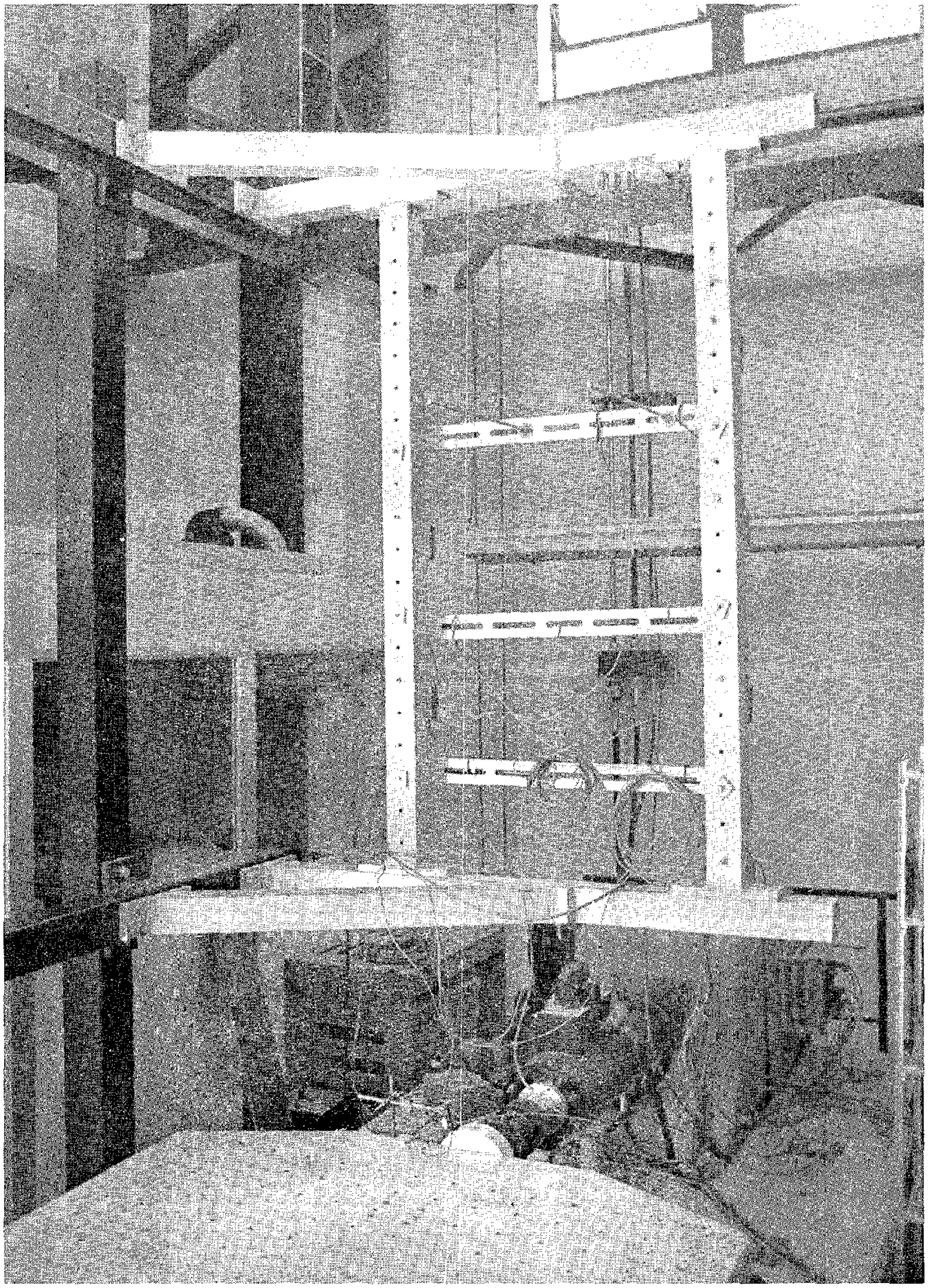

Figure 2.2: Reference Frame.

the journal bearings (2 x 10,000 = 20,000 lb).

2. Maximum overturning moment (pitch) moment, assuming uniformly distributed load on the table, should not exceed 125,000 lb.ft. (figure 2.3).

3. Maximum concentrated moment in any local zone (under any of the structure legs) on the table should not exceed $M= a^3 \times 3.0$, (Eqn. 2.1),

where M= maximum local moment in lb.inch, and a= footprint dimension in inches.

4. Maximum tensile force T in any of the structure legs should not exceed the foot print area multiplied by the atmospheric pressure: $T_{max}= a^2 \times 14.7$, (Eqn. 2.2), where T_{max}= maximum tensile force in lbs, and a= footprint dimension in inches.}

5. Maximum dynamic force applied by the driving actuator is 14.0 kips.

Limitations 2, 3, and 4 are intended to prevent the rupture of the oil film between the aluminum plate and the supporting granite block.

The mass on the table also limits its dynamic capabilities. Figure 2.4 shows the interaction between the load, acceleration, and maximum frequency of the table. It can be seen that the unloaded table can produce a 5.0 G acceleration at 100 Hertz. When the table is fully loaded with 20 kips (assuming other safety limitations are met), it can not be driven by more than 0.7 G, dictated by the maximum capacity of the hydraulic actuator (14.0 kips dynamic force).

2.6 Pretest Seismic Qualification

The main objective of this process is to reproduce a specific earthquake trace with minimum distortion when the shake table is loaded with the model structure. Table-structure interaction and the shake table's own response function are considered in this study.

Since the Cornell University shake table runs under closed loop displacement control, the displacement trace of the desired earthquake was used as the drive waveform. The resulting displacements were obtained by double integrating the corrected acceleration record to avoid problems associated with the non-correspondence between the corrected acceleration, velocity, and displacement records available in the literature [9]. This step can also be justified as the reproduction of the acceleration trace was the final purpose of the simulation.

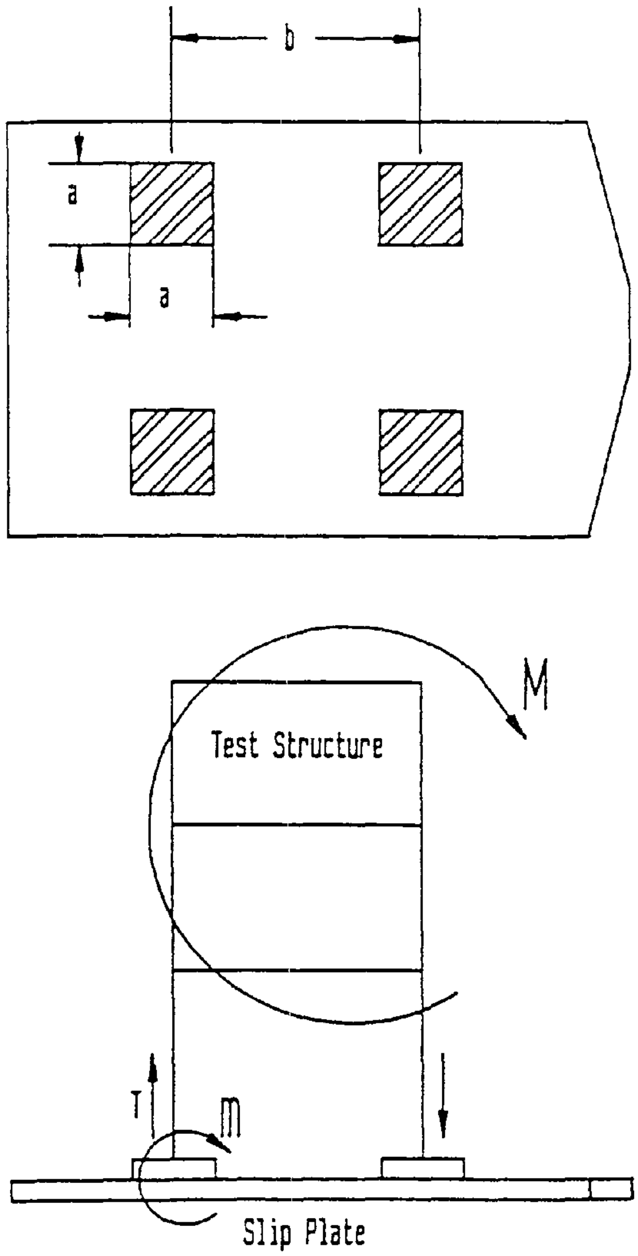

Figure 2.3: Overturning Moments and Local Bending Moments.

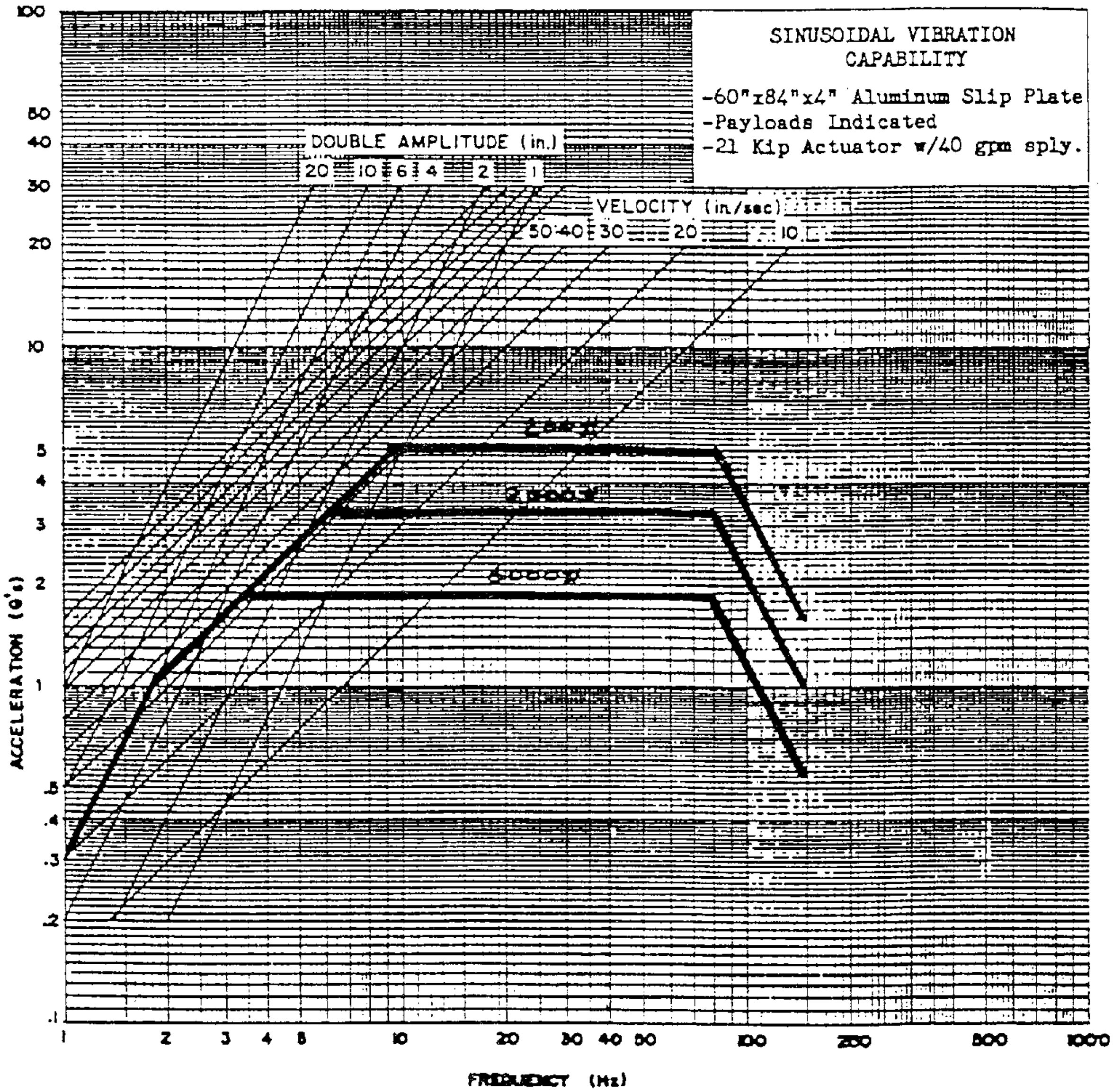

Figure 2.4: Interaction Between Load, Acceleration, and Maximum Frequency of The Shake Table.

Procedures used to account for the table-structure interaction, for off-line compensation, and for the evaluation of the table performance will be discussed in the following sections.

2.6.1 Table-structure interaction

All seismic qualification tests were carried out with the shake table running under loading conditions resembling as much as possible those developed when the actual concrete model was mounted on the table.

For the 2-story building test, an equivalent, single degree of freedom steel frame was used to simulate model load. The frame (figure 2.5) was designed to have the mass, overturning moment, and leg spacing similar to those of the model structure. The stiffness of the frame legs was selected in such a way that the natural frequency (10 Hz.) of the frame was between the first and the second mode frequencies of the concrete model (6.25 Hz and 17.0 Hz respectively).

2.6.2 Off-line compensation

The off-line compensation technique used in the present work accounts for offsets (or distortions) in the measured signal at different frequencies. The principal step in this process is to determine the transfer function of the shake table H(f) as expressed by equation 2.3.

$$Y(f) = H(f) \times X(f) \tag{2.3}$$

where:

X(f) = Fourier transformed input (drive signal).

Y(f) = Fourier transformed output (measured signal).

H(f) = Transfer function of the system.

The only requirements for the complete description of the frequency response function H(f) is that the input and output signals be Fourier transformable, a condition that is met by all physically realizable systems, and that the input signal be non-zero at all frequencies of interest [21]. Some investigators have proposed the use of a banded white noise source to obtain the transfer function [9].

In the present case, the desired earthquake displacement record (which is always Fourier transformable) was used as the input signal. The measured table displacement then forms the output signal. The transfer function H(f) was then obtained by direct division of the Fourier

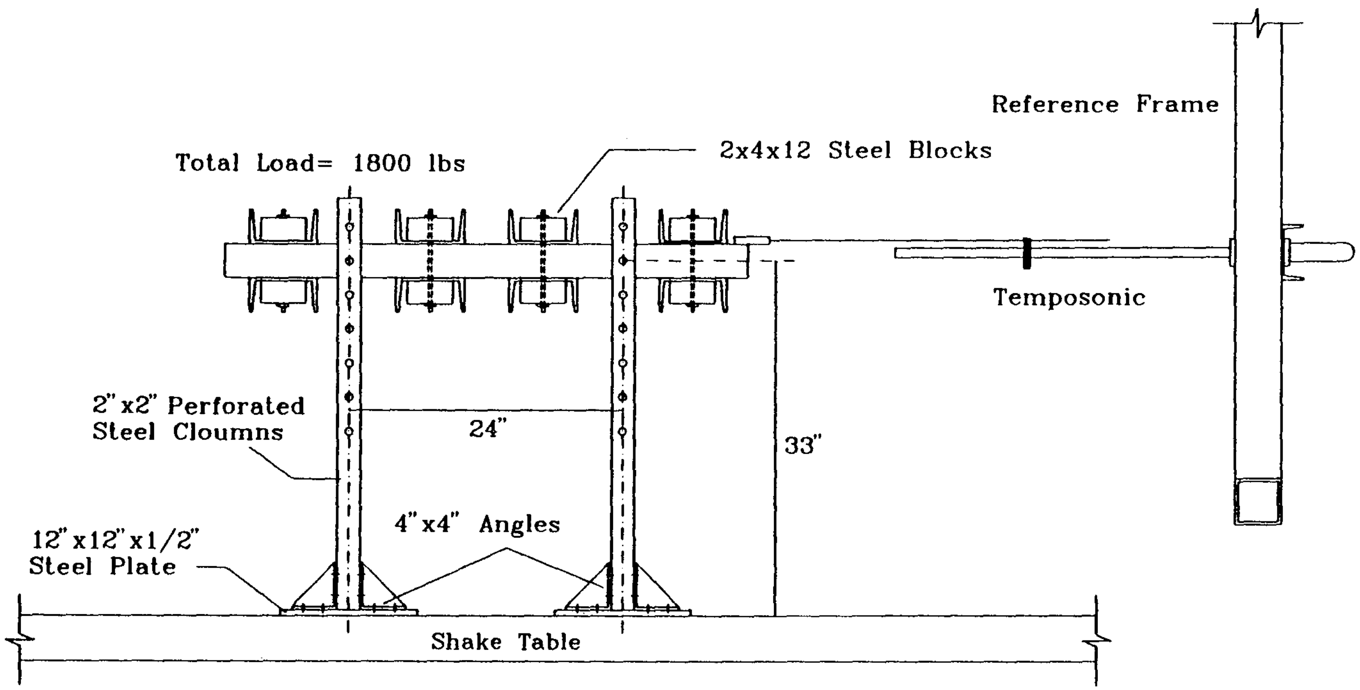

Figure 2.5: 2-story Building Equivalent Single Degree of Freedom System.

transforms of the input and the measured displacements:

$$H(f) = \frac{Y(f)}{X(f)} \tag{2.4}$$

The transfer function determined using equation 2.4 is unique only if the system is linear and time-invariant [9]. In the current study, the system non-linearity due to the continuously changing structure properties during the test was ignored.

Once the system transfer function is determined, a signal correction waveform DX(f) can be created as follows;

$$DY(f) = X(f) - Y(f) \tag{2.5}$$

$$DX(f) = H^{-1}(f) \times DY(f) \tag{2.6}$$

Where:

DX(f) = frequency domain drive signal correction.

DY(f) = frequency domain measured signal offset.

$H^{-1}(f)$= Inverted transfer function (complex function).

The correction signal DX(f) in the frequency domain (or a fraction of it) is added to the Fourier transformed original drive signal X(f), then the new corrected Fourier transformed drive signal given by equation 2.7 is transformed to the time domain to be as the new drive signal for the shake table.

$$X(f)_{corr} = X(f) + DX(f) \tag{2.7}$$

The amount (percentage) of drive signal correction at selected frequency ranges was manually monitored to account for the system non-linearity and time variance in an attempt to obtain the best possible performance.

2.7 Evaluation of the table performance

The reproduction of the desired acceleration record was of primary importance in the simulated earthquake tests. The different criteria used to evaluate the adequacy of the achieved table acceleration are discussed in the following sections.

2.7.1 Power spectrum (frequency domain analysis)

Comparing the power spectra of the measured and the desired accelerogram provides a direct evaluation of the energy content of the two traces at all frequency levels of concern. The comparison also helps detecting the ranges of frequencies to be enhanced, and the ranges to be suppressed during the off-line compensation process.

Special attention was always paid to the ranges of frequencies expected to affect the model structure. Figure 2.6 shows the Fourier transform of the original, uncompensated, and the compensated acceleration records for the 2-story model case. It can be seen that the off-line compensation technique significantly changed the table response especially in the second mode range (10 Hz. to 17 Hz).

2.7.2 Response spectrum

The response spectrum curve of the measured and the required accelerogram is another manifestation of the maximum response of the two traces at different periods. It can be seen from figure 2.7 that the off-line compensation technique enhanced the high period (low frequency) components, and suppressed the low period (high frequency) components of the measured table acceleration, resulting in a better reproduction of the desired accelerogram. Deviation of the response spectra of the measured table acceleration from the original Taft S69E 1952 spectrum at periods larger than first mode range were neglected.

2.7.3 Frequency ensemble work

The frequency ensemble work (equation 2.8) was proposed by Housner and Jennings [21] to represent the capacity of a ground motion to supply energy to a linear structure.

$$W_f = \frac{\pi}{2}\int_0^{t_1} a^2 \, dt \qquad (2.8)$$

Where:

W_f = frequency ensemble work.

t_1 = waveform time length.

Figure 2.8 shows the variation of the energy supplied to the structure with time (computed using equation 2.8) for the original Taft record, uncompensated table motion, and the compensated table motion for the 2-story building test. It can be seen that at the end of the acceleration history (at time 10.50 seconds), the uncompensated table motion provided about 9%

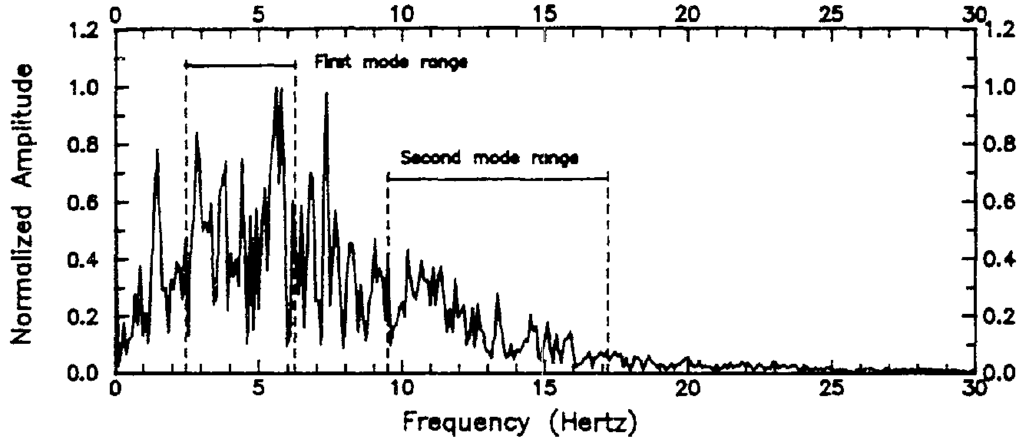

(a) Original Time Compressed Taft 1952 S69E Earthquake.

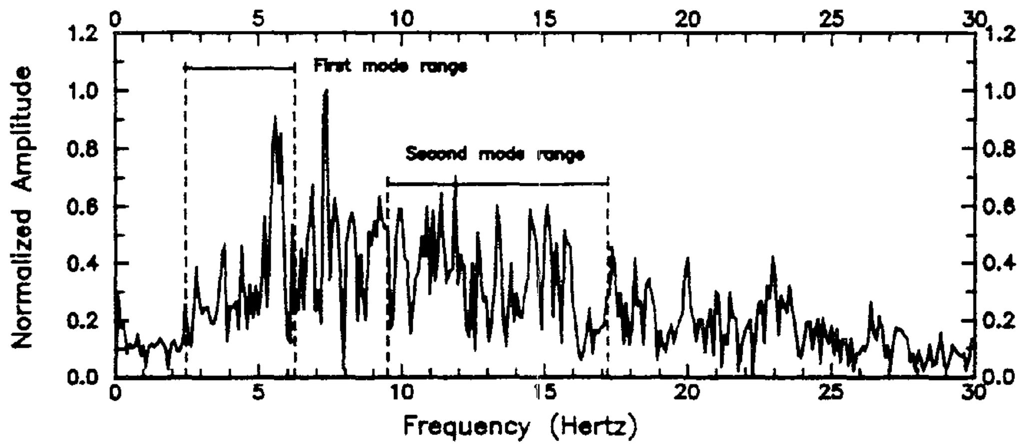

(b) Uncompensated Table Acceleration.

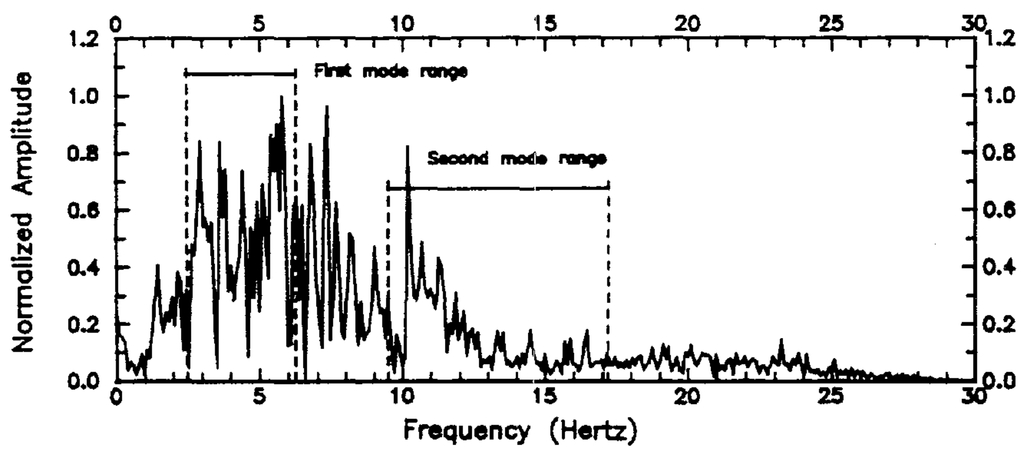

(C) Compensated Table Acceleration.

Figure 2.6: Power Spectrum of The Original Taft Accelerogram, Uncompensated, and Compensated Table Acceleration (2-Story Model Test).

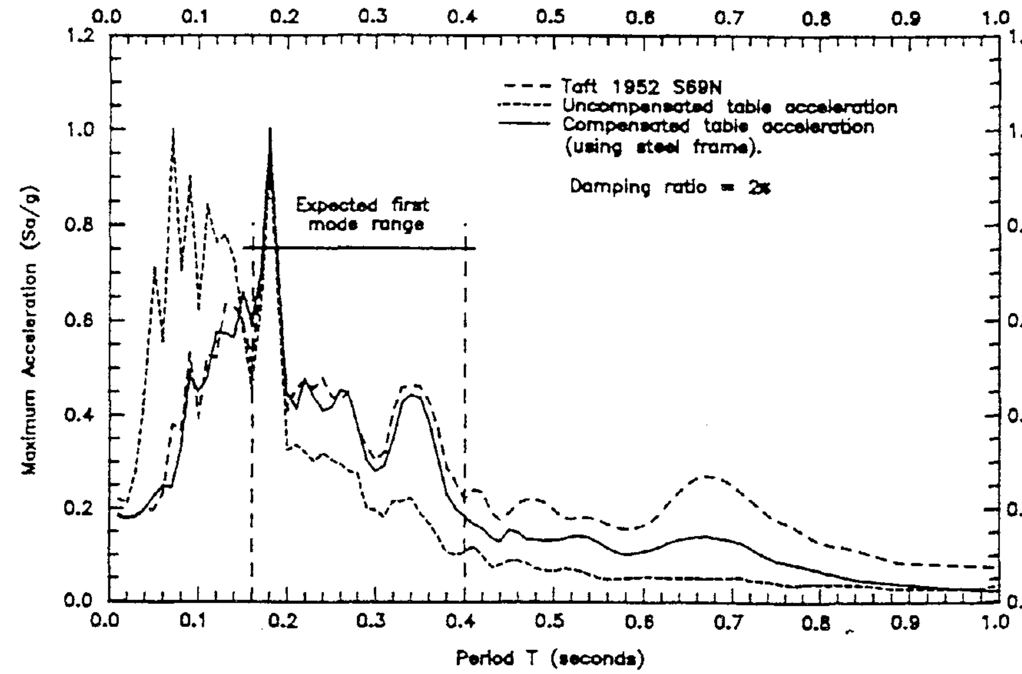

Figure 2.7: Effect of Off-Line Compensation on Response Spectra.

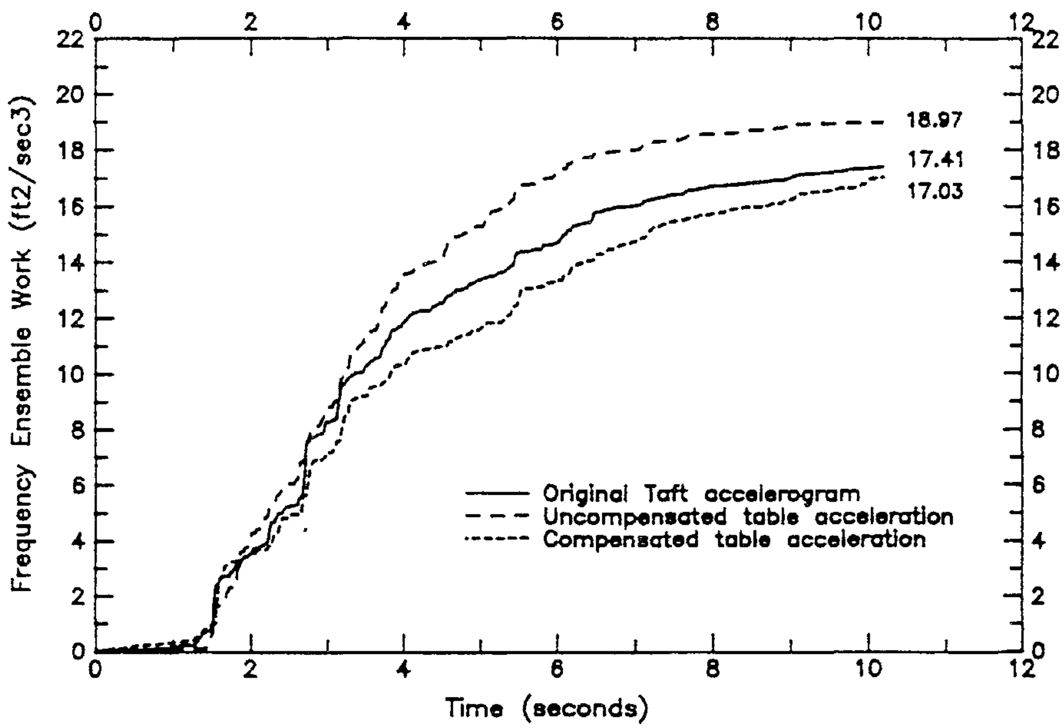

Figure 2.8: Accumulated Energy-Time Variation (2-Story Building Test).

more energy than the original Taft earthquake, while the compensated table motion provided only 2% less energy than the original Taft earthquake.

2.7.4 Direct comparison of the acceleration traces

This comparison was simply done by examining the first 3 or 5 spikes of the acceleration traces (figure 2.9). It can be seen that for the 2-story model test, when the maximum acceleration in the original time compressed Taft earthquake and the compensated records were almost the same, the second spike was underestimated by about 8%, while the third spike was overestimated by 7%.

2.8 Concluding remarks

The behavior of the Cornell University shake table has been characterized. Procedures implemented to minimize the displayed motion distortion were discussed and evaluated.

Experience at Cornell using the available control system showed that it is always possible to reproduce with acceptable accuracy a specific earthquake trace within a certain frequency band (1 Hz. to 15 Hz. in the present case). Attempts to improve the obtained trace beyond that limit resulted in over-correction of the drive signal. This was not considered as a serious problem since the dominant response of the tested models had a fundamental frequency range of 1.0 Hz. to 6.0 Hz.

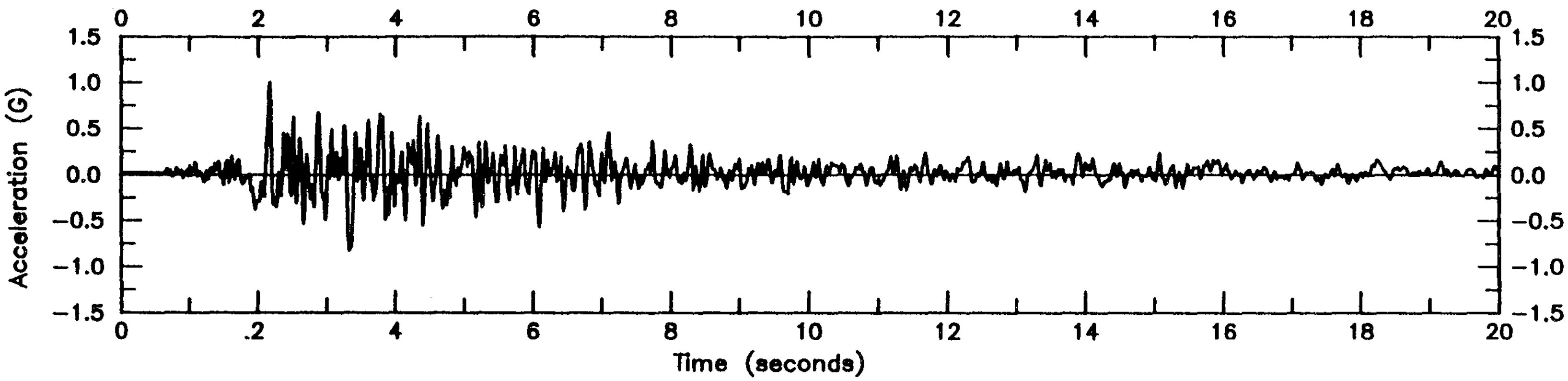

(a) Normalized Time Scaled Taft 1952 S69E Earthquake.

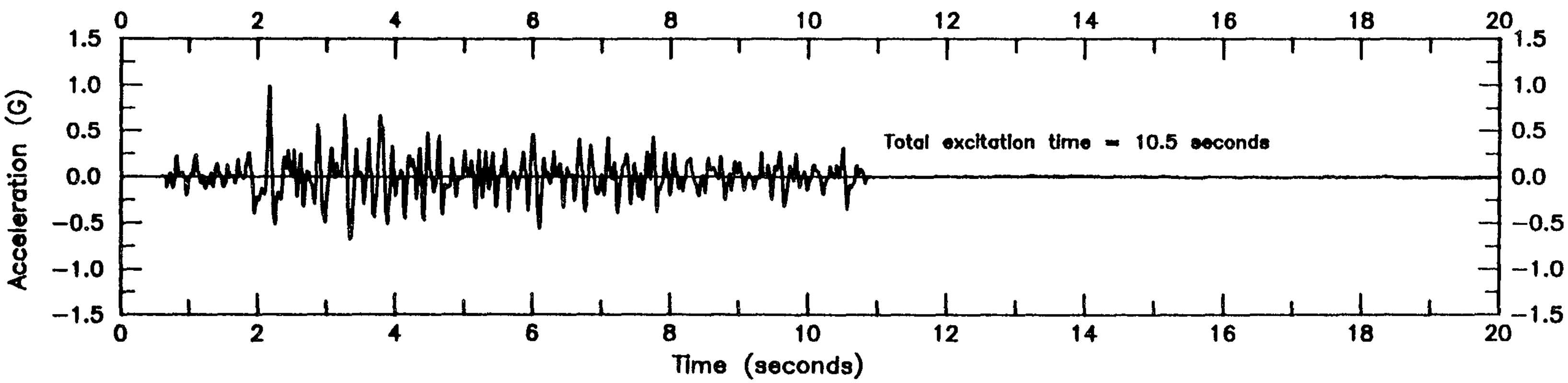

(b) Normalized Measured Table Acceleration After The Off-Line Compensation.

Figure 2.9: Required Versus Achieved Table Acceleration for The 2-Story Building Test.

CHAPTER 3
EXPERIMENTAL PROGRAM

This chapter is divided into two sections. The first section describes the test structure, including design and fabrication, mechanical properties, materials, and finally, the load set-up and instrumentation. The second section deals with the test procedure for the model structure. The three types of tests— static, free-vibration, and simulated-seismic are introduced and discussed.

3.1 Test structure

The test structure was a 1/6 scale, 2-story, one-bay by one-bay office building. It was designed and detailed to resist gravity loads only, with no consideration for any kind of lateral forces due to wind or earthquakes. Several buildings with similar design and reinforcement details were reported to suffer significant damage during Mexico City earthquake [19]. Details of the prototype building design are provided in appendix A of this report.

3.1.1 2-Story building model

Model design

The 2-story building is shown in figure 3.1. The model structure represented only one bay with two side half bays of the prototype structure (a center-line to center-line cut). The model was designed according to the similitude requirements provided in table 3.1. Geometric dimensions of the model were obtained by directly scaling the prototype dimension by the scale factor S_L= 6.

Since the microconcrete used in this model had an ultimate strain S_ε of 0.003 in./in. in contrast with a 0.002 in./in. prototype concrete ultimate strain (figure 3.2.a), a distorted model design was inevitable. The model reinforcement yield stress was modified to keep the strain distortion factor S_ε constant and equal to 0.67 (figure 3.2.b). The required yield strength of the model reinforcement f_{ym} was obtained using the following equation;

$$\frac{f_{ym}}{f_{yp}} = \frac{\epsilon_{cu_p}}{\epsilon_{cu_m}} = S_\epsilon \tag{3.1}$$

Where f_{yp}= yield strength of the prototype reinforcement, f_{ym} = yield strength of the model

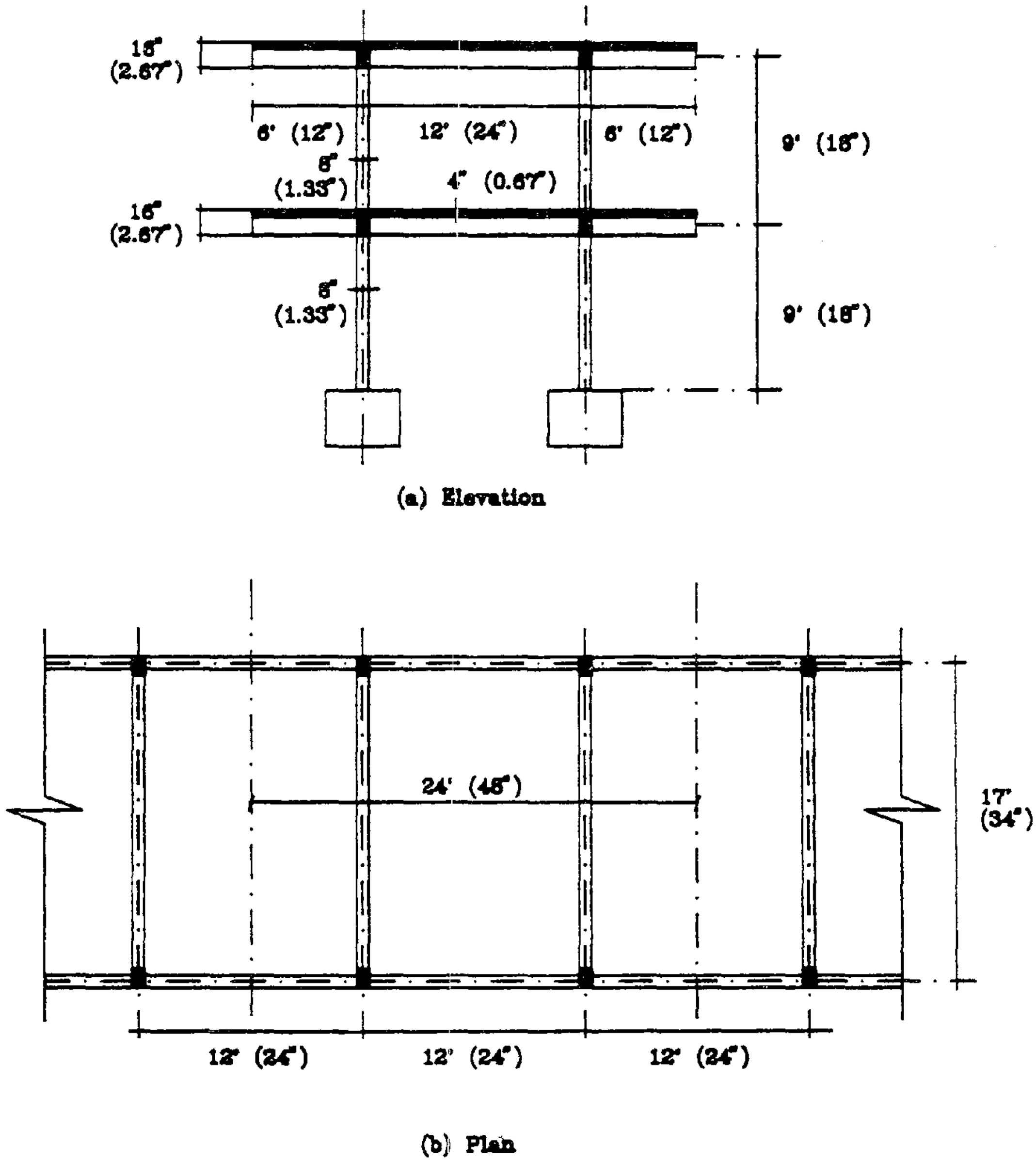

Figure 3.1: General Layout of The 2-Story Building.

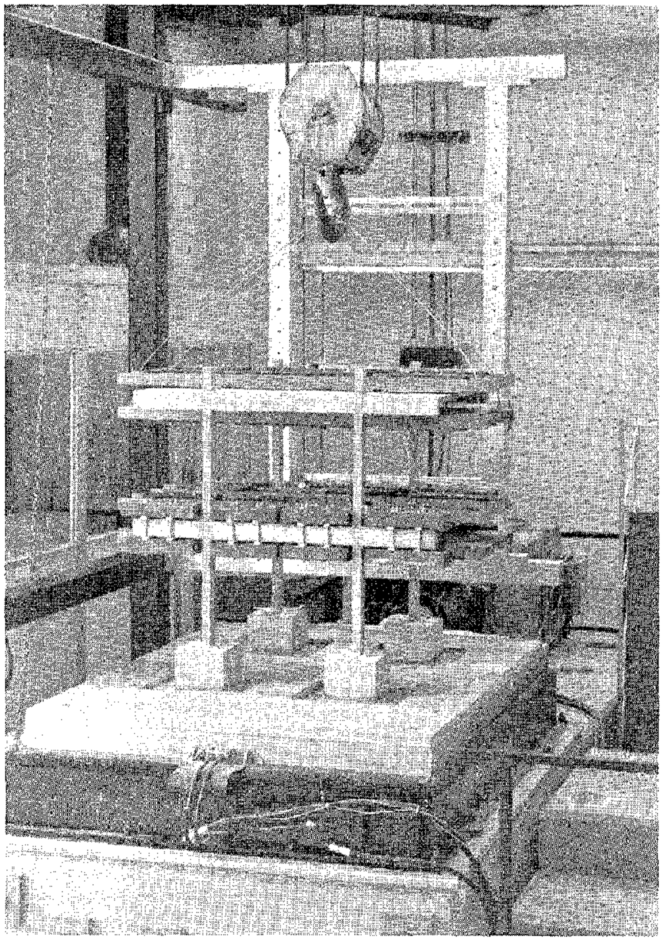

(c) Model on shake table

Figure 3.1 (Continued)

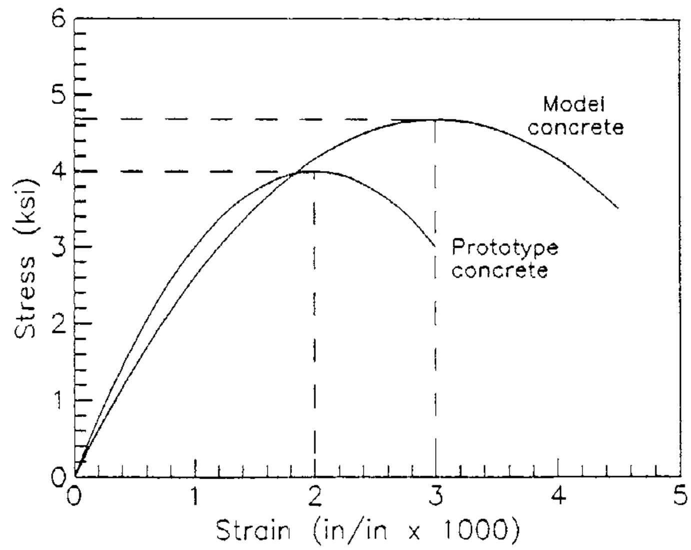

(a) Concrete Stress & Strain Scaling.

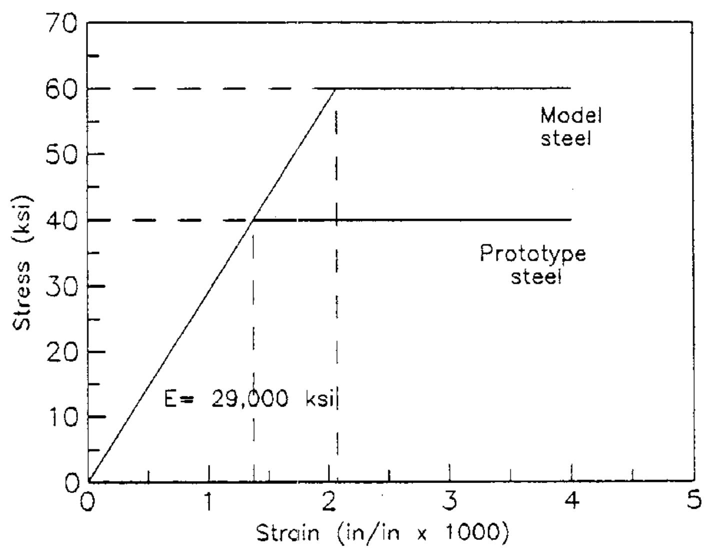

(b) Steel Stress & Strain Scaling.

Figure 3.2. Model Materials Stress & Strain Scaling.

reinforcement, ε_{cup}= ultimate compressive strain of the prototype concrete, and ε_{cum}= ultimate compressive strain of the model concrete.

Table 3.1: Similitude Requirements For The Model Structure

Quantity	Symbol	Dimension	Scale Factor
Linear dimension	L	L	S_L
Displacement	δ	L	$S_\varepsilon \times S_L$
Angular displacement	θ	---	S_ε
Time	T	T	S_t
Frequency	f	T^{-1}	S_t^{-1}
Velocity	V	LT^{-1}	$S_L \times S_t^{-1}$
Acceleration	a	LT^{-2}	$S_L \times S_t^{-2}$
Energy	E	FL	$S_f \times S_L^3$
Area of reinforcement	A_r	L^2	$S_f \times S_L^2 \times S_e^{-1}$
Concrete stress	fc	FL^{-2}	S_f
Steel stress	f_s	FL^{-2}	S_f
Concrete strain	ε_{cu}	---	S_ε
Steel strain	ε_s	---	S_ε
Concrete modulus	E_c	FL^{-2}	$S_f \times S_e^{-1}$
Steel modulus	E_s	FL^{-2}	1
Mass density	ρ	FL^{-3}	S_f
Concentrated load	Q	F	$S_f \times S_L^2$
Line Load	W	FL^{-1}	$S_f \times S_L$
Pressure	q	FL^{-2}	S_f
Bending moment	M	FL	$S_f \times S_L^3$

The required model reinforcement areas were then modified according to the similitude requirements (equation 3.2) to provide the scaled bar yielding force [15].

$$A_m = \frac{S_\varepsilon}{S_f \times S_l^2} \times A_p = \frac{0.667}{0.854 \times 6^2} \times A_p = 0.217\ A_p \qquad (3.2)$$

Where A_m= tensile stress area of the model reinforcement, A_p= prototype reinforcement area, S_ε= strain scale factor = 0.667, S_f= stress scale factor = 0.854, and S_L= length scale factor.

After the selection of the model bar sizes, the yield stress of each bar size was modified to account for any differences between the required and the selected bar areas in order to correctly scale the bar yield force. The required model reinforcement yield stress became;

$$f_{ym} = f_{ym_{calculated}} \times \frac{A_{m_{required}}}{A_{m_{chosen}}} \qquad (3.3)$$

The heat-treatment process was then carried out separately for each bar size to achieve the required yield stress according to equation (3.3).

Model Materials

(a) Model concrete:

The microconcrete used in the current model was based on the results of a previous study conducted at Cornell University on improving the modeling techniques of small scale concrete structures [10]. The microconcrete mix ratio was (Water : Cement : Model sand (Sm): Model aggregates (Am)= 0.7 : 1 : 3 : 3); where model sand was defined as particles that pass a #8 sieve and were retained on #200 sieve, and model aggregates were defined as particles that pass #4 sieve and were retained on #8 sieve. Figure 3.3 illustrates the grading curve for the aggregates. Type III cement was used since it has more rapid curing than type I cement. Superplastisizer EUCON 537 was added by the ratio of 1 % of the cement weight to increase the mix workability. The stress-strain curve of the microconcrete is shown in figure 3.4. where it can be seen that the strain distortion factor S_ε is equal to 0.667 and the stress distortion factor S_f is equal to 0.854. Model concrete properties at time of testing are given in table 3.2.

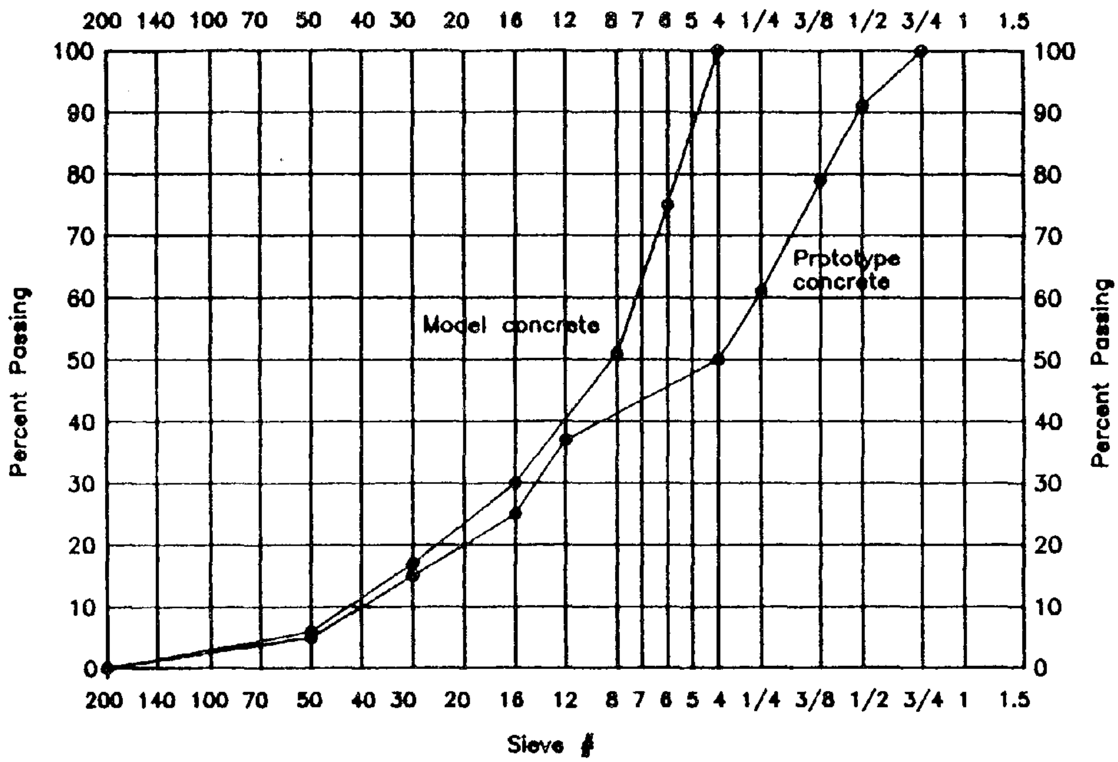

Figure 3.3: 2-Story Building Model Concrete Aggregate Grading.

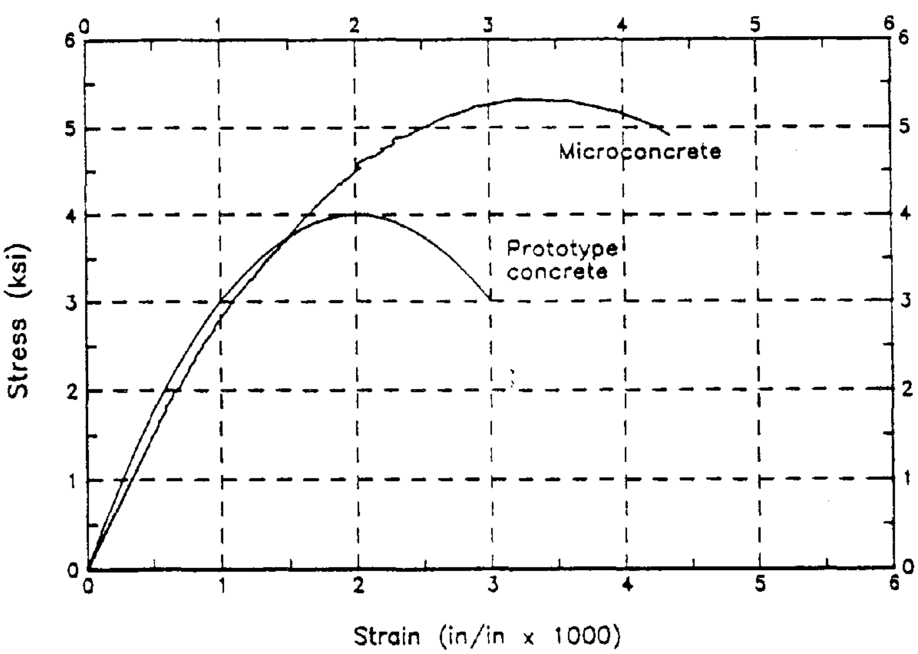

Figure 3.4: Prototype Concrete Vs. Microconcrete Stress-Strain Curve.

Table 3.2: 2-Story Model Concrete Properties

Property	Prototype Concrete	Model Concrete (2 weeks age)	Model Concrete (8 months age)
f_c'	4000 psi	4600 psi	5300 psi
ϵ_{cu}	0.002 in/in	0.003 in/in	0.0029 in/in
$E_{0.45f'_c}$	3600 ksi	2400 ksi	2900 ksi
f_t'	380 psi	450 psi	510 psi

(b) Model reinforcement:

It has been shown in reference [10] that the use of threaded rods as model reinforcement is the best available option for small scale modeling of reinforced concrete structures since this type of reinforcement provides (a) nearly perfect modeling of low level flexural cycles, (b) correct ultimate strength even after severe loading, and (c) an acceptable cracking behavior through the different stages of loading. It was also reported [10] that cold forming of the threaded rods significantly increases the yield strength, and a heat-treatment process was essential to reduce the yield strength to the required level and to produce an adequate yield plateau. A full account of the heat-treatment technique adopted in the current work can be found in references [8] and [10]. A sample of the model reinforcement stress-strain curves before and after the heat-treatment is shown in figure 3.5.

A fundamental aspect of the model construction was to adopt realistic reinforcement details that reflected construction practices during the 1950 to 1970 period. Special attention was paid to critical details such as the beam-column joints and column lap splices. Figure 3.6 shows a non-seismically detailed joint and a modern seismically detailed joint. The differences between the two joints can be summarized in the following points:

For a seismically detailed joint (Figure 3.6.a): (a)Full development length is provided for both top and bottom beam reinforcement, (b) Beam and column concrete zones are highly confined around the joint area to provide joint ductility, (c) Column stirrups continue through the joint length, (d) Lap splice is positioned at the middle half of the column length and the splice length is longer, and (e) Lap splice is confined by stirrups over its entire length.

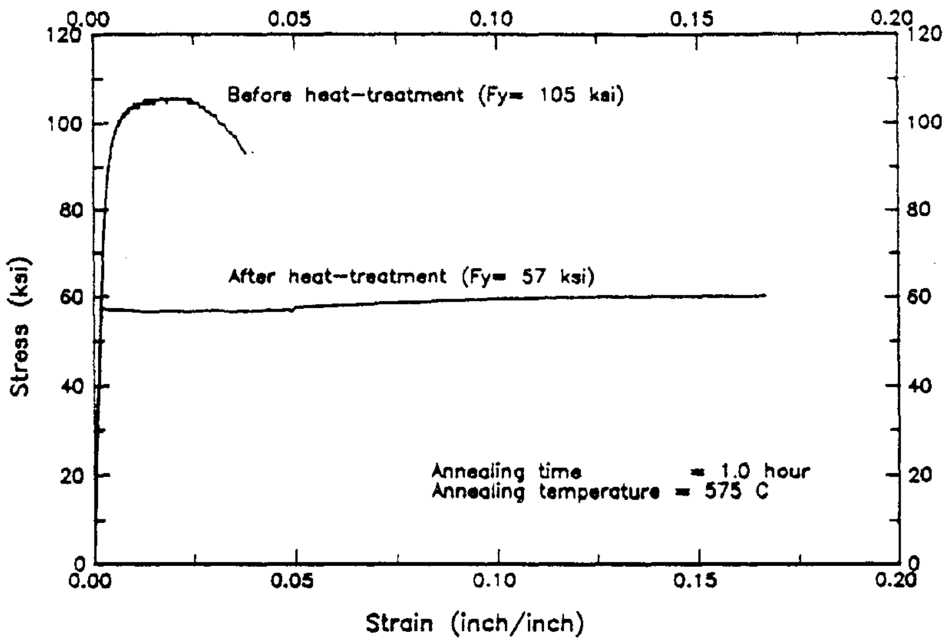

Figure 3.5: Stress-Strain Curve of Original Versus Heat-Treated Model Reinforcement (Size 8-32).

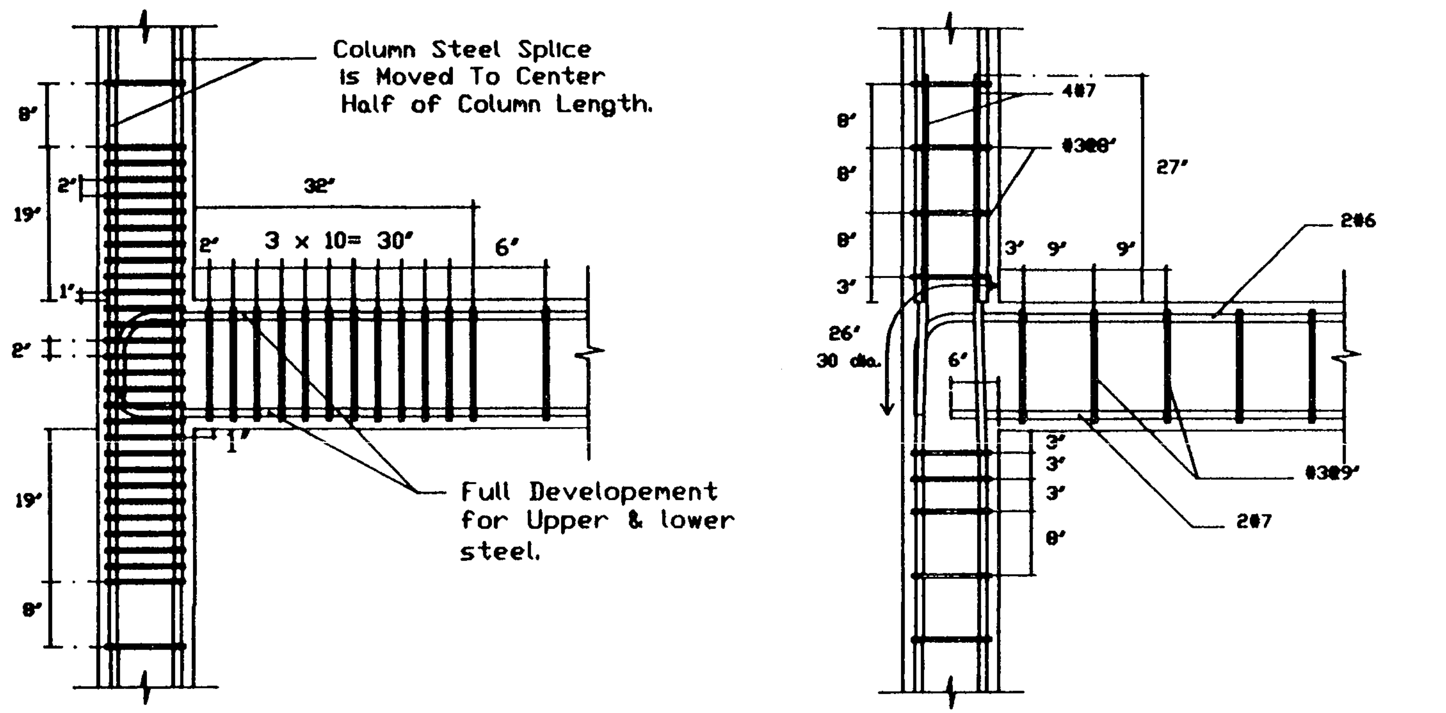

(a) **Modern Seismiaclly Detailed Joint.**

(b) **Typical Non-seismically Detailed Joint.**

Figure 3.6: Exterior Beam-Column Joint Details.

On the other hand, the basic features of a typical 1950-1970 beam-column joint (figure 3.6.b) were: (a) Discontinuous bottom beam reinforcement with a very short embedment length (6"), (b) No beam or joint confinement except for several stirrups at a spacing of 3" (usually) located at 3" distance below the beam bottom face. These stirrups were meant to resist the reaction of the sloping column steel, (c) No joint reinforcement. The column stirrups do not continue through the joint length, (d) Lap splice is designed as a compression splice (short splice) and located immediately above the beam top face, and (e) No special confinement was provided for the lap splice.

Although the ACI-318 code recommended the use of a compression lap splice in reinforced concrete columns, inspection of the reinforcement details of actual projects executed during the period 1950-1970 indicated that it was a common practice to use an empirical splice length varying from 24 to 30 bar diameters. This resulted in a longer splice than required by the ACI code. For the 2-story model, a splice length of 30 bar diameter was used. The full reinforcement details of the prototype structure main supporting frame are shown in figure 3.7.

The fabrication procedure of the model building was designed to resemble as closely as possible the construction steps of full scale buildings. The technique can be summarized in the following steps;

1. Footings were cast in wooden forms and cured for 1 week under wet burlap and plastic sheeting.
2. First story columns were cast on the footings, extending up tp 1/2 in. below the bottom surface of the beam.
3. The individual footings and columns assemblages were positioned accurately on a stiffened wooden base table (figure 3.8a).
4. Formwork for the beams and slabs were positioned and the steel cages put in place (figure 3.8.b).
5. Slab and beam concrete was placed (figure 3.8c) and wet cured for 1 week.
6. The second story was built following similar procedures.

Load set-up and model instrumentation

(a) <u>Load set-up</u>

Additional masses were used to simulate the dead weight of the prototype building

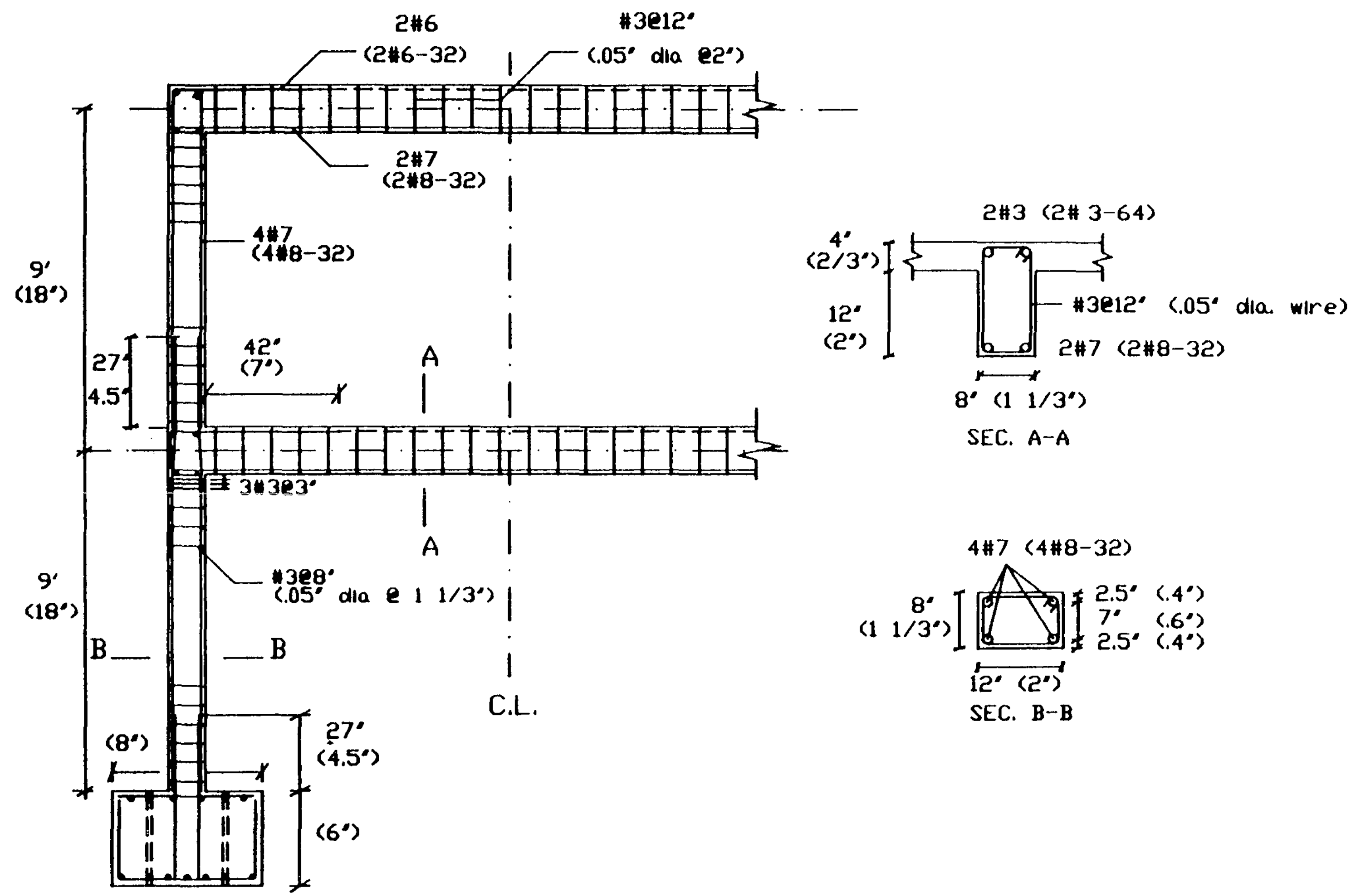

Figure 3.7: Reinforcement Details of The 2-Story Prototype (Model) Building.

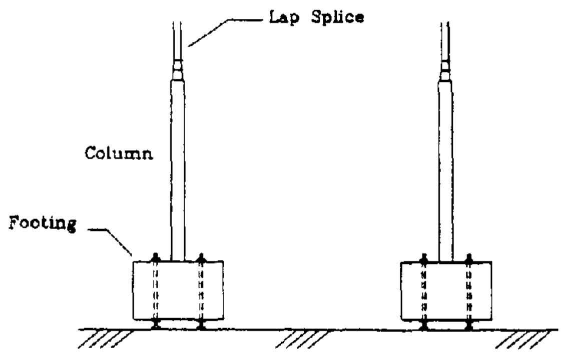

(a) First Story Columns.

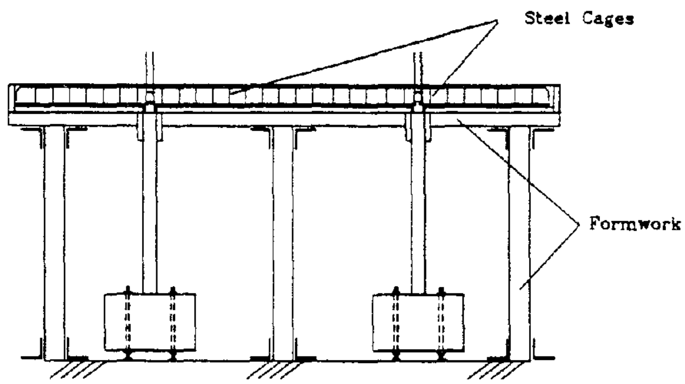

(b) First Story Steel Cages Placed in The Form.

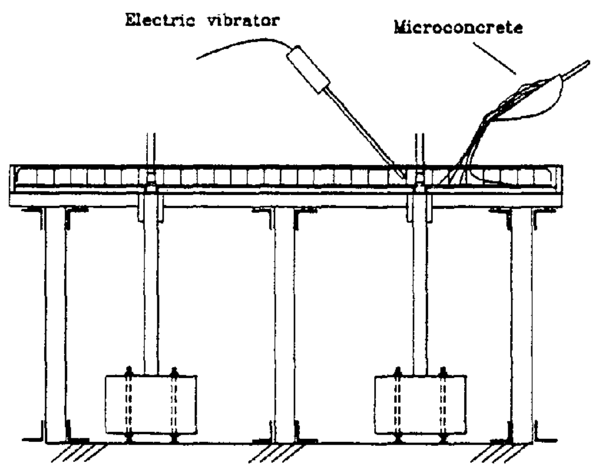

(c) Casting of The First Story Slab.

Figure 3.8: Fabrication of The 2-Story Model Building.

according to the similitude requirements in table 3.1. For the first story, the added masses were computed as follows;

$$M_{m1} = \frac{M_{p1}}{S_l^2 \times S_f} - M_{m_{o.w}} = \frac{44.1}{36 \times 0.854} - 0.14 = 1.29\ kips \quad (3.4)$$

Where M_{m1}= additional mass to be added on the model first story, M_{p1}= prototype first story dead load. $M_{mo.w}$ = own weight of the model floor.

For the second story, the additional mass M_{m2} was equal to 0.75 kips. The loads actually added were slightly less than those required according to the similitude laws due to the fixed size of the steel blocks (figure 3.9).

The slab loads on each floor were lumped at two points as shown in figure 3.9, where two 6 x 2 steel channels were used to collect the steel blocks load and transfer it directly to the beams at their third points through two, one inch wide steel blocks.

Blocks simulating the exterior wall loads were needed only on the first floor. These blocks were mounted directly on the transverse beams where two rectangular 1/4" x 1" x 4" aluminum washers were used for the load transfer. The stiffened portion of the transverse beams due to this loading scheme was 4" long.

(b) Model instrumentation

The model displacements were measured using linear displacement transducer (MTS Temposonic) at two points 25" apart at each floor level (figure 3.10). This set-up would also capture any rotational motion of the model during vibration. More information about these devices can be found in [13].

The table acceleration along with the floor accelerations were measured using ENDEVECO piezoresistive accelerometers model 7265 [6].

3.2 Test procedure

3.2.1 Introduction

The model structure was subjected to a series of tests to evaluate its performance before, during, and after earthquakes of different magnitudes. The general behavior of the model was studied through the following parameters: (a) base shear, (b) inter-story shear, (c) inter-story drift

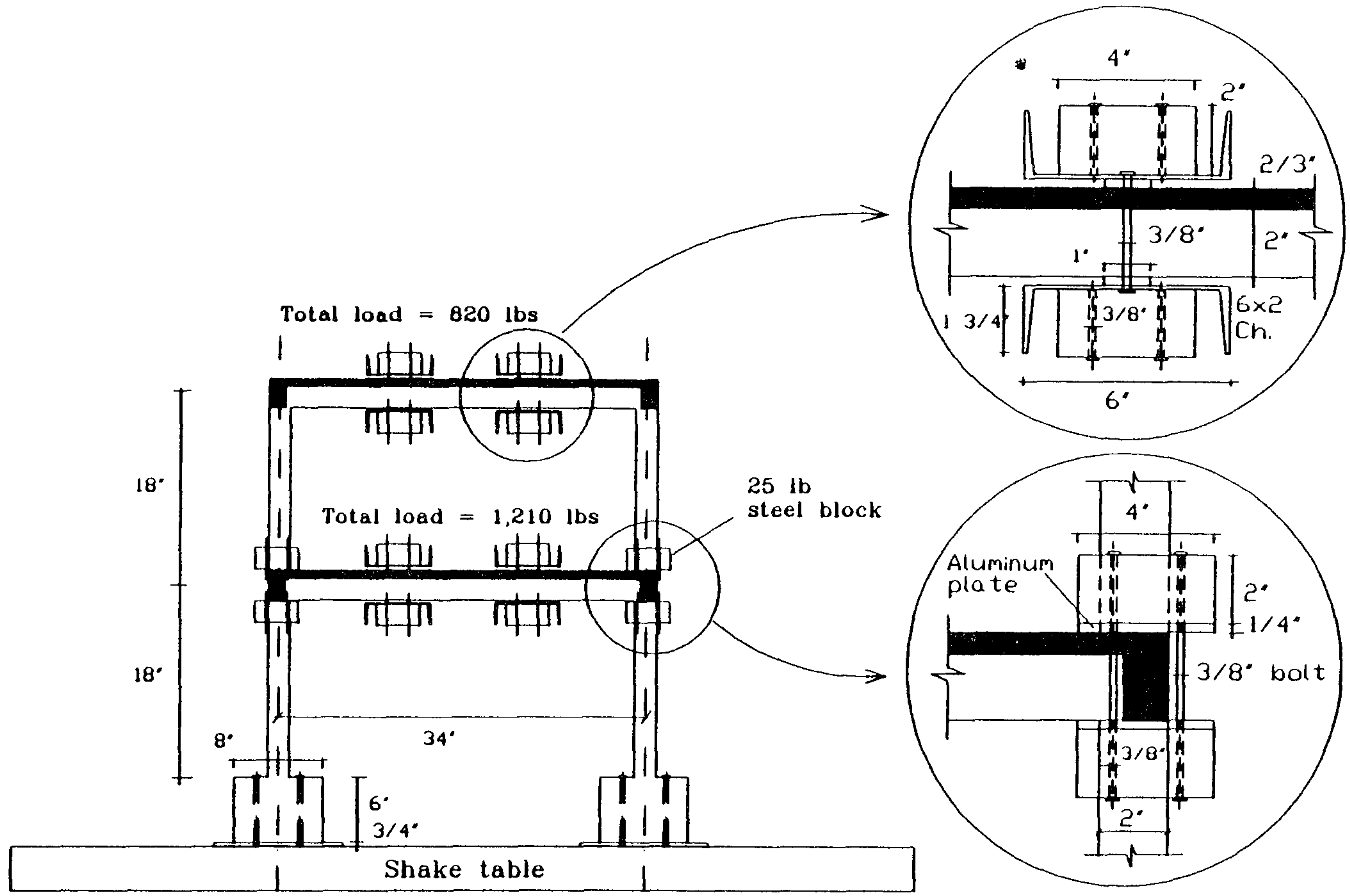

Figure 3.9: Loading System for The 2-Story Model Building.

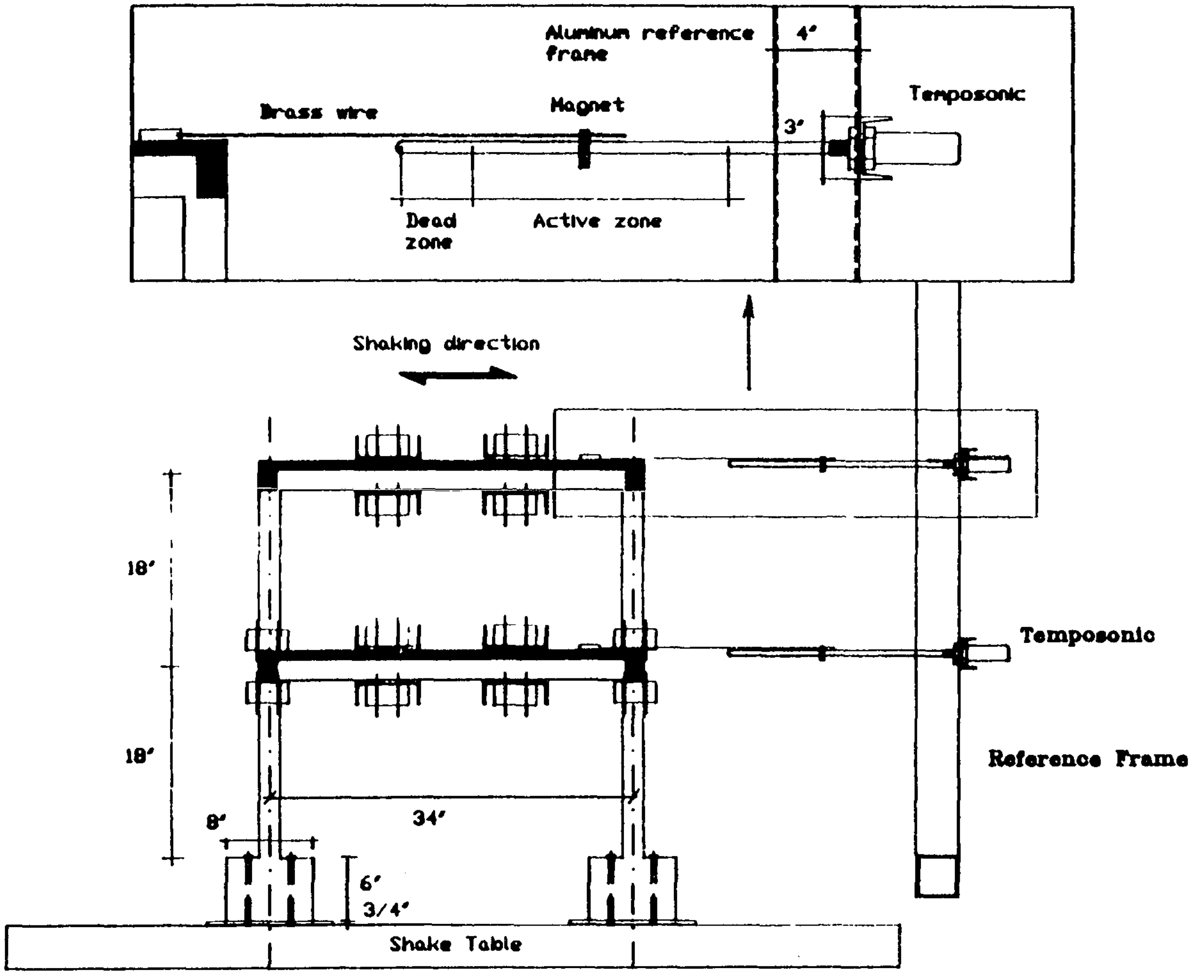

Figure 3.10: Displacement Measurements of The 2-Story Model.

(time history), (d) flexibility matrix coefficients, (e) natural frequencies, (f) damping ratios (assuming viscous damping model), and (g) cracking behavior and visual damage.

Three types of tests were conducted to study these parameters: (a) flexibility matrix determination test (static test), (b) free vibration test, and (c) simulated earthquake tests (seismic test).

The first two tests were carried out before and after each seismic test to evaluate the changes in structural properties from the seismic test. The third test consisted of applying the time scaled Taft S69E 1952 earthquake component to the model structure at different amplitudes until significant damage was observed. The techniques used to perform these tests are discussed in the following sections.

3.2.2 Static flexibility matrix determination

Figure 3.11 shows the load set-up used to determine the static flexibility matrix coefficients of the 2-story building . A 200 lb static concentrated load (applied in 4 increments) was applied at each floor level using a 1000 lb capacity manual jack. The flexibility matrix coefficients were computed at each load increment and finally all four values were averaged to obtain a 2 x 2 symmetric matrix.

The obtained flexibility matrix along with the mass matrix were used to compute the eigenvalues (natural frequencies) of the system using equation 3.5. These frequencies were compared with those obtained from the free vibration test to check the validity of the two tests.

$$[M] \times \{q\} = \frac{1}{\omega^2} \times [F] \times \{q\} \tag{3.5}$$

Where [M] = measured mass matrix, [F]= measured flexibility matrix, {q}= eigen vector(s), and ω= circular frequency.

3.2.3 Free vibration test

Figure 3.12 shows the load set-up used for the free vibration test of the 2-story model. The model structure was pulled back (displaced) by 0.05 inches at the second floor level using a steel wire. The wire was then suddenly released (cut) and the structure was allowed to vibrate freely. Accelerations and displacements were measured at each floor level until the structure

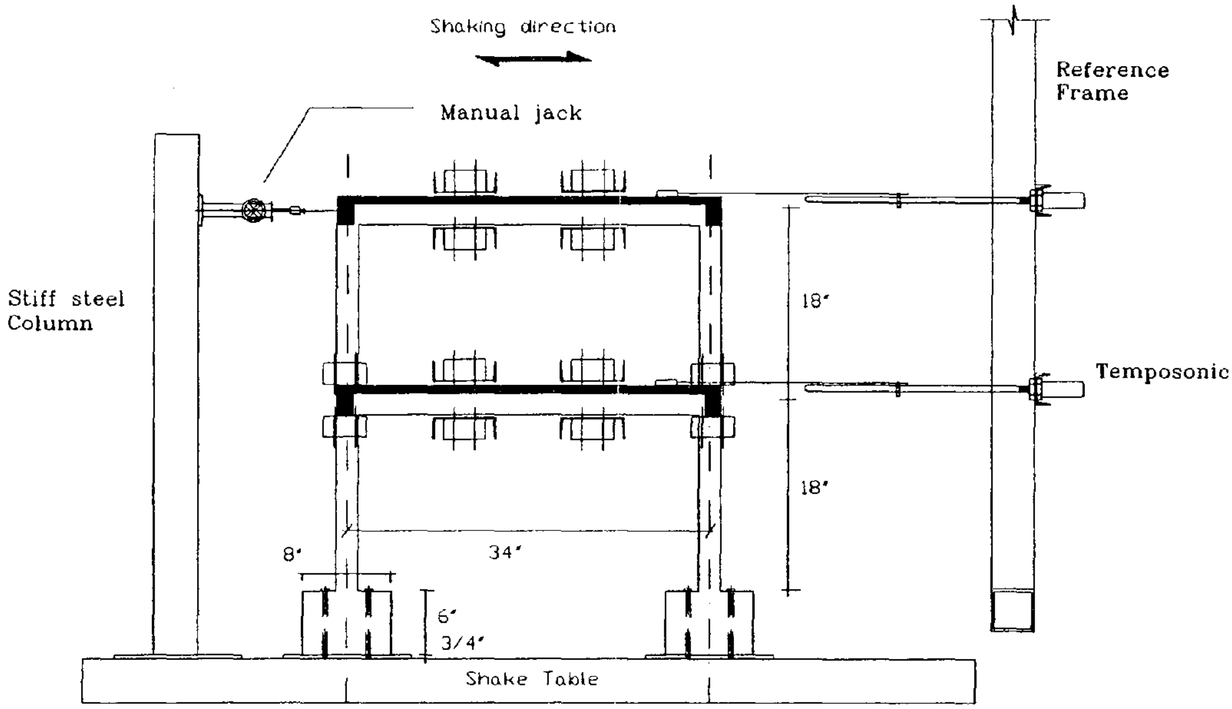

Figure 3.11: 2-Story Building Static Test Load Set-Up.

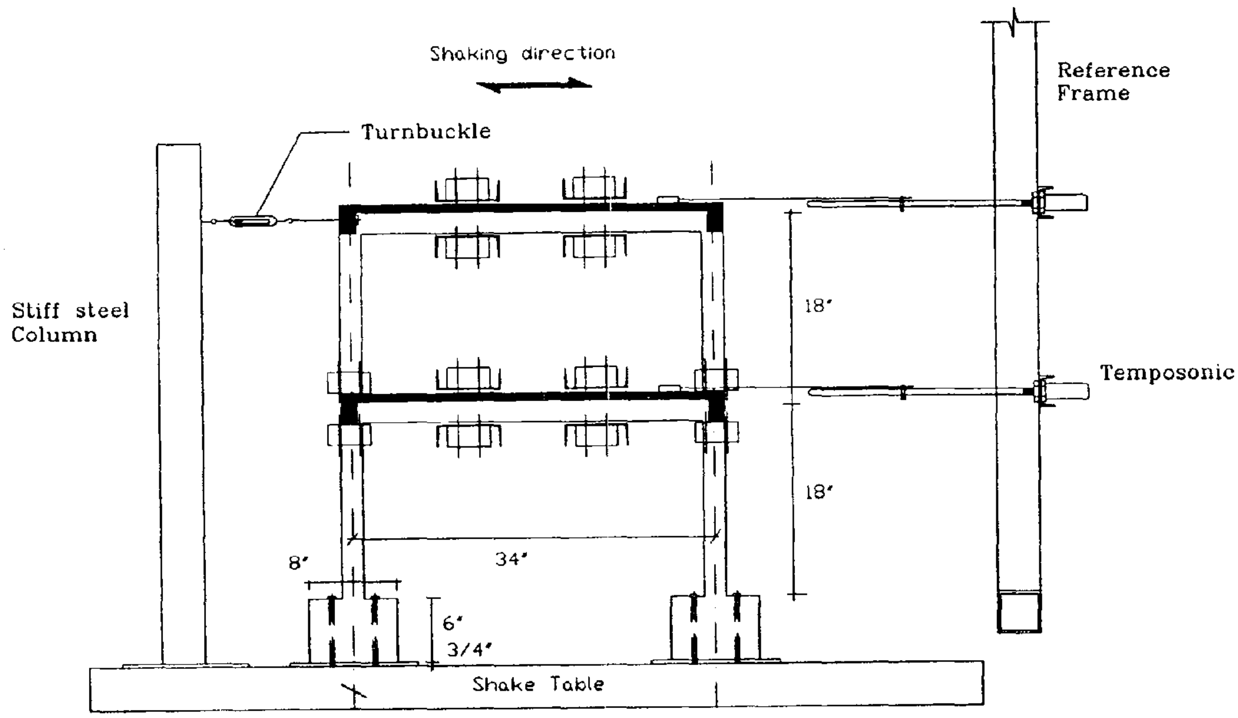

Figure 3.12: 2-Story Building Free Vibration Test Load Set-Up.

motion damped out. A typical data gathering time was about 20 seconds.

The gathered data was used to compute the natural frequencies of the model using a Fast Fourier Transform algorithm (FFT). Knowing the natural frequencies of the model, the same data was band-pass filtered to isolate the response corresponding to each vibration mode (figures 3.13.a and 3.13.b). These separated motions were again used to obtain the damping ratios of each mode using the well-known "Logarithmic Decrement" technique, assuming a viscous damping model.

The second story acceleration data was used to evaluate both the natural frequencies and the damping ratios of the model structure after every seismic test. A curve fitting algorithm was then used to obtain the logarithmic curve that best fit the envelope of the acceleration trace within the concerned range. The viscous damping ratio for both modes were directly obtained from the fitted curve equation (figures 3.13.a and b).

3.2.4 Simulated earthquake tests

The first 10 seconds of the Taft S69E 1952 earthquake (figure 3.14) were applied at different amplitudes to evaluate the model structure performance under seismic excitation. The used record was time-compressed by a factor of $S_t = S_L^{1/2}$ to satisfy the similitude requirements. This resulted in the shift of the response spectrum curve shown in figure 3.15. Although the active seismic excitation time was about 10 seconds (after time compression), the model responses were recorded for 30 seconds to capture the free vibration response after the earthquake.

The magnitude of the earthquake was defined as the maximum ground acceleration applied to the model building. Although the shake table was "prequalified" using a loading condition similar to that of the reinforced concrete model, it was still difficult to reproduce a certain earthquake with specific maximum amplitude during the actual test. This was due to the fact that the transfer function of the shake table was determined using a linear elastic structure while the actual reinforced concrete model was highly non-linear.

All seismic tests were video taped for later, slow motion display. This was found to be useful in reviewing and visually comparing different tests.

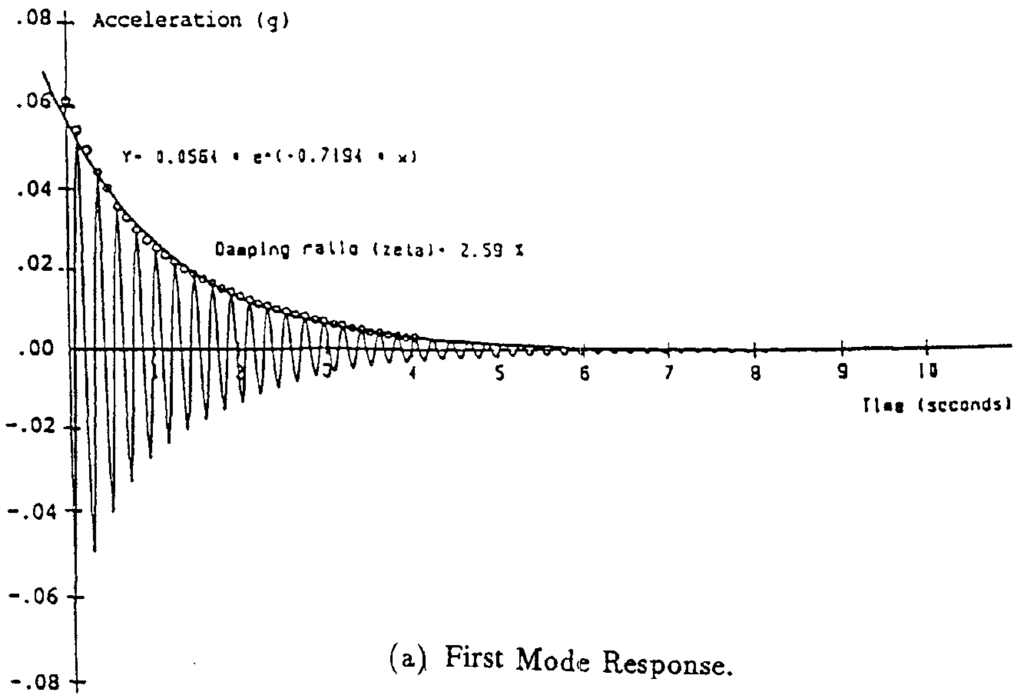

(a) First Mode Response.

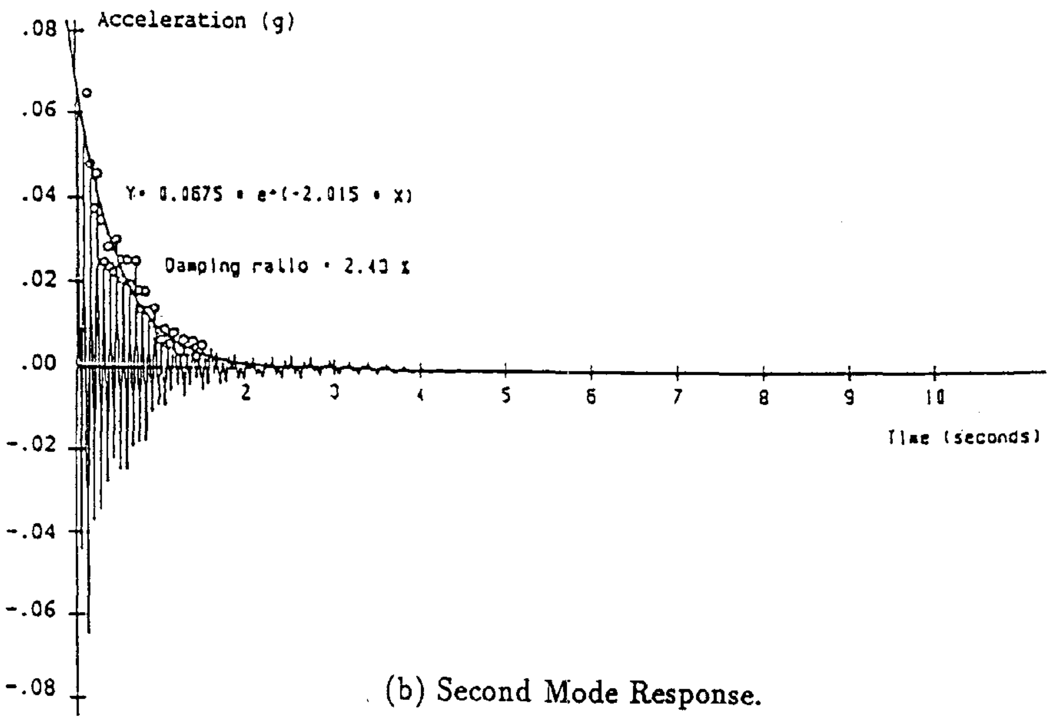

(b) Second Mode Response.

Figure 3.13: Sample Results of The 2-Story Building Free Vibration Test.

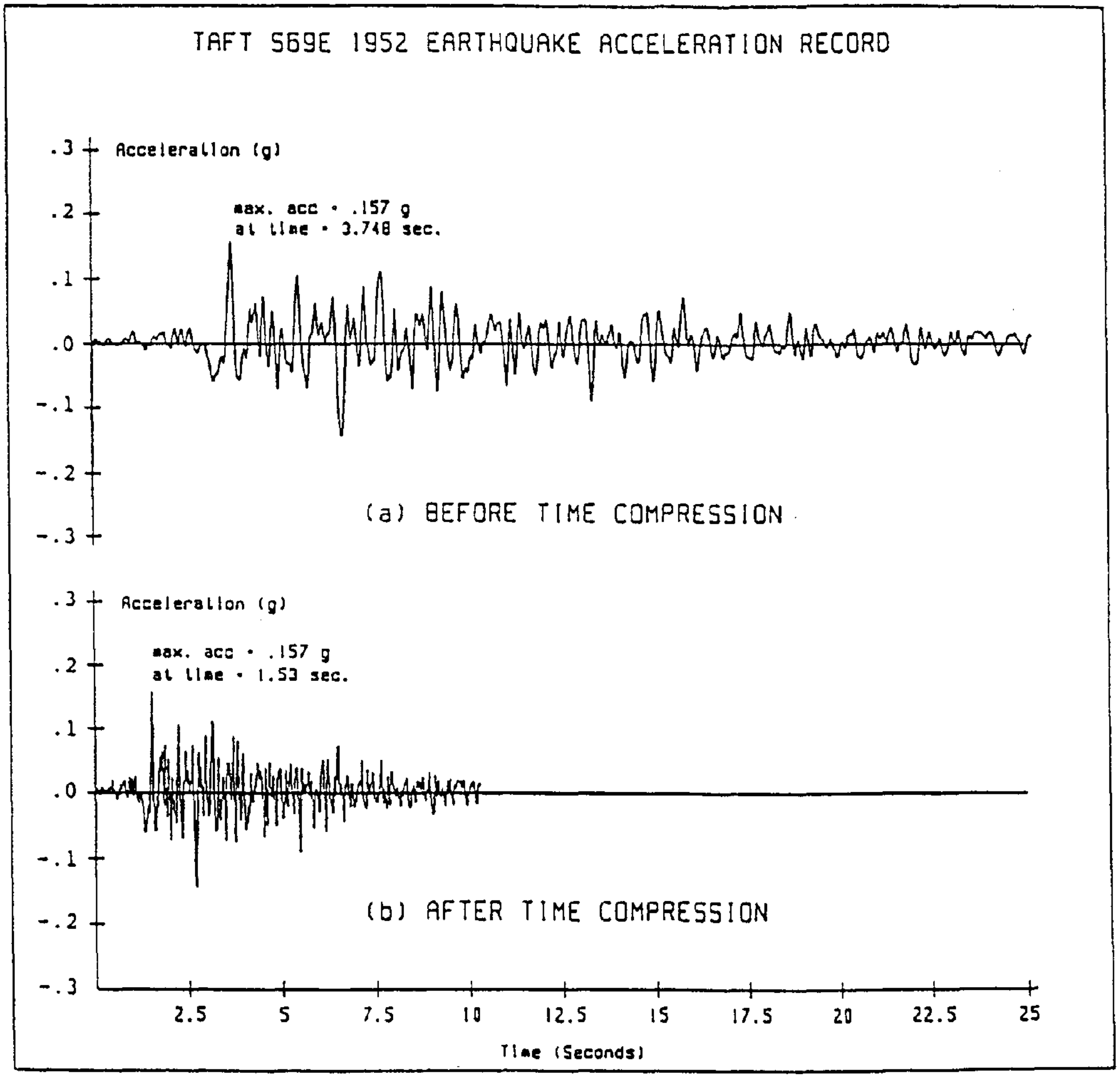

Figure 3.14: Original Versus Time-Compressed Taft 1952 S69E Earthquake.

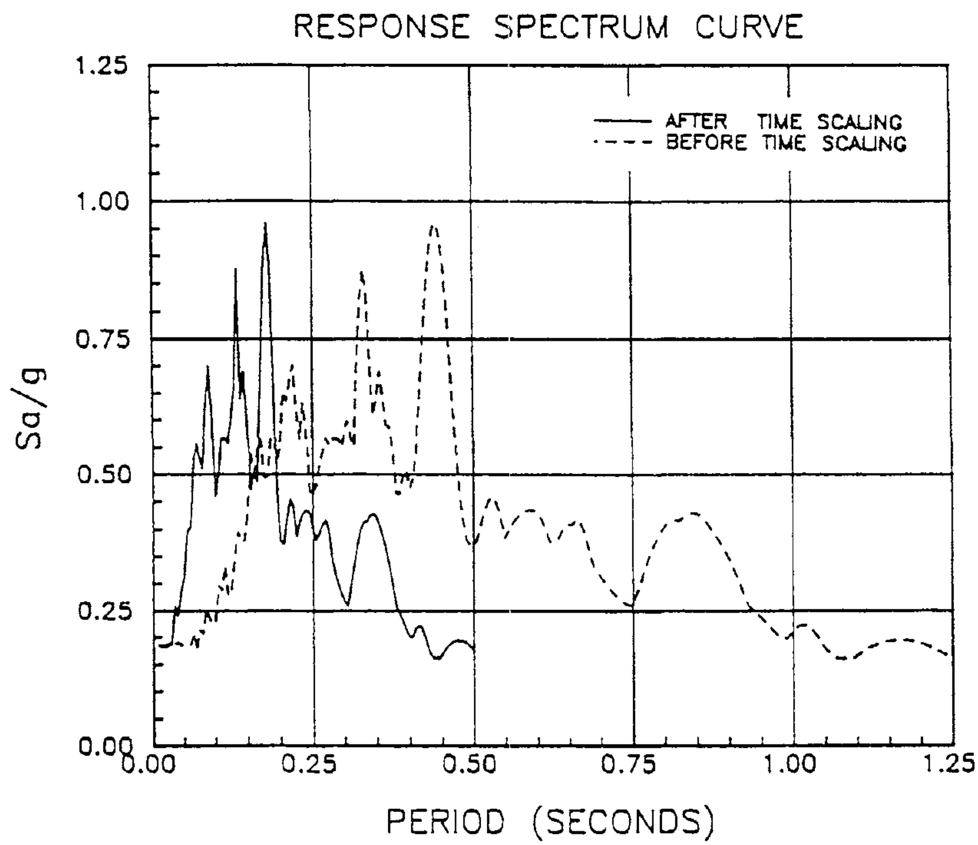

Figure 3.15: Effect of Time-Compression on Response Spectrum.

CHAPTER 4
2-STORY BUILDING TEST RESULTS

4.1 Introduction

The model structure was tested using the time compressed Taft S69E 1952 earthquake at different amplitudes. Traces of the story displacement, story acceleration, and table motion were recorded during each test. Also, the main structural properties of the model (natural frequencies, damping ratios, and flexibility matrix coefficients) were determined before and after every seismic test. Results of these tests will be presented and discussed in this chapter. Results will also be compared (when feasible) with those of a similar seismic detailed model tested at 0.7 scale at the UCB (University of California at Berkeley) [4].

4.2 Test program

Since the model structure was not seismically detailed, it was difficult to predict the ground motion magnitude that would develop sufficient damage without risking an unsafe complete destruction of the model. It was decided that the series of one weak (0.079 g) and two strong ground motions (0.57 g, and 0.65 g) used for the UCB test could cause significant damage to the model building and possibly to the model instrumentation. On the other hand, a gradually increasing earthquake amplitude may not reveal the actual seismic resistance of the structure since the accumulative damage of the building will continuously reduce its stiffness, and consequently lower the magnitude of the lateral forces acting on it as the fundamental period of the structure moves towards the descending portion of the response spectrum curve of the given ground motion (figure 4.1).

The test program was thus selected as an intermediate solution between the two extreme cases. First the model was exposed to two consecutive runs of amplitude 0.26 g representing a mild earthquake, where the second run was carried out to investigate the response of the cracked building with minor damage to the same ground motion. After that, two runs of amplitudes 0.36 g and 0.45 g were performed to increase the level of damage to the building, then two runs of amplitude 0.75 g were applied to simulate a strong ground motion case. Finally a 0.90 g amplitude run was carried out to study the failure mechanism of the structure.

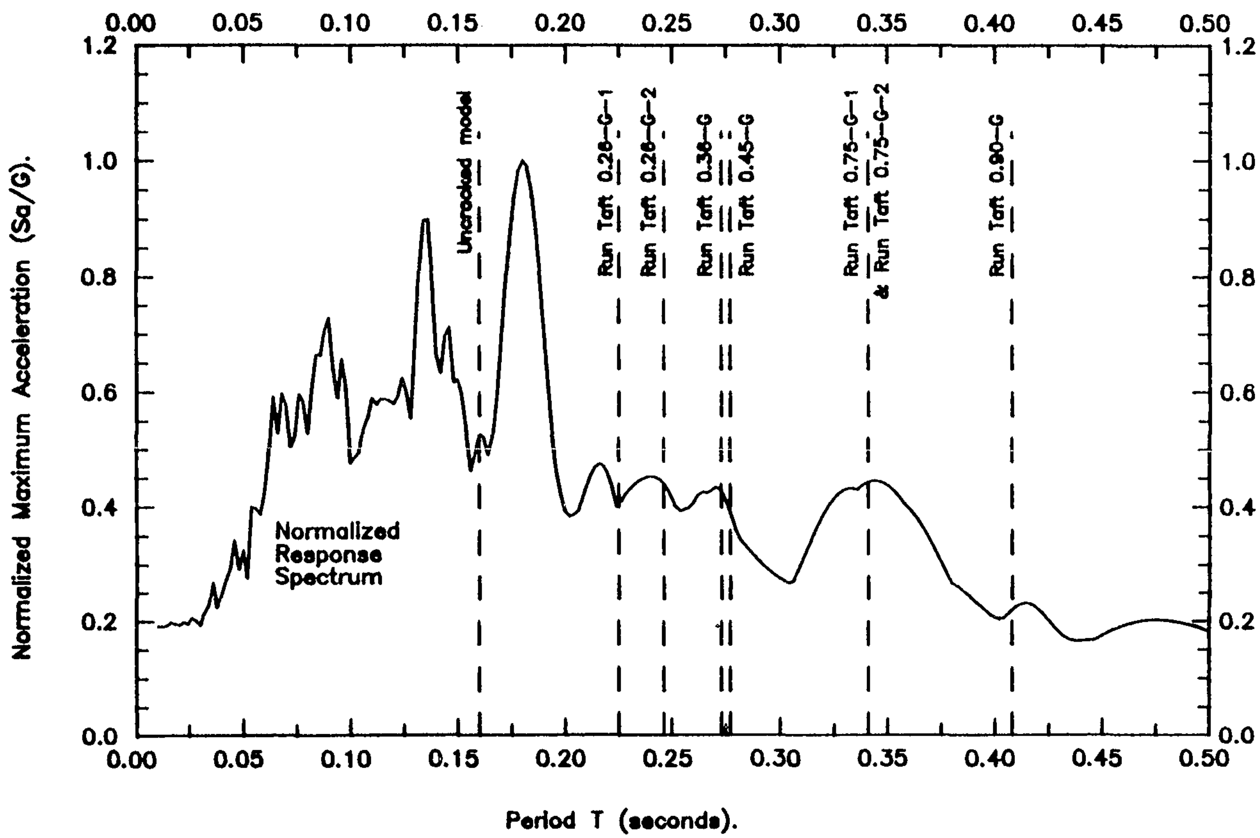

Figure 4.1: Normalized Response Spectrum Curve of The 2-Story Model Input Ground Motion with Selected Test Events.

4.3 Initial properties of the model structure

Initial properties of the model structure along with those of the UCB model (scaled to the Cornell model scale) are presented in table 4.1. It can be seen that the Cornell model fundamental frequencies were lower than those of the UCB model by about 20% and 14% for the first and the second modes respectively. Less discrepancy was observed in the flexibility matrix coefficients where the maximum difference was less than 13%.

Table 4.1: Initial Properties Of Cornell Model Versus UCB Model

Property	UCB Model	UCB Model at Cornell Scale	Cornell Model	Difference%
First natural frequency	3.80 (Hz)	7.79 (Hz)	6.25 (Hz)	-19.8%
Second natural frequency	9.80 (Hz)	20.08 (Hz)	17.19 (Hz)	14.4%
Flexibility Coefficient f11	0.148×10^{-4} (in/lb)	0.888×10^{-4} (in/lb)	1.000×10^{-4} (in/lb)	12.6%
Flexibility coefficient f12	0.167×10^{-4} (in/lb)	1.002×10^{-4} (in/lb)	1.130×10^{-4} (in/lb)	12.8%
Flexibility coefficient f22	0.393×10^{-4} (in/lb)	2.358×10^{-4} (in/lb)	2.250×10^{-4} (in/lb)	-4.58%

Differences can be attributed to many factors such as the different material properties of the two models, loading scheme, testing technique, and even the prototype design of the two structures. For example, table 4.2 shows that the two models had almost the same prototype weight on each floor, but comparison of figures 4.2 and 3.10 illustrates the substantial difference in the loading technique of the two models.

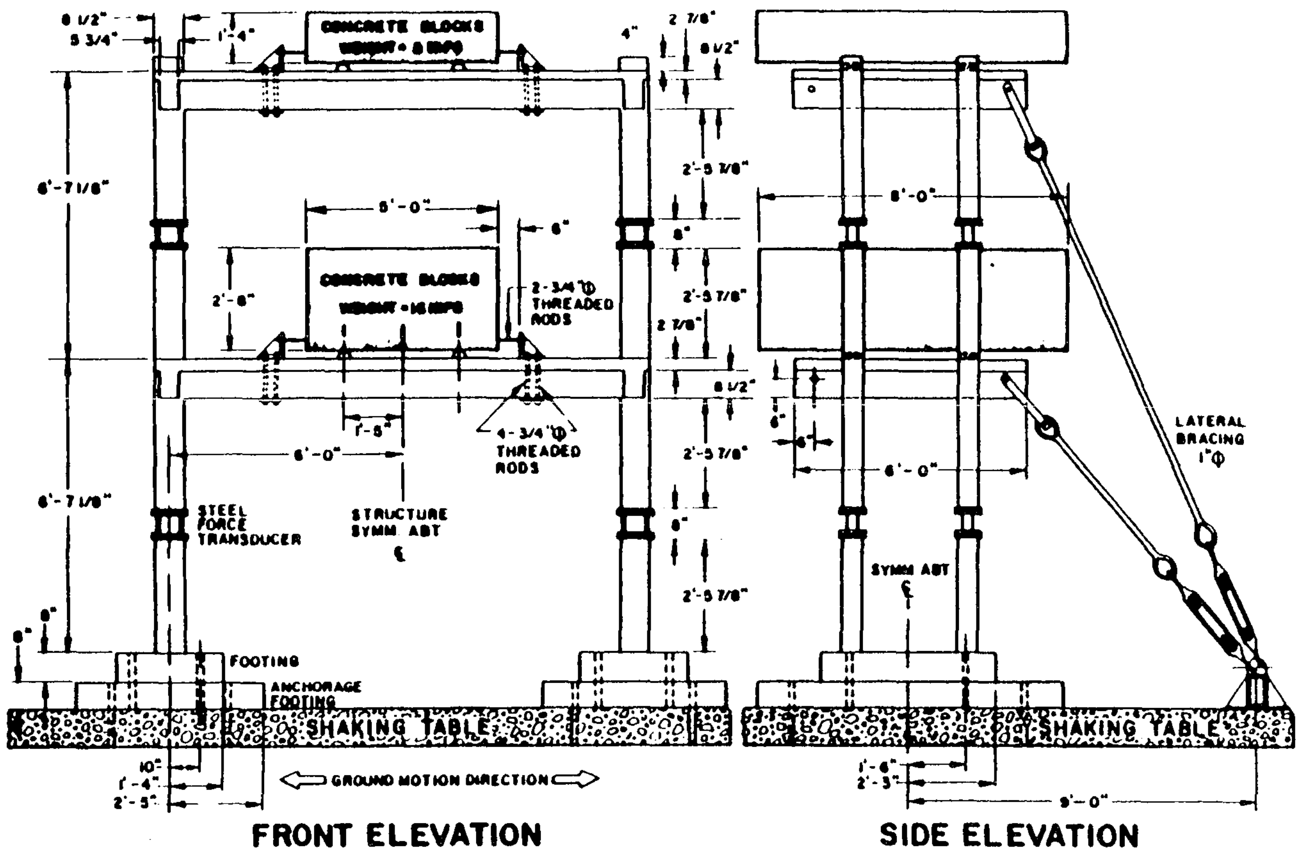

Figure 4.2: Load Set-Up of The UCB 2-Story Building Test (Blondet el.al 1980).

Table 4.2: Loading of Cornell and UCB Models [4]

Model	Scale	First Story Load (kips)		Second Story Load (kips)	
		Model	Prototype	Model	Prototype
Cornell	1/6	1.21	43.56	0.82	29.52
UCB	7/10	21.44	43.76	13.44	27.43

4.4 Runs Taft 0.26 g-1, and Taft 0.26 g-2

Run Taft 0.26 g-1 was applied to the model structure to examine its response during a mild earthquake and to produce a modest level of damage. Figures 4.3.a through 4.3.e represent the measured story displacements, story accelerations and base shear during the seismic test. The inter-story shear is also plotted against the inter-story drift in figures 4.4.a and 4.4.b.

Inspection of the recorded displacements indicates that both stories were moving in phase, with their peak values occurring at the same time. It was concluded that the first mode of motion dominated the response in this run. The same result could also be reached by inspecting the story acceleration records.

The fundamental frequency of the model was reduced by about 29% after this run due to concrete cracking (table 4.3). It was also observed that the natural frequencies obtained from the free vibration test were consistently higher by about 10% than those obtained from the static test. This can be attributed to the loading rate effects in reinforced concrete structures where the concrete modulus E_c increases with increasing the rate of loading.

The stable, narrow banded shear-displacement hysteresis loops of each of the two stories (figure 4.4) indicate that although the model stiffness was reduced due to cracking, minor damage occurred to the building at this stage and the response was nearly elastic.

When the same run was repeated (run Taft 0.26 g-2), very minor changes in the model deformations and base shears were recorded (figures 4.5.a through e). The maximum story displacement was increased by 7% and 2% for the first and the second stories respectively. On the other hand, the maximum story acceleration increased by 37% and 21% for the first and the second stories, but the two maximum values did not occur simultaneously resulting in only 7% increase in the maximum base shear.

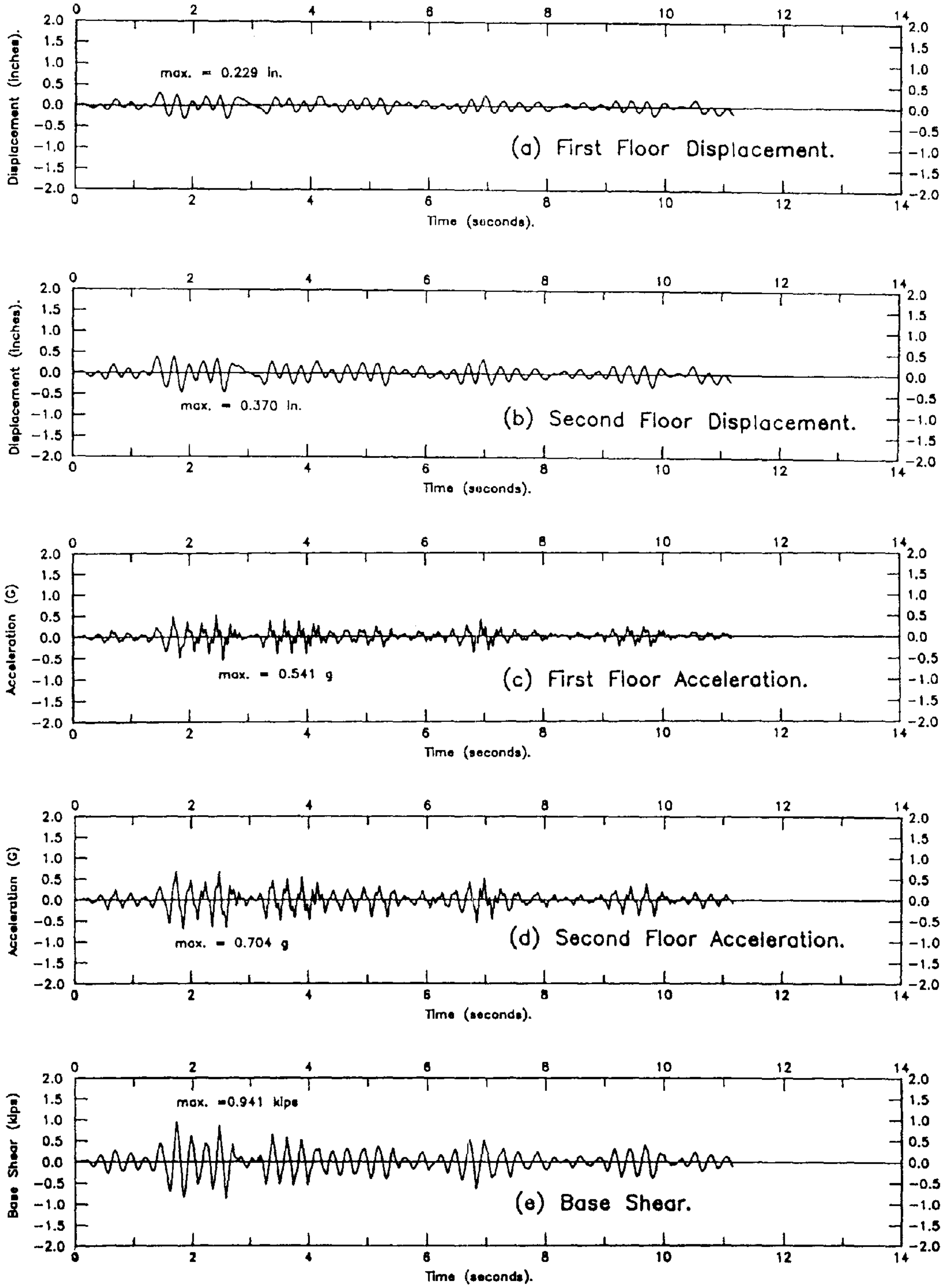

Figure 4.3: Measured 2-Story Model Response During Run Taft 0.26-G-1.

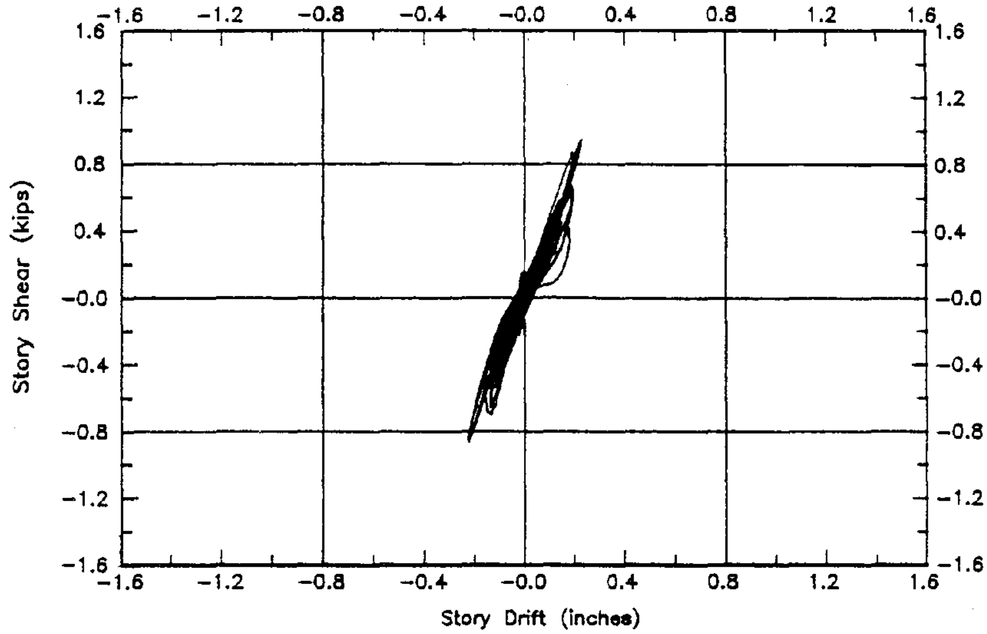

(a) First Story.

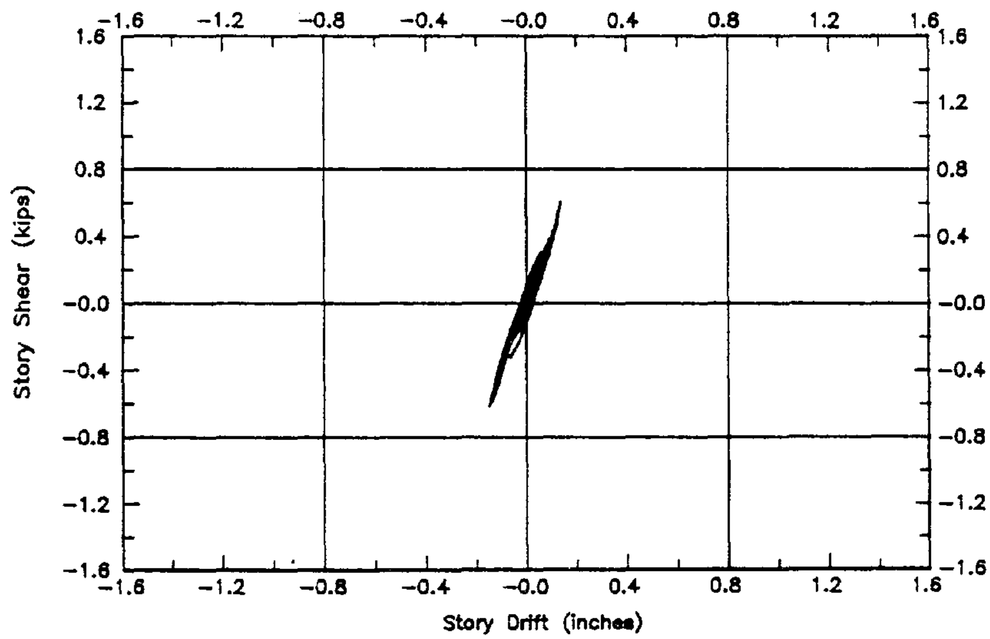

(b) Second Story.

Figure 4.4: Story Shear Versus Inter-Story Drift Hysteresis (Run Taft 0.26-G-1).

Table 4.3: Variation of Natural Frequencies and Damping Ratios

Test	Natural Frequencies				Damping ratio (% Critical)	
	Free Vibration		Static			
	f_1	f_2	f_1	f_2	ξ_1	ξ_2
Uncracked	6.25	17.19	---	---	---	---
Taft 0.26g-1	4.44	13.18	4.06	12.15	2.64	2.44
Taft 0.26g-2	4.07	12.10	3.69	10.87	3.06	3.14
Taft 0.36g	3.66	11.70	3.46	10.74	4.19	3.85
Taft 0.45g	3.61	11.48	3.24	10.47	4.76	3.72
Taft 0.75g-1	2.93	10.31	2.70	9.54	4.49	3.46
Taft 0.75g-2	2.93	10.30	2.52	9.07	4.50	3.43
Taft 0.90g	2.45	9.48	2.52	8.65	4.53	3.42

The level of damage in terms of cracking at the joints was slightly increased after this run, where the natural frequencies of the model were reduced by an average value of 8%, and its flexibility matrix coefficients were increased by about 20% (Table 4.4). The first mode damping ratio increased from 2.64% to 3.06%.

Table 4.4: Variation of Static Flexibility Matrix Coefficients

Test	Flexibility Matrix Coefficient inch/lb x 10^{-3}			
	f_{11}	f_{12}	f_{21}	f_{22}
Uncracked	0.100	0.113	0.113	0.225
Taft 0.26g-1	0.254	0.292	0.292	0.532
Taft 0.26g-2	0.300	0.350	0.350	0.660
Taft 0.36g	0.345	0.406	0.406	0.733
Taft 0.45g	0.426	0.473	0.473	0.773
Taft 0.75g-1	0.544	0.682	0.682	1.192
Taft 0.75g-2	0.640	0.763	0.790	1.338
Taft 0.90g	0.775	0.995	0.995	1.578

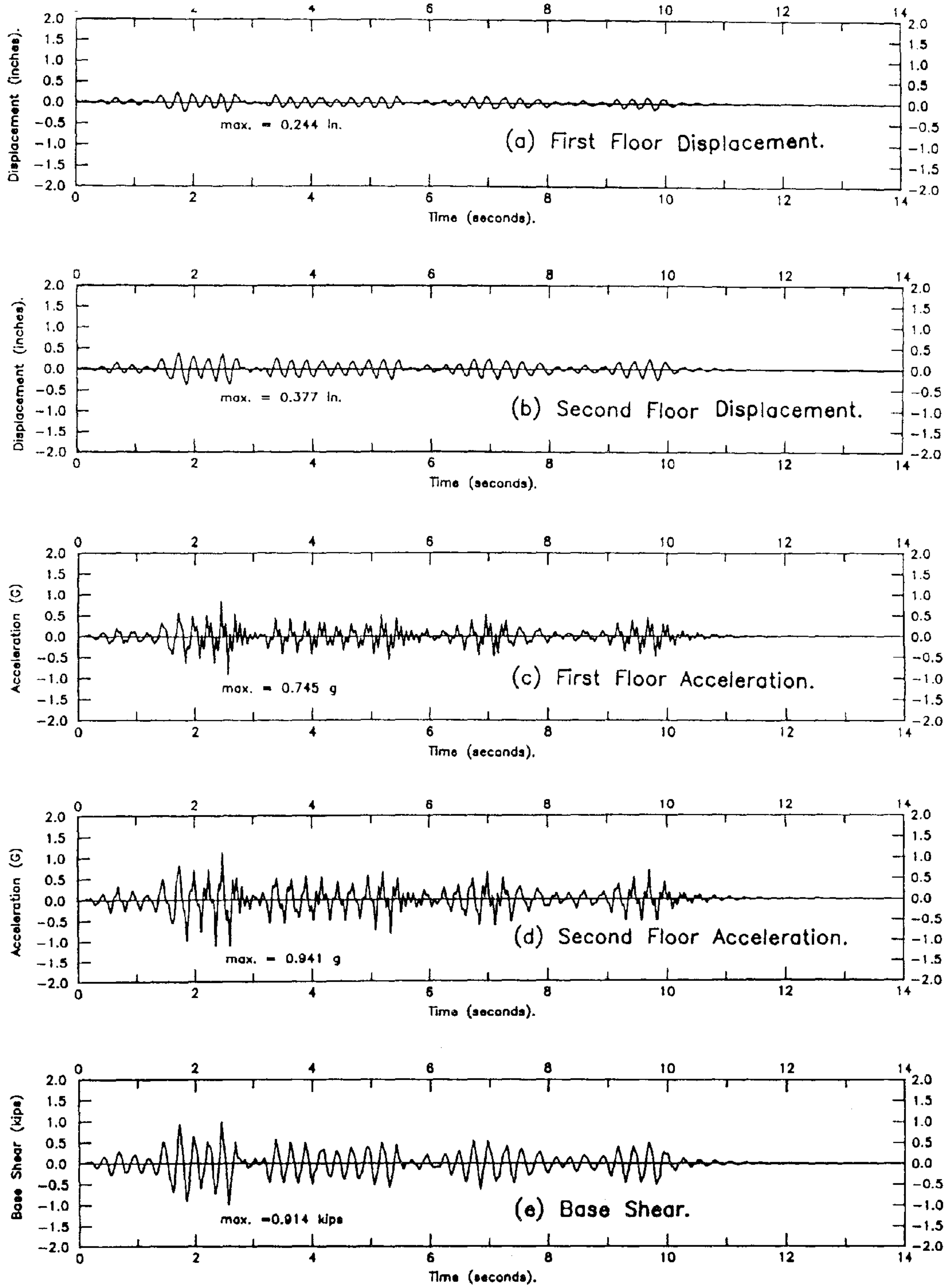

Figure 4.5: Measured 2-Story Model Response During Run Taft 0.26-G-2.

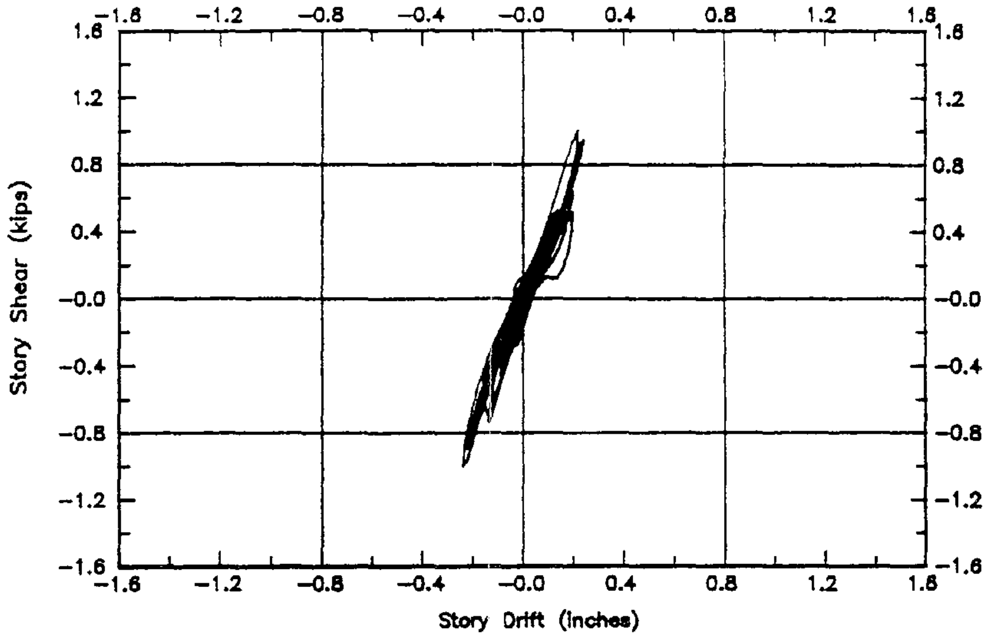

(a) First Story.

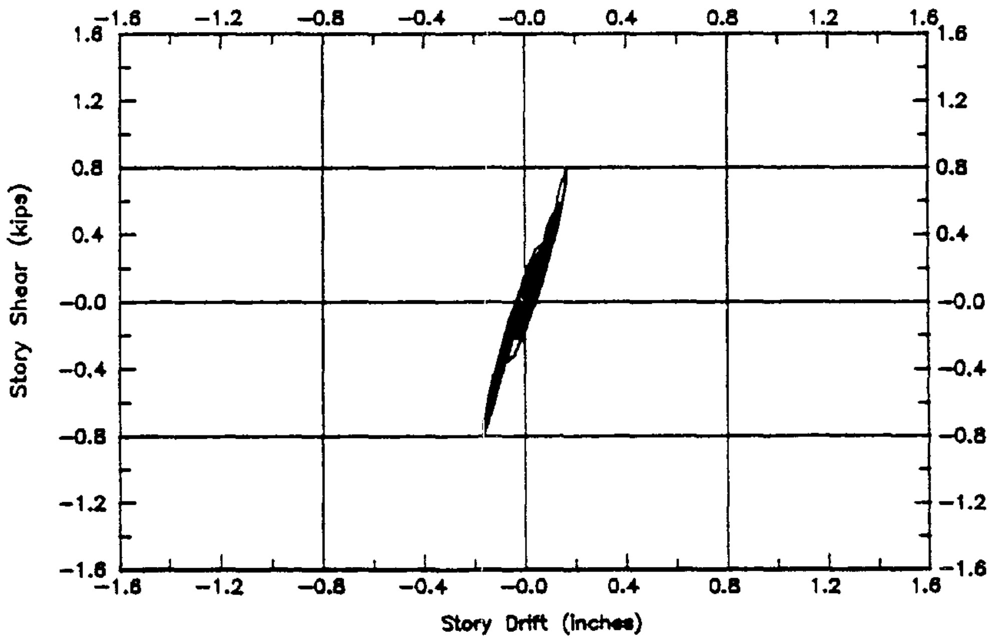

(b) Second Story.

Figure 4.6: Story Shear Versus Inter-Story Drift Hysteresis (Run Taft 0.26-G-2).

The total energy dissipated by the model at this run was about 31% higher than that of run Taft 0.26 g-1 (table 4.5). This increase can be explained by comparing figures 4.4.b, and 4.6.b, where it can be seen that the high second story shear forces in this run caused cracks to develop resulting in wider hysteresis loops and consequently more energy absorption.

Table 4.5: Energy Dissipation

Test	Energy Dissipated (kips.inch)		
	First floor	Second floor	Third floor
Taft 0.26g-1	0.423	0.289	0.712
Taft 0.26g-2	0.418	0.513	0.931
Taft 0.36g	0.692	0.408	1.099
Taft 0.45g	1.148	0.379	1.527
Taft 0.75g-1	3.667	1.841	5.508
Taft 0.75g-2	1.597	0.451	2.047
Taft 0.90g	2.484	0.330	2.814

4.5 Runs Taft 0.36 g and Taft 0.45 g

Run Taft 0.36 g (figures 4.7 and 4.8) was associated with a significant increase in the model deformations, with maximum displacements of both stories 44% higher than those obtained during the previous run. Maximum story accelerations recorded -3% and 20% increase in the first and the second stories respectively, resulting in 11% increase in the maximum base shear (table 4.6).

It was clear that the level of cracking of the model was increased as the fundamental frequency was reduced by about 10%, and the flexibility matrix coefficients were increased by an average value of 14% (Table 4.4). The total energy dissipated by the structure was 18% higher than that dissipated during the previous run.

At run Taft 0.45 g (figures 4.9 and 4.10), the amount of damage introduced to the model was less than that caused by the run Taft 0.36 g. This was manifested in the very minor changes in the model natural frequencies (1% and 2% reduction for the 1st and the 2nd modes), and a

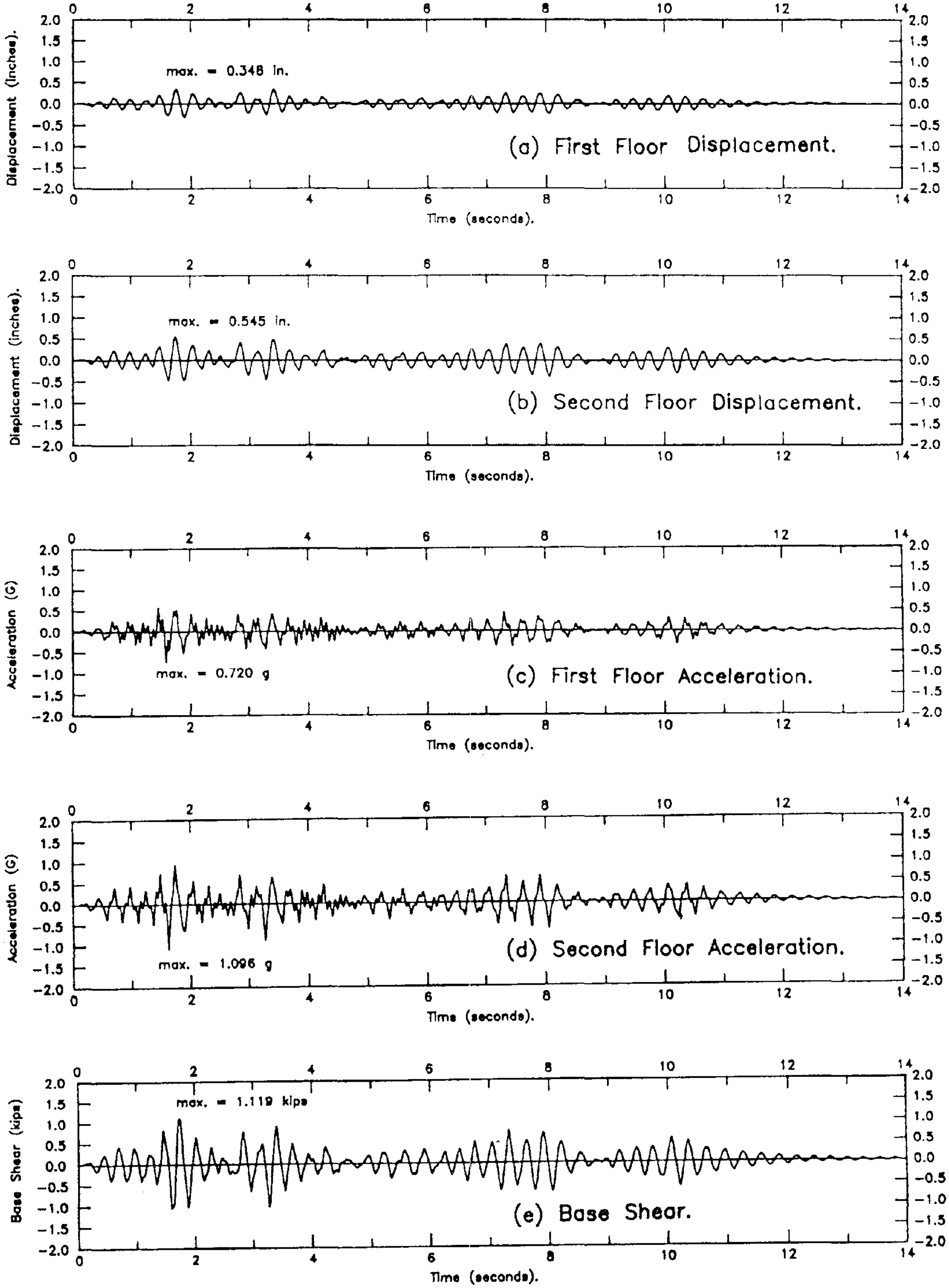

Figure 4.7: Measured 2-Story Model Response During Run Taft 0.36-G.

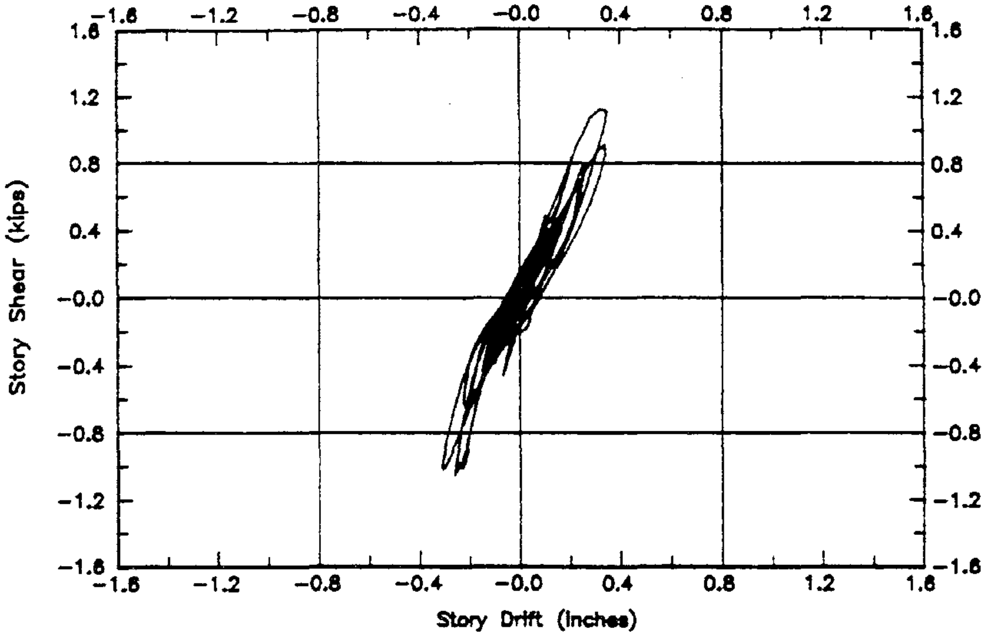

(a) First Story.

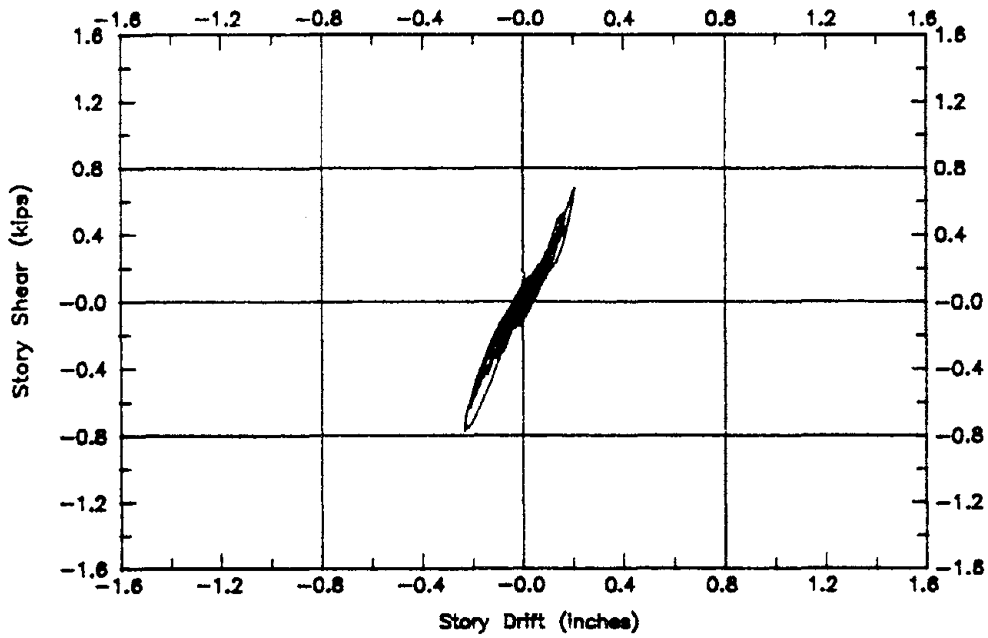

(b) Second Story.

Figure 4.8: Story Shear Versus Inter-Story Drift Hysteresis (Run Taft 0.36-G).

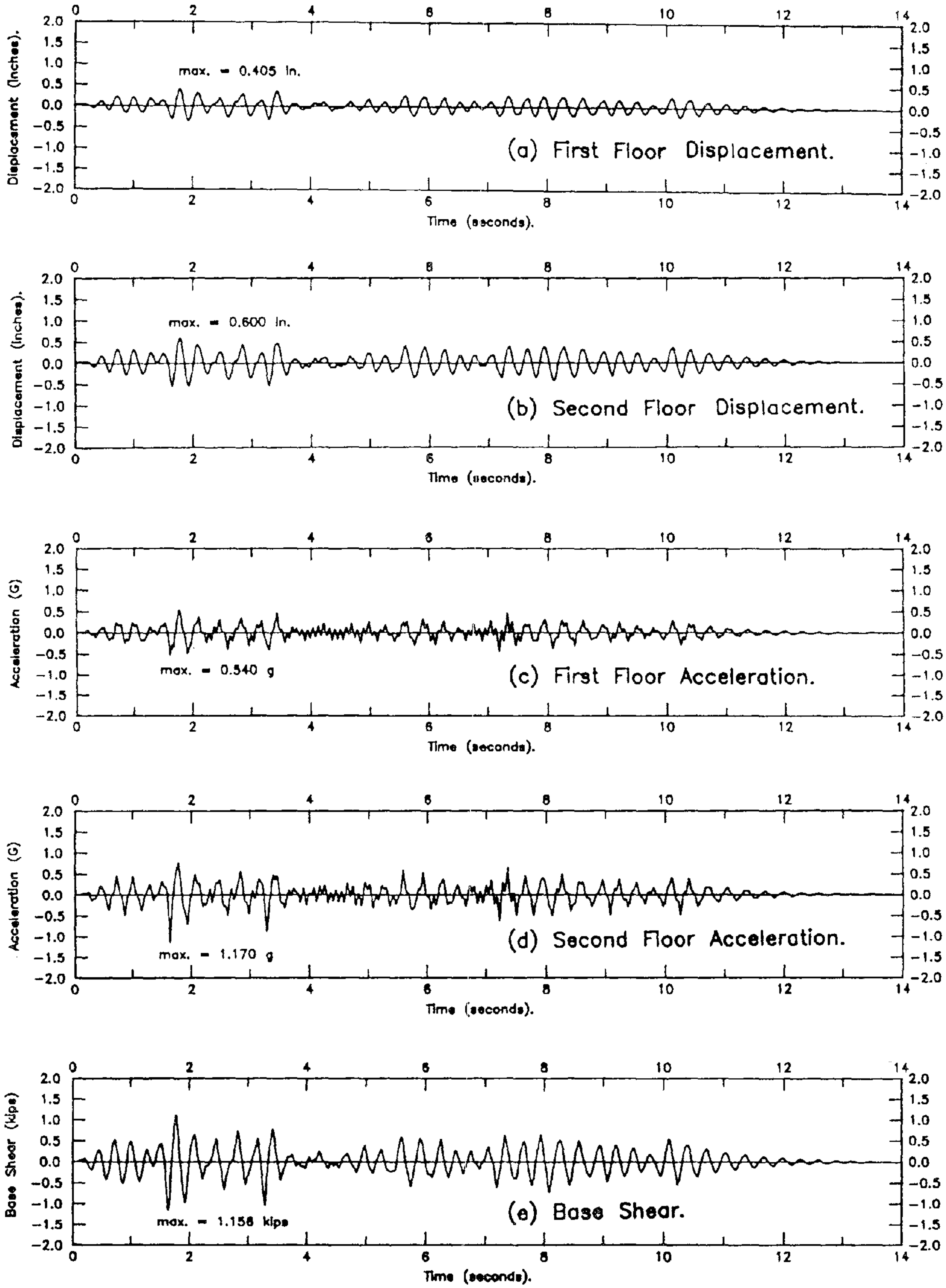

Figure 4.9: Measured 2-Story Model Response During Run Taft 0.45-G.

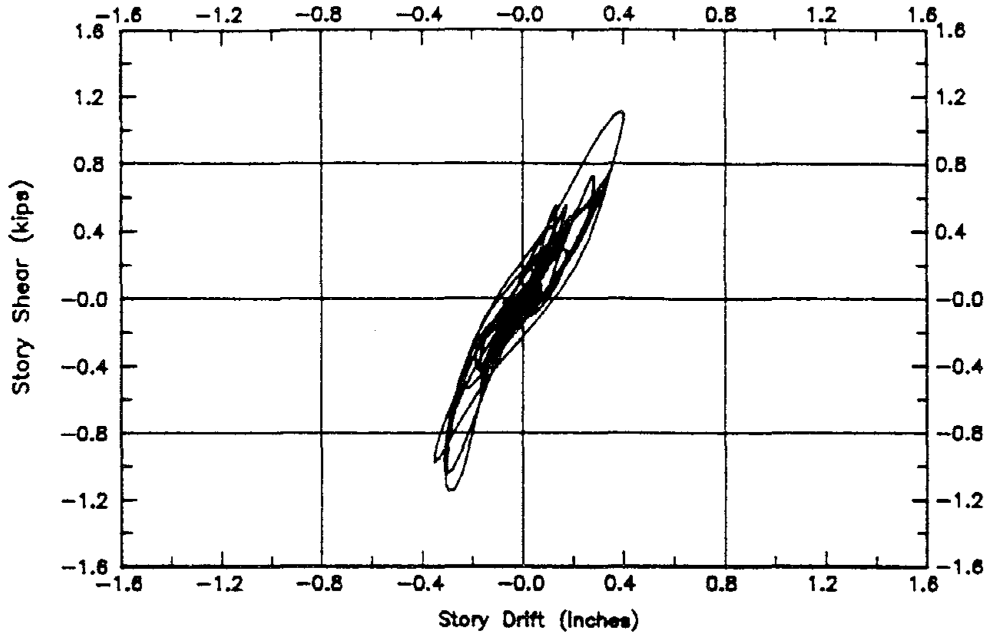

(a) First Story.

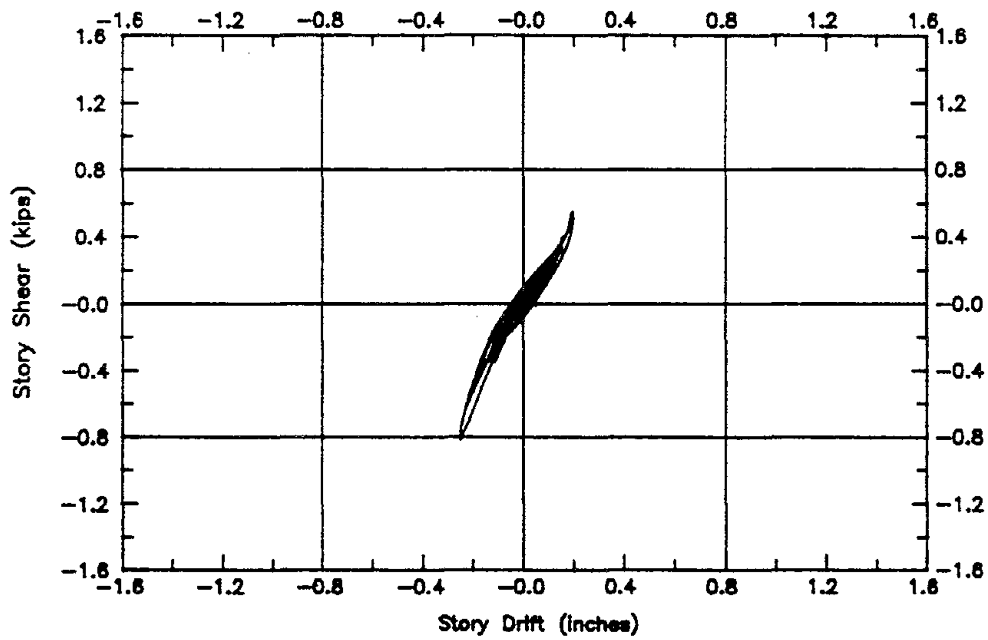

(b) Second Story.

Figure 4.10: Story Shear Versus Inter-Story Drift Hysteresis (Run Taft 0.45-G).

comparatively small increase in all the flexibility matrix coefficients (an average of 11% increase).

Table 4.6: Summary of Simulated Earthquake Test Results

Test	Maximum Story Displacement (inches)		First Story Drift (%)	Maximum Story Acceleration (g)		Maximum Base Shear (Kips)
	1st story	2nd story		1st story	2nd story	
Taft 0.26g-1	0.229	0.370	1.27%	0.542	0.706	0.943
Taft 0.26g-2	0.224	0.377	1.36%	0.745	0.914	1.005
Taft 0.36g	0.348	0.545	1.93%	0.720	1.096	1.119
Taft 0.45g	0.405	0.600	2.25%	0.540	1.167	1.156
Taft 0.75g-1	0.741	1.227	4.12%	0.767	1.343	1.307
Taft 0.75g-2	0.789	1.036	4.38%	0.643	0.920	1.104
Taft 0.90g	0.911	1.146	5.06%	0.367	0.525	0.569

The maximum story responses (displacements and accelerations) also showed less changes than those recorded for run Taft 0.36 g as shown in table 4.5 and figure 4.9. As a result, the maximum base shear was increased by only 4% over the previously recorded value. On the other hand, as a result of the damage accumulation, the extension of old cracks and the generation of new ones, the energy dissipated at this run was about 39% higher than that dissipated by the previous run.

4.6 Runs Taft 0.75 g-1 and Taft 0.75 g-2

At run Taft 0.75 g-1, large flat portions of the story drift-story shear curves were obtained in both directions for the first story, indicating that the first story columns yielded in both directions. This was associated with pull-out of the discontinuous beam bottom reinforcement under positive moments, resulting in very large deformation of the two stories (figures 4.11.a and 4.11.b). The first story maximum displacement was 83% higher than that recorded during run Taft 0.45 g, and 223% higher than that of run Taft 0.26 g-1, while the second story maximum displacement was 105% and 231% higher than the values for runs Taft 0.45 g and Taft 0.26 g-1,

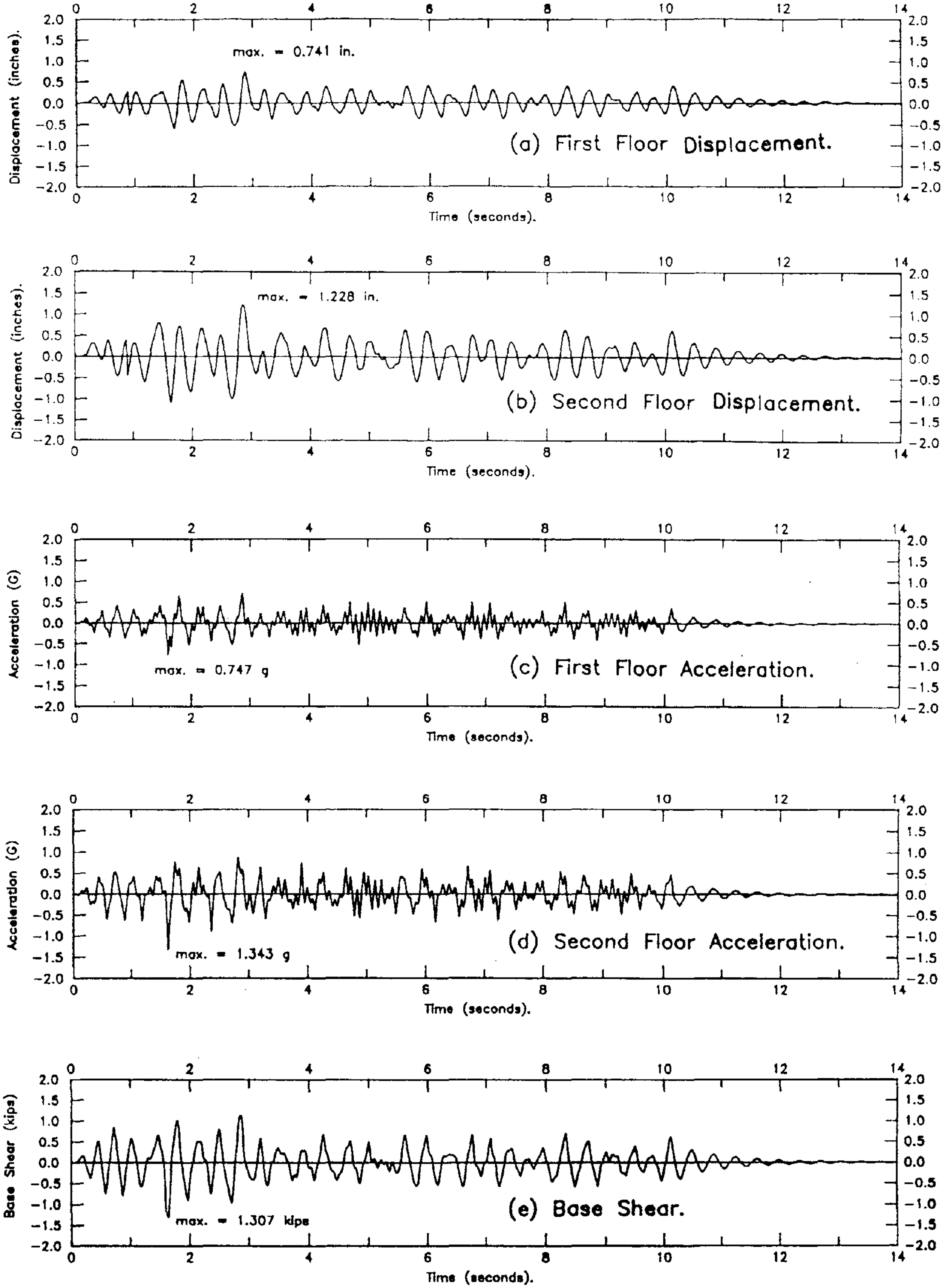

Figure 4.11: Measured 2-Story Model Response During Run Taft 0.75-G-1.

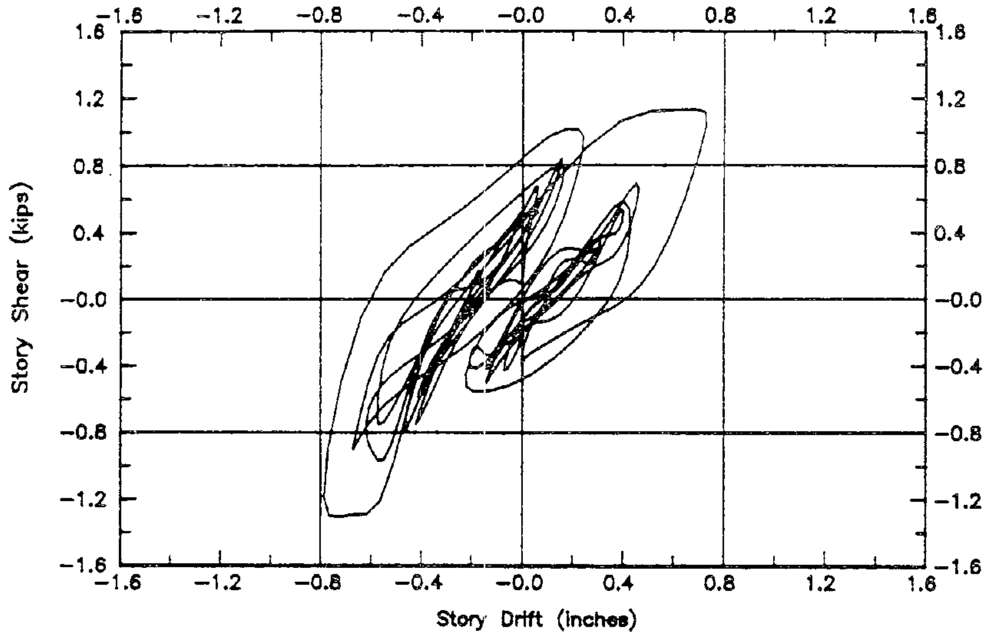

(a) First Story.

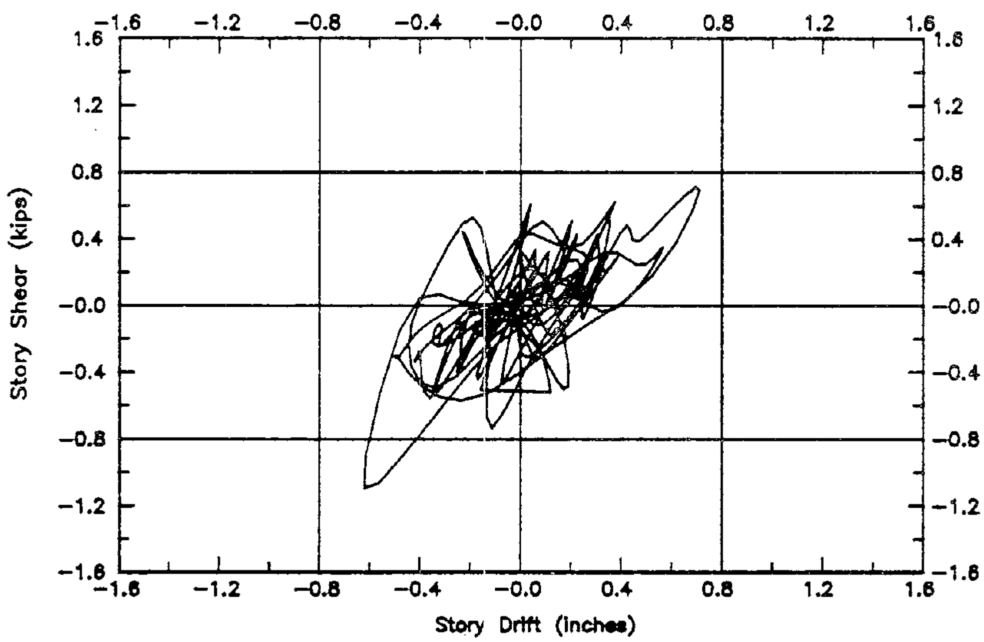

(b) Second Story.

Figure 4.12: Story Shear Versus Inter-Story Drift Hysteresis (Run Taft 0.75-G-1).

respectively (table 4.6).

The increase in maximum story accelerations was less than that of the story displacement (figures 4.11.c and d). An increase of 42% and 15% over the previous run values was recorded for the first story and the second story, respectively. The two peak values were synchronized resulting in a maximum base shear increase of 13% over the previous run and 39% increase over the Taft 0.26 g-1 maximum value (figure 4.11.e).

The total energy dissipated by the model during this run was 261% higher than that dissipated during the previous run and 674% higher than that of run Taft 0.26 g-1. This can be attributed to the yielding of the first story columns and the increased level of cracking of the second story. It was also observed that the first story dissipated 67% of the total amount of energy while the second story dissipated only 33% as its columns did not yield (figures 4.12.a and b).

The model stiffness was significantly reduced due to this run as the model flexibility matrix coefficients were increased by an average value of 42% while the natural frequencies were reduced by 19% and 10% for the first and the second modes respectively. The total increase in the flexibility matrix coefficients after this run as compared to the elastic uncracked model values were 440%, 504%, and 430% for f_{11}, f_{12}, and f_{22} respectively (table 4.4).

A 6% reduction in the first mode damping ratio was recorded due to this run. For the second mode, only a 1% damping ratio reduction was obtained (table 4.3).

As a direct result of the significant change of the model properties due to run Taft 0.75 g-1, the measured model responses during run Taft 0.75 g-2 were less than those of the previous run. The maximum story accelerations were reduced by 16% and 31% for the first and the second stories respectively. This resulted in a 16% reduction in the maximum base shear (figures 4.13.c, d and e).

The combined action of the model softening, and the reduction of the model lateral forces resulted in only a 6% increase in the first story maximum displacement and 16% reduction in the second story maximum displacement (figures 4.13.a, and b). The flexibility matrix coefficients were increased by an average value of 14% over the previous run values, indicating an increase in the damage level.

The total energy dissipated by the model during this run was reduced by 63%, while no changes were detected in the natural frequencies and the damping ratios after this run.

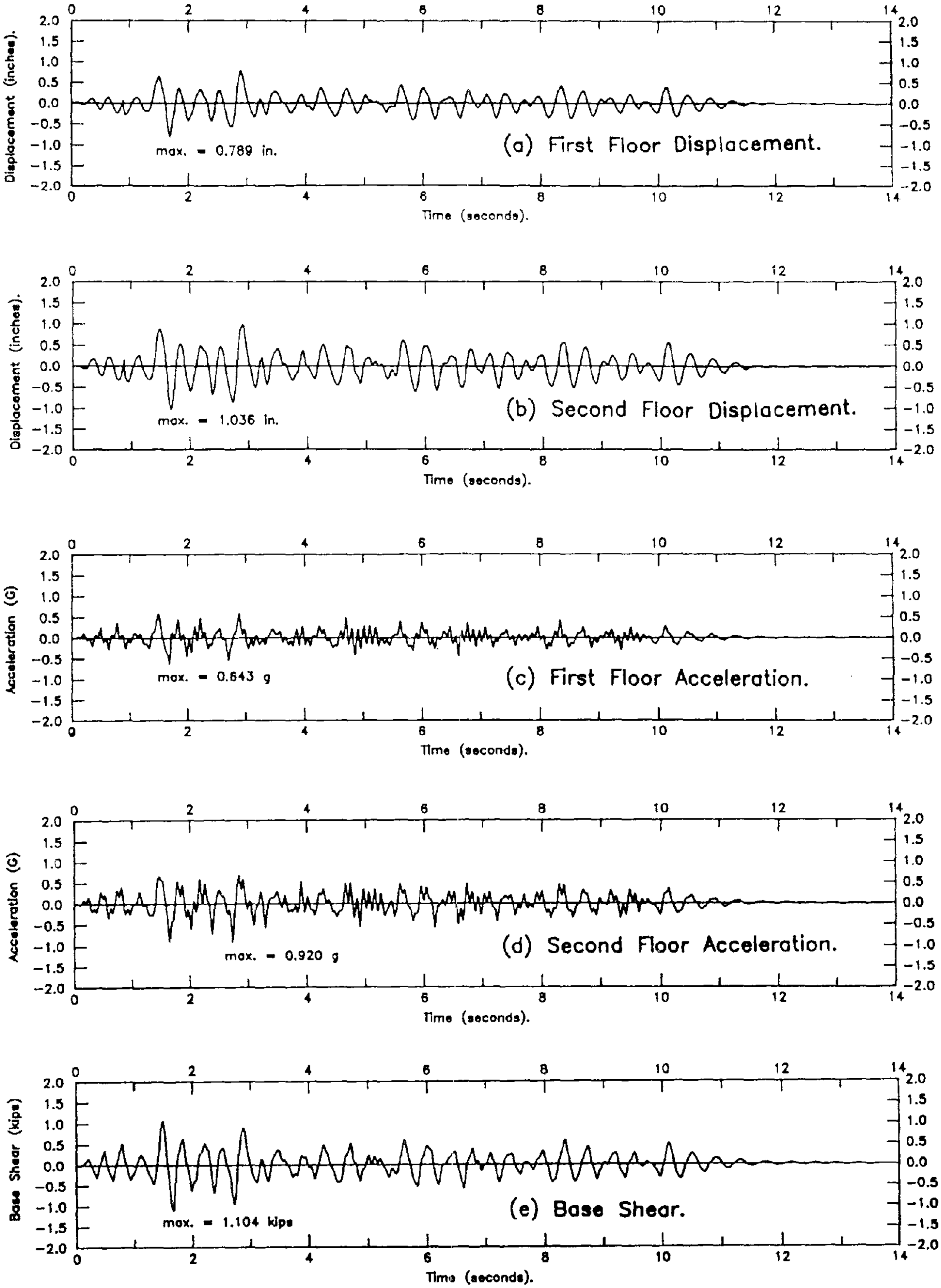

Figure 4.13: Measured 2-Story Model Response During Run Taft 0.75-G-2.

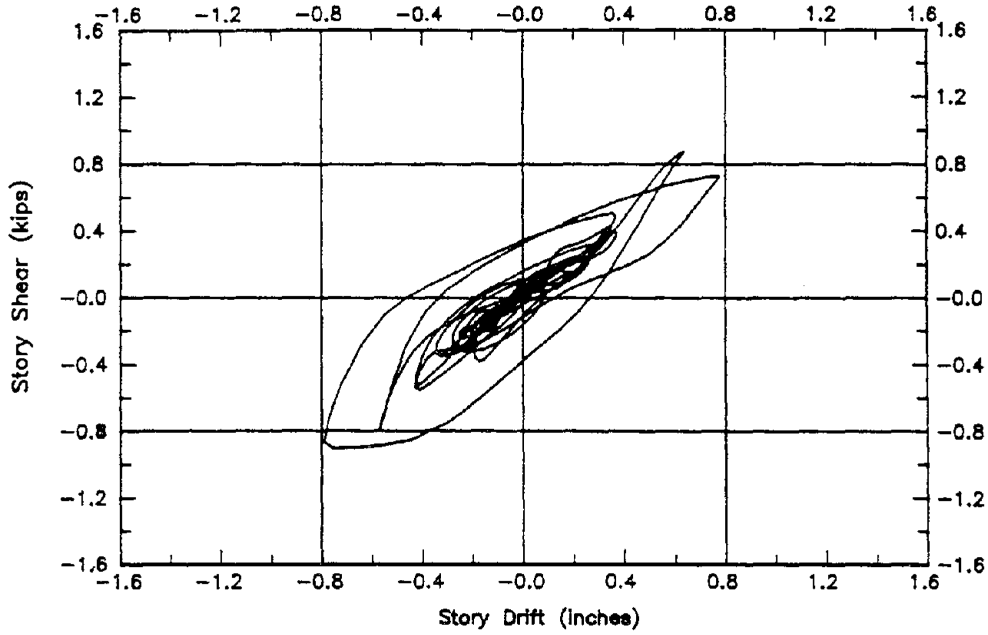

(a) First Story.

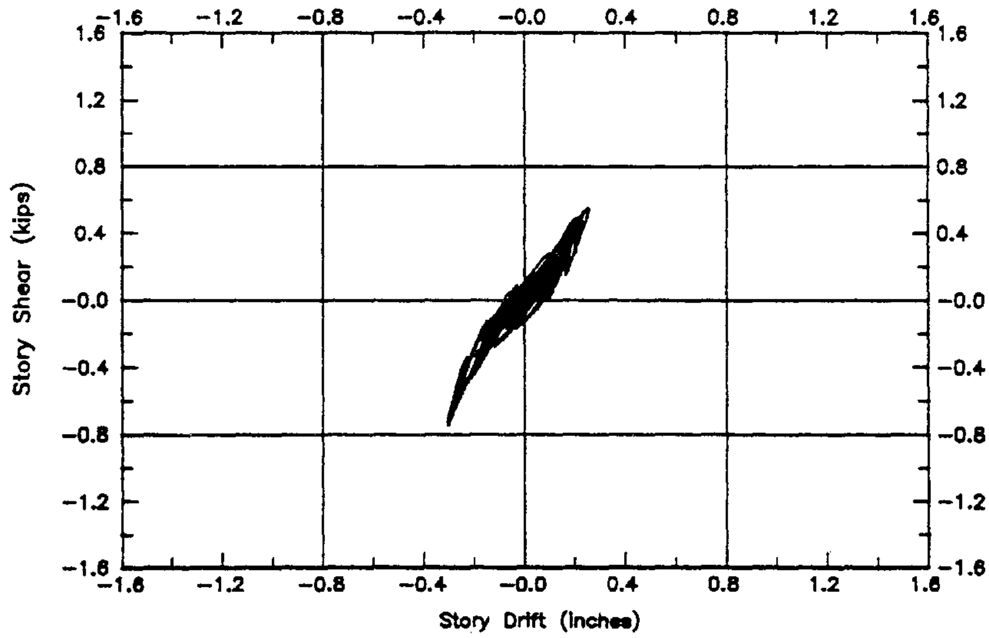

(b) Second Story.

Figure 4.14: Story Shear Versus Inter-Story Drift Hysteresis (Run Taft 0.75-G-2).

4.7 Run Taft 0.90 g

At run Taft 0.90 g, the level of lateral forces was significantly reduced due to the model softening. The maximum story accelerations were reduced by 43% for both stories, resulting in a 48% reduction of the maximum base shear, while the maximum story displacement recorded an increase of 23% and 11% for the first and the second stories respectively (figure 4.15).

The natural frequencies of the model were reduced by 16%, and 8% for the first and the second modes respectively, while the flexibility matrix coefficients were increased by an average value of 22%. The total increase of the flexibility matrix coefficients after this run as compared to the uncracked model values were 675%, 745%, and 601% for f_{11}, f_{12}, and f_{22} respectively. The corresponding reduction of the model natural frequencies was 61% and 49% for the first and the second modes, respectively.

The total energy dissipated at this run was 37% higher than that of the previous run but still 49% less than that dissipated during run Taft 0.75 g-1 (table 4.5).

After run Taft 0.90 g, the critical sections of the building at the construction joints of the first story columns, and at locations of the discontinuous bottom beam reinforcement, were severely damaged. It was decided to terminate the seismic testing at this stage, since no additional useful information could be obtained.

4.8 Summary

The 2-story office building model was tested on the Cornell University shake table using the time-compressed Taft 1952 S69E earthquake at different amplitudes. The model response was characterized by the domination of the first mode of vibration and high flexibility and stiffness degradation. Pull-out of the discontinuous positive beam reinforcement did occur, resulting in an even higher degree of flexibility.

A complete failure mechanism was not achieved, but the model was so damaged in terms of large cracks, steel pullout, and stiffness reduction that it was impossible to increase the base shear to cause failure using the same earthquake record with the current shake table capabilities.

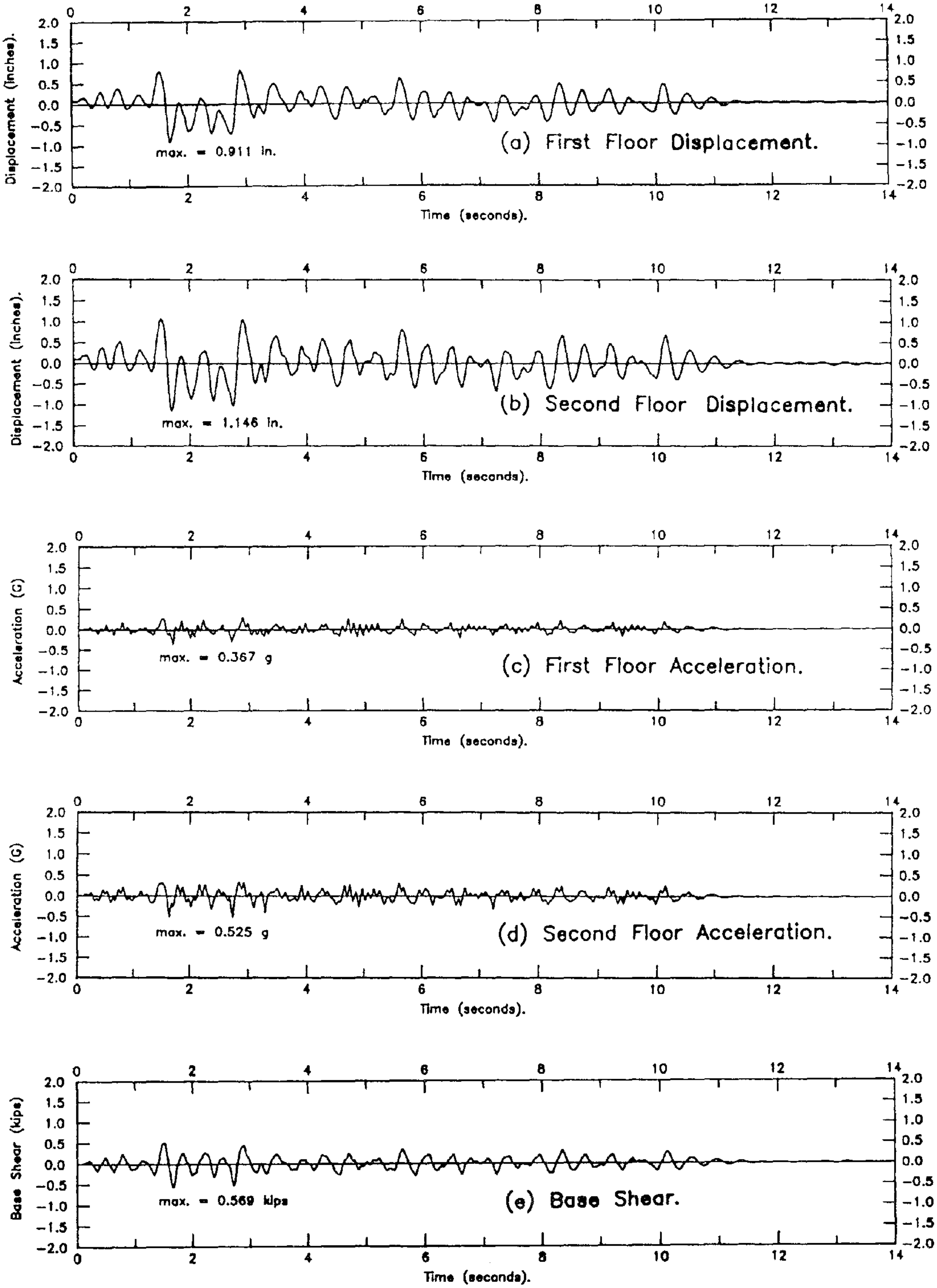

Figure 4.15: Measured 2-Story Model Response During Run Taft 0.90-G

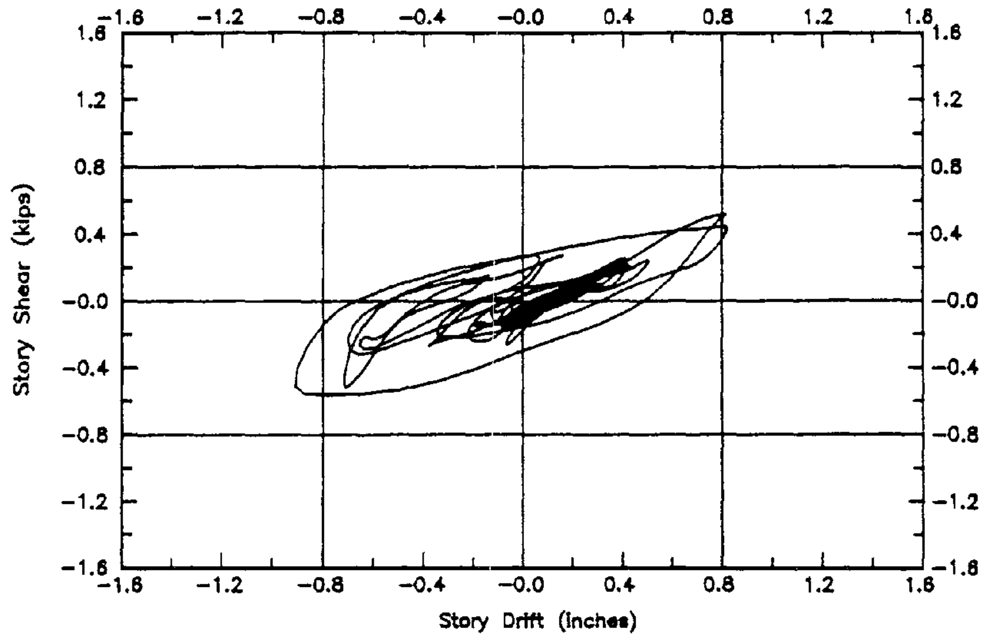

(a) First Story.

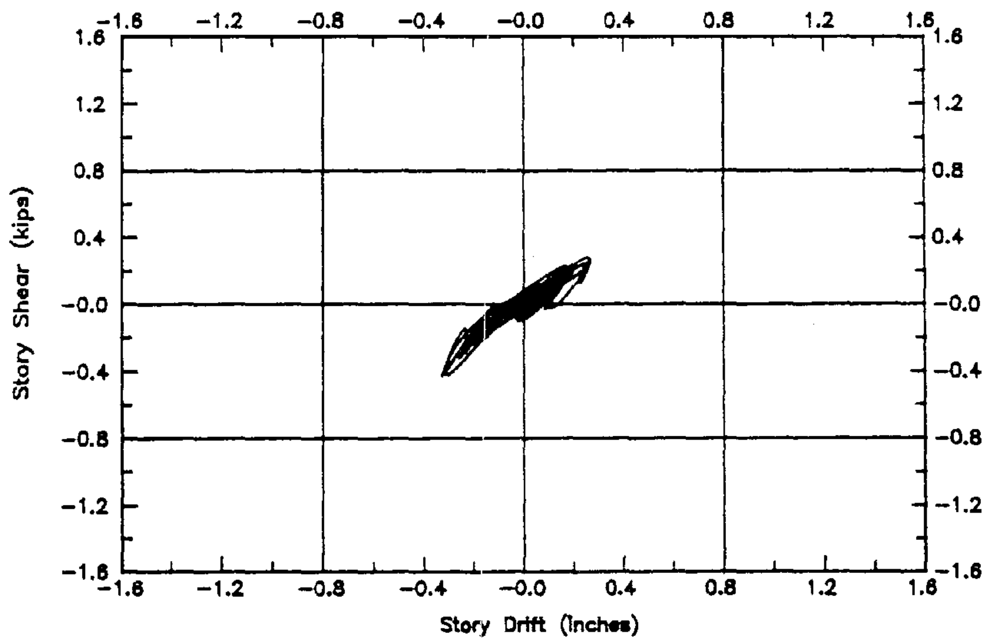

(b) Second Story.

Figure 4.16: Story Shear Versus Inter-Story Drift Hysteresis (Run Taft 0.90-G).

CHAPTER 5
ANALYTICAL RESULTS

5.1 Introduction

Results of the numerical analyses performed for the 2-story model structure using program IDARC (Inelastic Damage Analysis of Reinforced Concrete structures) [16,18] are presented, discussed, and compared with the experimental results in this chapter. A brief description of the program organization, model idealization, and input data is provided first, followed by a detailed presentation of the analytical results for the 2-story model. Since the current model did not have any internal force measurements, only the global response of the model (story displacements and story shears) was compared to the theoretically predicted response.

5.2 Program IDARC

5.2.1 General

The program was developed at the State University of New York at Buffalo [1985-1987] to perform complete damage analysis of reinforced concrete structures subjected to earthquakes. The library of elements includes beams, columns, shear walls, edge columns, and transverse beams for proper modeling of concrete structures. The program is organized into three computational phases: (a) system identification, (b) dynamic response analysis, and (c) damage analysis.

In the first phase, information such as the structure configuration, material properties, and element reinforcement are used to determine the component properties, ultimate member capacities, fundamental period, and the static failure mode. In the second phase, a dynamic analysis of the structure is performed using the Newmark-β method to solve the equations of motion based on the three parameter hysteretic model to trace force-deformation relationships. In the final portion of the program, a damage analysis is performed, resulting in damage indices for individual members, for stories, and for the whole structure.

5.2.2 Structural modeling

The structure as a whole is modeled with one degree of freedom at each floor level, ignoring any axial deformations in the members. Individual members (beams, columns, etc.) are represented by non-linear springs, taking into consideration the effect of the flexibility distribution along the members and the rigid zones at the ends of each member. During the dynamic analysis, the force deformation relationship of each critical section is traced by the three parameter hysteretic model shown in figure 5.1, in which stiffness degradation, strength deterioration, and pinching behavior are controlled by the three parameters α, β, and γ, respectively. With the proper selection of these parameters, the response of different reinforced concrete elements can be simulated. The monotonic loading behavior of reinforced concrete is described by the tri-linear envelope shown in figure 5.2, in which the two break points correspond to the cracking and the yielding moments of the section. The additional load capacity due to the reinforcement strain hardening is represented by the additional strength beyond the yield point. More information on the structural modeling can be found in references [16,18].

5.3 2-Story model analysis

5.3.1 Input data

The input information of program IDARC used to perform the seismic test simulation is summarized in the following data sets:

1. Structure configuration

The model structure (figure 5.3) is composed of two one-bay by 2-story identical frames with a centerline to centerline span of 24", and a story height of 18". A total weight of 1.21 and 0.82 kips was assigned to the first and the second stories respectively for the dynamic analysis.

2. Material information

One type of concrete was used for all members, where the measured microconcrete properties defined in figure 5.4. A reduced modulus of elasticity of $E_{0.45fc'}$= 1400 ksi was used to account for the effect of concrete cracking due to the static loads and shrinkage. For the steel reinforcement, a yield stress of f_y= 40 ksi and a Young's modulus E_s= 29,000 ksi were adopted. The strain hardening portion of the steel stress-strain curve was assumed to start at a 3% strain and a strain hardening modulus of E_{sh}= 500 ksi was used beyond that point (figure 5.5).

3. Element information

All columns had the same cross section of 1.33" x 2.0" and a clear span of 15.33". The

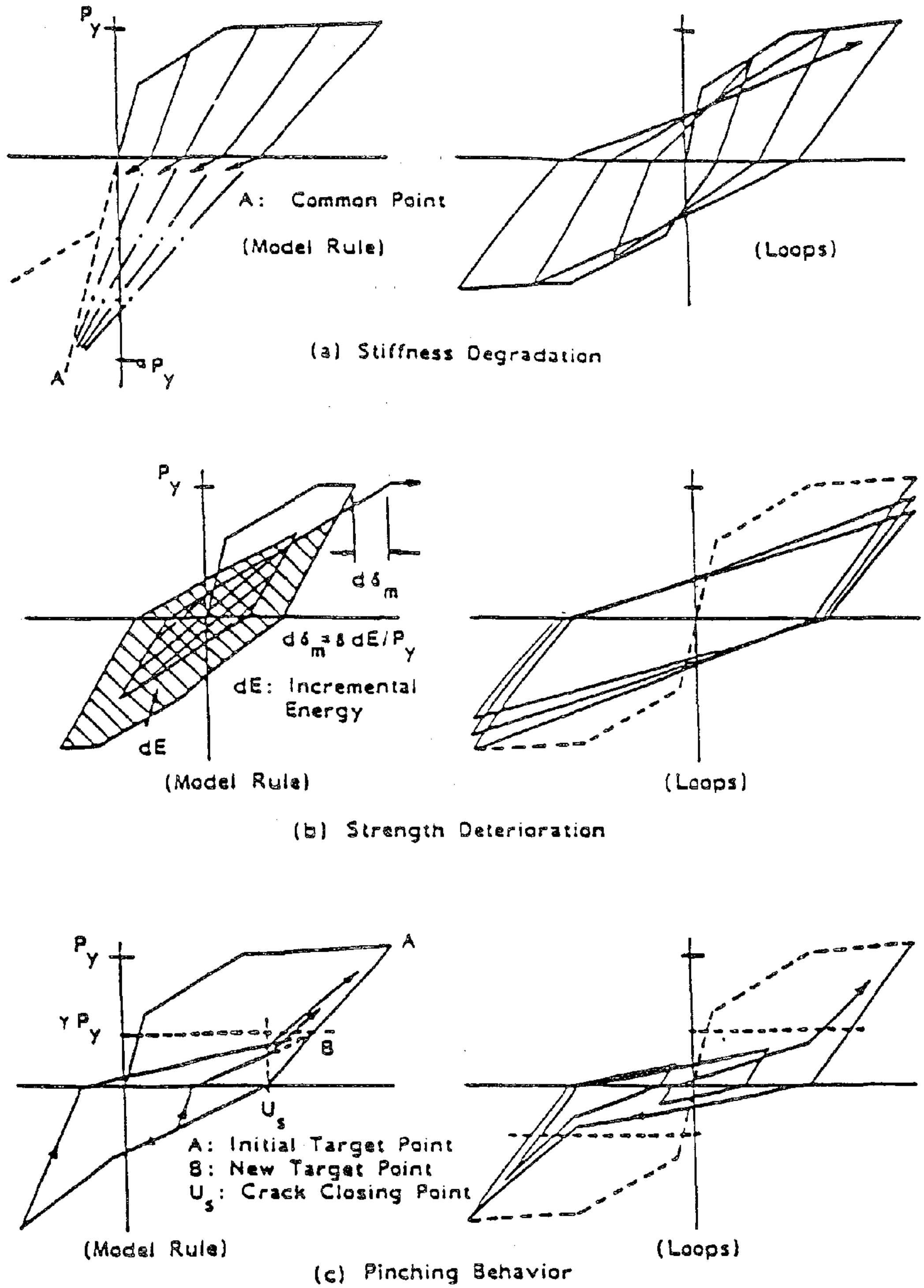

Figure 5.1: Three Parameter Model Used in Program IDARC [Park et.al 1987].

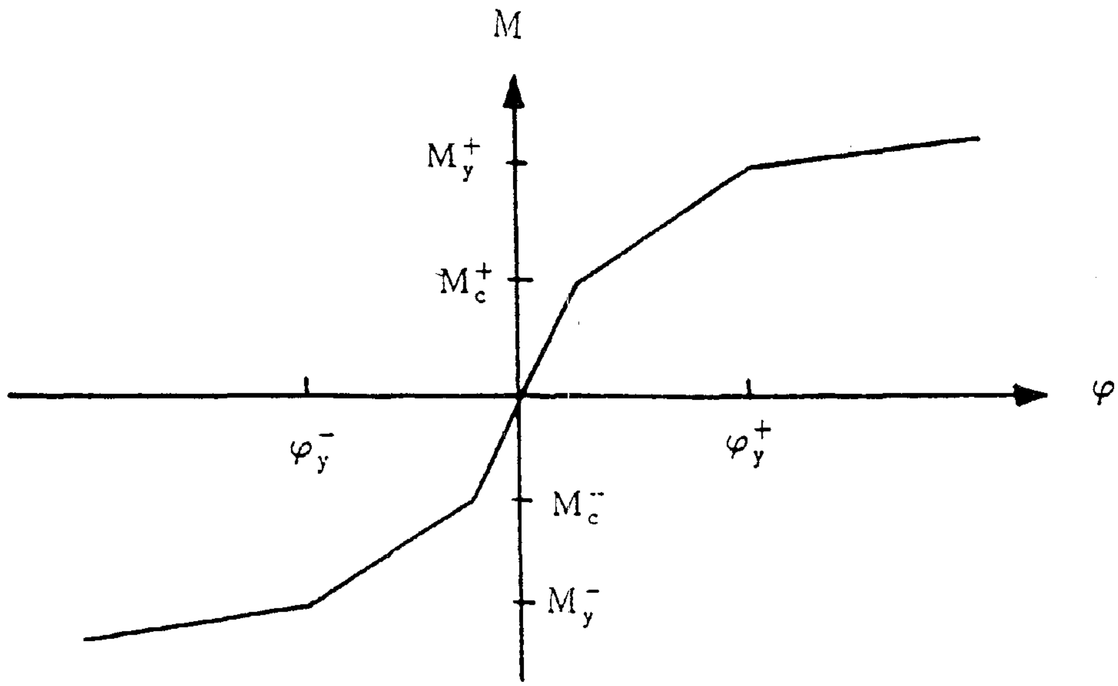

Figure 5.2: Tri-linear Envelope Curve [Reinhorn et.al 1989].

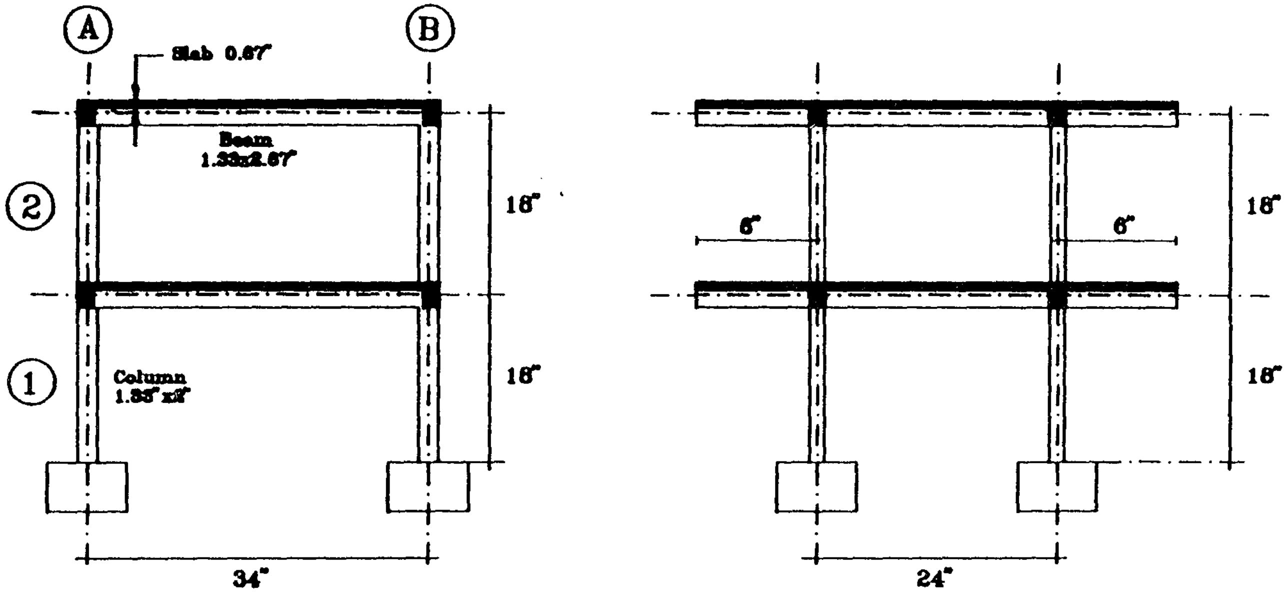

(a) Elevation.

(b) Side View.

Figure 5.3: General Layout of The 2-Story Model.

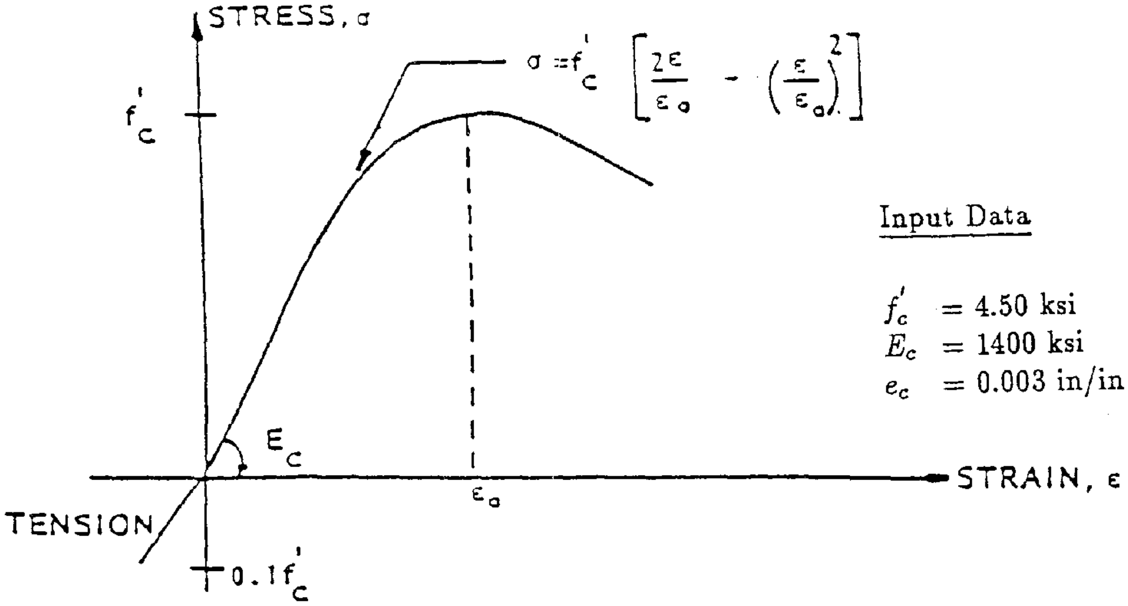

Figure 5.4: Idealized Microconcrete Stress-Strain Curve [Park et.al 1987].

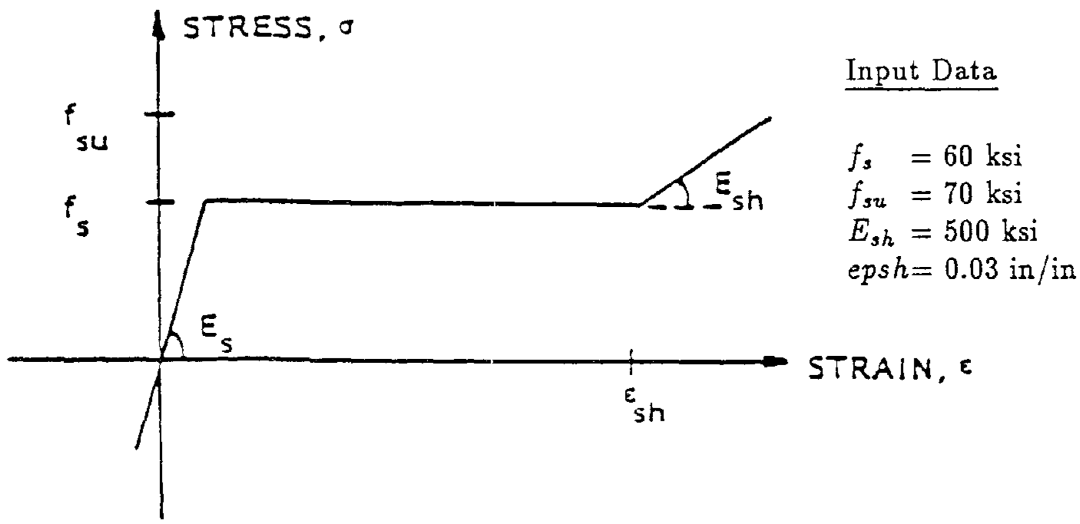

Figure 5.5: Idealized Steel Reinforcement Stress-Strain Curve (Park et.al 1987].

column reinforcement and confinement ratios were obtained from figure 3.7. Beams had a common cross section of 1.33" x 2.67" and a 32" clear span. Tee sections had a slab thickness of 0.67" and an effective width of span/4= 5.5".

Both web and slab reinforcement are illustrated in figure 3.7. Since program IDARC requires the static reactions on each member, an elastic analysis was conducted using program STRAND-2D [20] to obtain the axial forces on the columns and the bending moments at each beam end.

4. Dynamic analysis information

The measured table accelerations were used as the input ground motion to eliminate any error in the calculated response due to the differences between the required and the measured acceleration traces. The first mode damping ratio obtained from the free-vibration test performed prior to the seismic tests was used in the analysis. Based on the values recommended in references [17] and [18], the three parameters α, β, and γ were taken equal to 2.0, 0.05, and 1.0 respectively. It should be kept in mind that these parameters were based on prototype tests, and not on small scale models that have properties resembling those of the present model. Also, these parameters do not account for the positive beam steel pull-out.

The same data was used for run Taft 0.26g-2, but with two exceptions: (1) the concrete modulus of elasticity was modified to 0.5 $E_{0.45fc'}$= 1000 ksi to account for the stiffness reduction caused by run Taft 0.26g-1, and (2) the ground acceleration trace measured at the shake table surface during that run was used as input.

5.4 2-Story Model Analysis

5.4.1 Run Taft 0.26-G-1

The computed story shears are plotted against the measured shears in figures 5.6.a and 5.6.b for the first and the second stories respectively. It can be seen from both figures that the computed shears were significantly less than the measured shears. The computed base shear recorded a maximum value of 0.576 kips, which was 61% of the measured value of 0.943 kips. The same observation was true for the second story where the maximum computed shear of 0.318 kips represented only 66% of the maximum measured value of 0.484 kips. Figures 5.7.a and 5.7.b show the computed story displacements during this run. The two figures indicate the

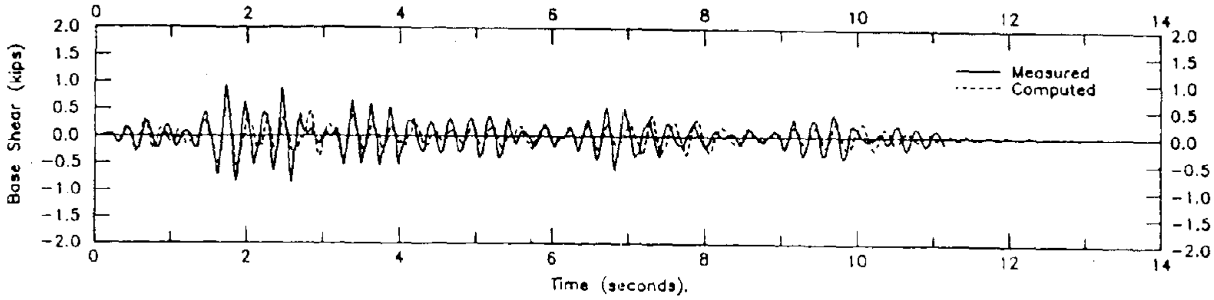

(a) Base Shear.

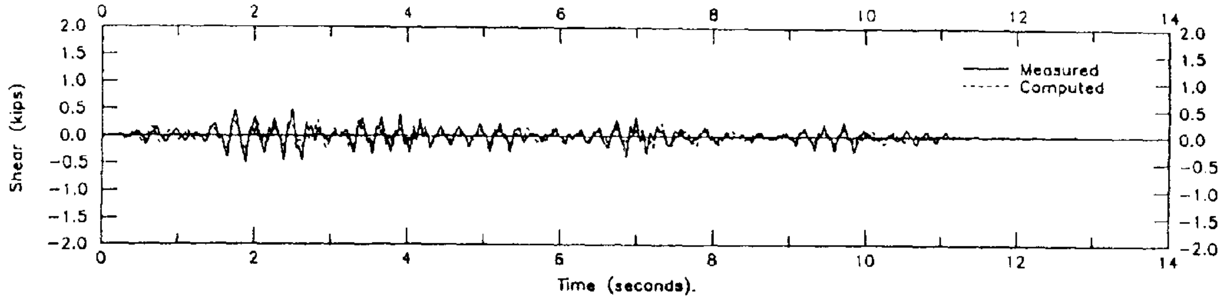

(b) Second Story.

Figure 5.6: Computed Versus Measured Story Shears (Run Taft 0.26-G-1).

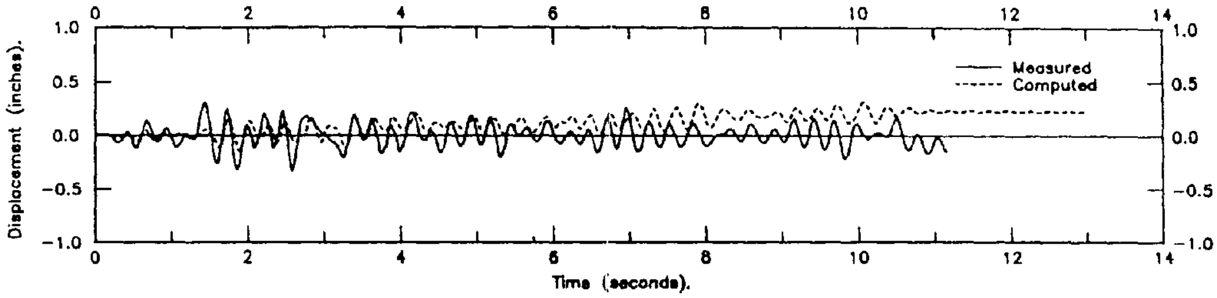

(a) First Story.

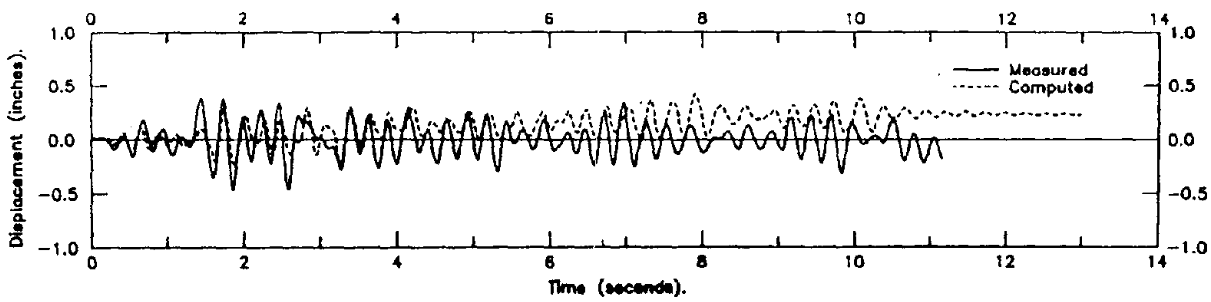

(b) Second Story.

Figure 5.7: Computed Versus Measured Story Displacements (Run Taft 0.26-G-1).

large drift caused by accumulated numerical errors.

The lack of correlation between the analytical and the experimental results for the current case could be attributed to the fact that the column moment-normal force interaction, which is believed to play an important role in the present building response, was ignored in the analysis. The program relies only on the static reactions given at the beginning of the analysis and assumes that they will not change during the earthquake. This approach may be acceptable for buildings with extremely low height to length ratio, but is not for the current type of buildings.

Another factor that may have contributed to the aforementioned discrepancy is neglecting the P-Δ effect which was proven from other Cornell tests to be of vital importance in the analysis of this type of buildings.

5.4.2 Run Taft 0.26-G-2

The analysis performed for the Taft 0.26-G-2 resulted in the same conclusions of the previous run where the story shears (figure 5.8) was highly under-estimated, and the story displacements (figure 6.9) showed large drift.

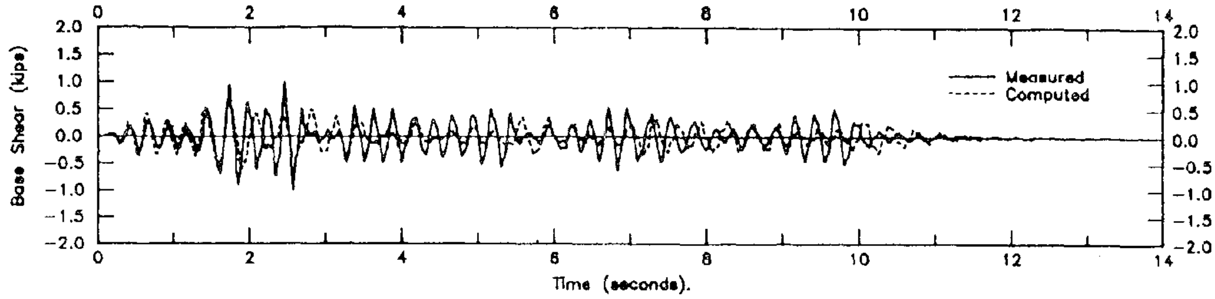

(a) Base Shear.

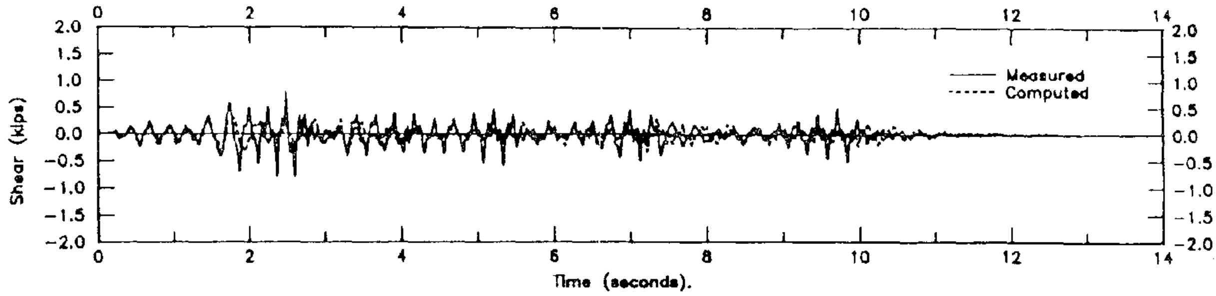

(b) Second Story.

Figure 5.8: Computed Versus Measured Story Shears (Run Taft 0.26-G-2).

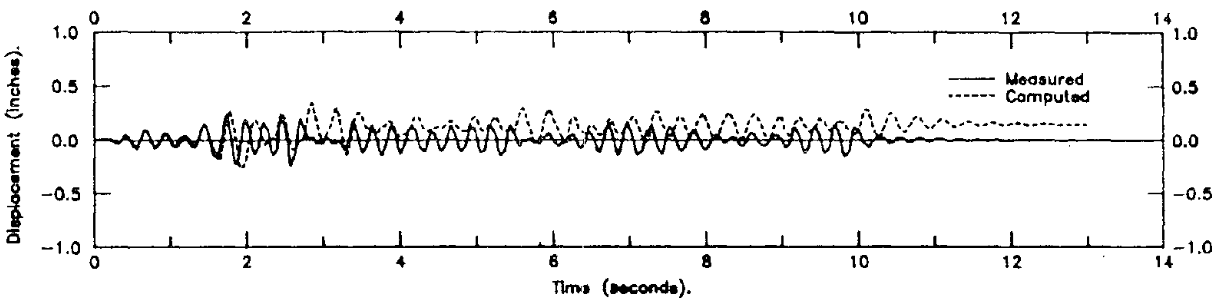

(a) First Story.

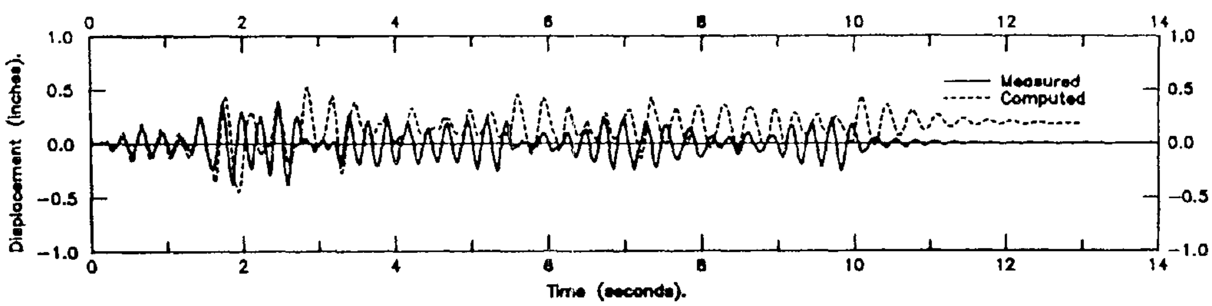

(b) Second Story

Figure 5.9: Computed Versus Measured Story Displacements (Run Taft 0.26-G-2).

CHAPTER 6
SUMMARY AND CONCLUSIONS

6.1 Summary

6.1.1 Experimental work

A 1/6 scale one-bay by one-bay by two story office building was tested on the Cornell University shake table. The model was designed for gravity loads only and detailed in such a way to reflect as closely as possible the common design practice during the 1940-1970 period. The model contained no walls or partitions. Experimental results are summarized in the following section.

Test results

The 2-story model building was tested using the Taft 1952 S69E recorded ground motion at peak accelerations of 0.26g, 0.36g, 0.45g, 0.75g, and 0.90g. The behavior of the bare frame during these runs can be summarized in the following points:

1. The building response was dominated by the first mode of vibration during all seismic tests.
2. The model experienced very large deformations associated with severe stiffness degradation even during the low amplitude runs.
3. Hinging zones formed in the columns outside the joint panels, and not in the beams.
4. Column lap splices (location and reinforcement details) did not form a potential source of damage to the columns.
5. Most of the deformation and energy dissipation took place in the first story columns.
6. Column cracks were concentrated at the top and bottom construction joints.
7. Discontinuous positive beam reinforcement pullout was detected after run Taft 0.45 g, causing a significant reduction in the model stiffness.
8. The high model flexibility prevented the formation of a complete failure mechanism. Maximum base shear was reached at the 0.75 g-1 run (1.307 kips) and decreased sharply to 0.569 kips at the 0.90 g run.

6.2 Analytical results

The non-linear dynamic analysis for reinforced concrete program IDARC [18] was used to predict the response of the model buildings. The input data included geometric information, material properties, hysteretic rules parameters, and the ground motion (measured table acceleration). The findings of the analysis can be summarized in the following points:

1. A poor correlation between the experimental and the analytical global responses was obtained for the 2-story model test. This was attributed to (a) ignoring the overturning moment, and (b) neglecting the P-Δ effect.

2. The effect of the continuously changing axial forces in the columns was not taken into account when evaluating the yield status of the columns. IDARC recognizes only the initial static axial forces in the analysis. This is expected to misrepresent the exterior column behavior where large axial force changes might occur.

3. The effective slab width was found to be of vital importance in the analysis since it can directly affect the structure failure mechanism by increasing beam flexural strength to the point that column behavior governs.

6.3 Conclusions

The experimental work presented in this report is the first to address the performance of lightly reinforced concrete buildings tested under realistic seismic loading conditions. Test results of the 2-story model building revealed many important aspects of the behavior of such buildings during earthquakes. Based on the current experimental results and the analytical study, the following conclusions may be drawn:

1- Although the inadequate reinforcement details of lightly reinforced concrete structures may form a potential source of damage, they are probably not sufficient to develop a local failure mechanism under moderate earthquake forces. In fact, a large increase in the structure period might shift it to a descending part on the response spectrum of the given ground motion, resulting in a reduction in the level of lateral forces.

2. The currently existing lightly reinforced concrete (LRC) buildings may be subjected to very large deformations associated with a significant reduction in stiffness during a moderate earthquake.

3. Due to their high flexibility, the P-Δ effect is significant in LRC structures and should be considered in the analysis.

4. Low and medium height LRC buildings most likely will collapse in a soft-story mechanism due to the higher flexural strengths of beams with respect to the columns. The situation is aggravated by the very low ductility of these columns caused by their high axial forces and poor confinement of primary longitudinal reinforcement.

5. Small-scale reinforced concrete models can be used as a powerful tool to study the performance of complete buildings or large subassemblies.

CHAPTER 7
REFERENCES

1. ACI Committee 318, "Building Code Requirements for Reinforced Concrete," American Concrete Institute, Detroit 1989.

2. ACI-ASCE Committee 352, "Recommendations for Design of Beam-Column Joints in Monolithic Reinforced Concrete Structures," ACI Structural Journal Vol. 86, No. 2/ May-June 1985.

3. Blondet, J.M., "Studies on Evaluation of Shaking Table Response Analysis Procedures", Report No. UCB/EERC-81/18,November 1981.

4. Blondet, J.M., Clough, R.W., and Mahin, S.A., "Evaluation of A Shaking Table Test Program on Response Behavior of A Two Story Reinforced Concrete Frame," Earthquake Engineering Research Center, University of California/ Berkeley, California. Report No. UCB/EERC-80/42.

5. Brigham, Oran E. ,"The Fast Fourier Transform", Prentice-Hall, Inc., 1974.

6. ENDEVCO CORPORATION/ DYNAMIC INSTRUMENTS DIVISION, "Instruction Manual For ENDEVCO Peizoresistive Accelerometers", September 1978.

7. Harris, H.G., Sabnis, G.M., White, R.N., "Reinforcement for Small Scale Direct Models of Concrete Structures," Models for Reinforced Concrete Structures, SP-24, American Concrete Institute, Detroit, 1970, pp. 141-158.

8. Harris, H.G., Sabnis, G.M., White, R.N., "Small Scale Direct Models of Reinforce and Prestressed Concrete Structures," Report No.326, Department of Structural Engineering, Cornell University,Ithaca, N.Y., September 1966.

9. Hwang, J.S., Chang, K.C., Lee, G.C. ,"The System Characteristics And Performance of a Shake Table", Technical Report NCEER-87-0004, June 1, 1987.

10. Kim,W., El-Attar, A., and White, R.N. ,"Small-Scale ModeLing Techniques For Reinforced Concrete Structures Subjected To Seismic Loads", National Center for Earthquake Engineering Research. Technical Report NCEER-88-0041, November 22, 1988.

11. Lund, R., "Environmental Simulation With Digitally Controlled Servo- Hydraulics ", Institute of Environmental Science, Philadelphia, 1976.

12. Micro-Measurements Division, Catalog 500/Part A ,"Strain Gage Listing", Measurements Group Inc., P.O. Box 27777, Nc (1989).

13. MTS SYSTEMS CORPORATION/ MACHINE CONTROLS DIVISION, "Temposonics TM Linear Transducer System With Analog Output/ Installation and Instruction Manual", 1989.

Nilson, A.H., and Winter G., "Design of Concrete Structures",Tenth Edition, McGraw-Hill Book Company, New York 1986.

15. Sabnis, G.M., Harris, H.G., White, R.N., and Mirza, M.S.,"Structural Modeling And Experimental Techniques", Prentice-Hall Inc., Engelwood Cliff, New Jersey, 1983.

16. Reinhorn, A.M., Seidel, M.J., Kunnath, S.K., and Park, Y.J.,"Damage Assessment of Reinforced Concrete Structures In Eastern United States", National Center for Earthquake Engineering Research. Technical Report NCEER-88-0016, June 15, 1989.

17. Park, Y.J., Ang, A.H-S., and Wen, Y.K., "Seismic Damage Analysis and Damage-Limiting Design of R/C Buildings", Civil Engineering Studies, SRS No. 516, University of Illinois, Urbana, October 1984.

18. Park, Y.J., Reinhorn, A.M., and Kunnath, S.K., "IDARC: Inelastic Damage Analysis of Reinforced Concrete Frame-Shear-Wall Structures", National Center for Earthquake Engineering Research. Technical Report NCEER-87-0008, July 20, 1987.

19. Pessiki S.P., Conley, C.H., Gergely, P., and White, R.N., "Seismic Behavior of Lightly-Reinforced Concrete Column and Beam-Column Joint Details", National Center for Earthquake Engineering Research. Technical Report NCEER-90-0014, August 27, 1990.

19. STRAND-2D, A Program for STRuctural ANalysis and Design of Two dimensional Plane Frame Structures, Group 2000 Engineering Corp., 3520 Long Beach Boulevard, Long Beach, California 90807.

20. William, G.H., and David, L.B., "Impulse Technique for Structural Frequency Response Testing", Sound and Vibration, Nov. 1977, pp. 8-21.

21. Housner, G.W. and Jennings, P.C., "The Capacity of Extreme Earthquake Motion to Damage Structures," Structural and Geotechnical Mechanics, a Volume Honoring Nathan Newmark, edited by J.W. Hall, Prentice Hall, New Jersey, 1977.

Appendix A

2-Story Prototype Building Design

A.1 Design Loads

The prototype 2-story building (figure 3.1) was designed for gravity loads of self weight, and live loads of 50 psf for the first floor and 20 psf for the roof. Detailed design loads are given in table A.1.

A.2 Load Distribution on Girders

Slab is continuous in the transverse direction (12 ft span) and simply supported in the longitudinal direction (17 ft span) (figure A.1).

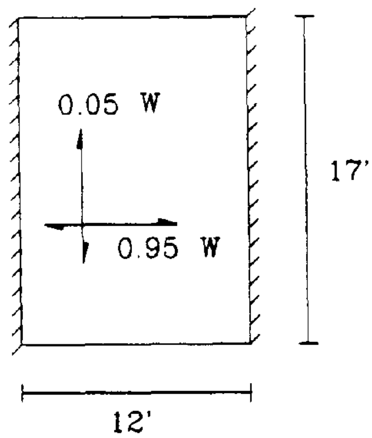

Figure A.1: Slab Load Distribution.

Aspect ratio $= \frac{12}{17} = 0.7$

$W_l = 0.95 \times 12 \times W = 11.4$ W

$W_t = 0.05 \times 8.5 \times W = 0.425$ W

Load on longitudinal girders;

Self weight $= 0.15 \times \frac{8\times12}{144} = 0.1$ kip/ft

Bottom story girder;

Dead load $= W_D = 11.4 \times 0.052 + 0.14 + 0.10 = 0.833$ k/ft

Live load $= W_L = 11.4 \times 0.050 = 0.57$ k/ft

Table A.1: Loads on Prototype 2-Story Building

Item	Bottom story	Top story
Dead load		
Slab (4 inches thick)	0.050 k/ft^2	0.050 k/ft^2
Ceiling (10 $lb/ft^3 \times 1.2"$)	0.001 k/ft^2	0.001 k/ft^2
Roofing	—	0.010 k/ft^2
Exterior Wall on transverse		
girders (Hollow brick wall)	0.200 k/ft	—
Glass	0.007 k/ft	—
Permanent wall on		
longitudinal girders	0.140 k/ft	—
Weight of columns and		
girders for both stories	9.5 kips	—
Live Load	0.050 k/ft^2	0.020 k/ft^2

Top story girder;

$$W_D = 11.4 \times 0.061 + 0.1 = 0.794 \text{ k/ft}$$

$$W_L = 11.4 \times 0.02 = 0.228 \text{ k/ft}$$

Load on transverse girders;

Bottom story;

$W_D = 0.425 \times 0.052 + 0.207 + 0.10 = 0.329$ k/ft

$W_L = 0.425 \times 0.050 = 0.021$ k/ft

Top story;

$W_D = 0.425 \times 0.061 + 0.10 = 0.126$ k/ft

$W_L = 0.425 \times 0.02 = 0.0085$ k/ft

A.3 Design Load Cases

The building was designed for the load cases shown in figure A.2.

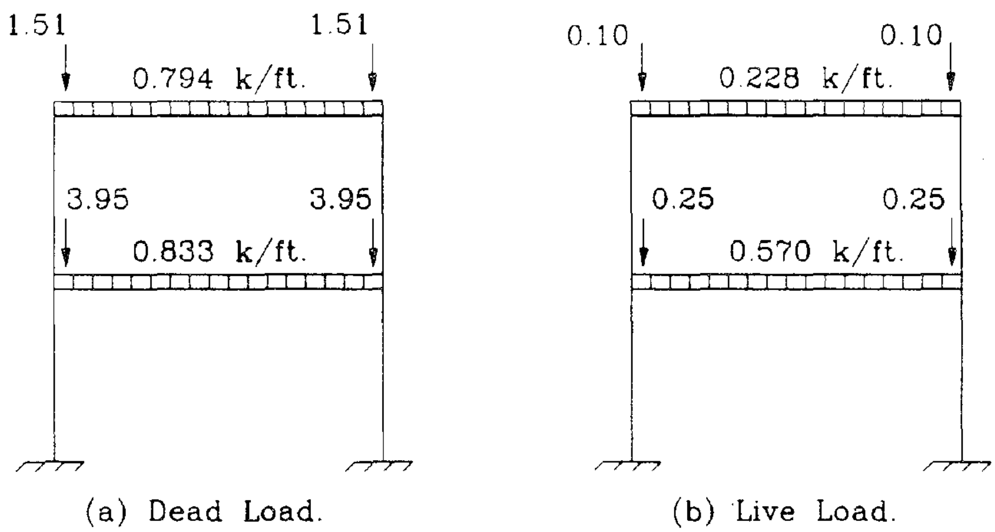

Figure A.2: Design Load Cases.

A.4 Relative Member Stiffness

Column: (8" × 12")

$I_{col} = \frac{8\times 12^3}{12} = 1152\ in^4$

Beam: (8" × 16")

Span length = 17' (204 in.)

Effective width = C.L. to C.L. distance = 72 in

= span / 4 = 51.0 in. (governs)

= 8 + 16 × 4 = 72 in.

I_{beam} = 5602 in^4 (figure A.3)

$\frac{I_{beam}}{I_{col.}} = \frac{5602}{1152} = 4.863$

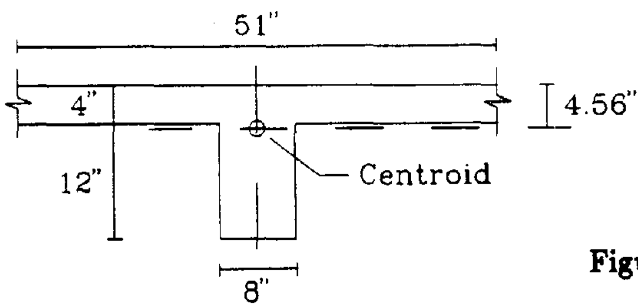

Figure A.3: Longitudinal Beam Cross Section.

A.5 Stress Resultants

The bending moment, shearing force and normal force diagrams of the main supporting frame (in the direction of motion) are shown in figure A.4. Critical sections of the frame (figure A.5) were designed using a load combination of (1.4 D.L.+ 1.7 L.L.) presented in table A.2.

A.6 Design of Members

Assume f_y = 40 ksi f'_c = 4 ksi

E_s = 29,000 ksi $E_c = 57000\sqrt{4000}$ = 3,610 ksi

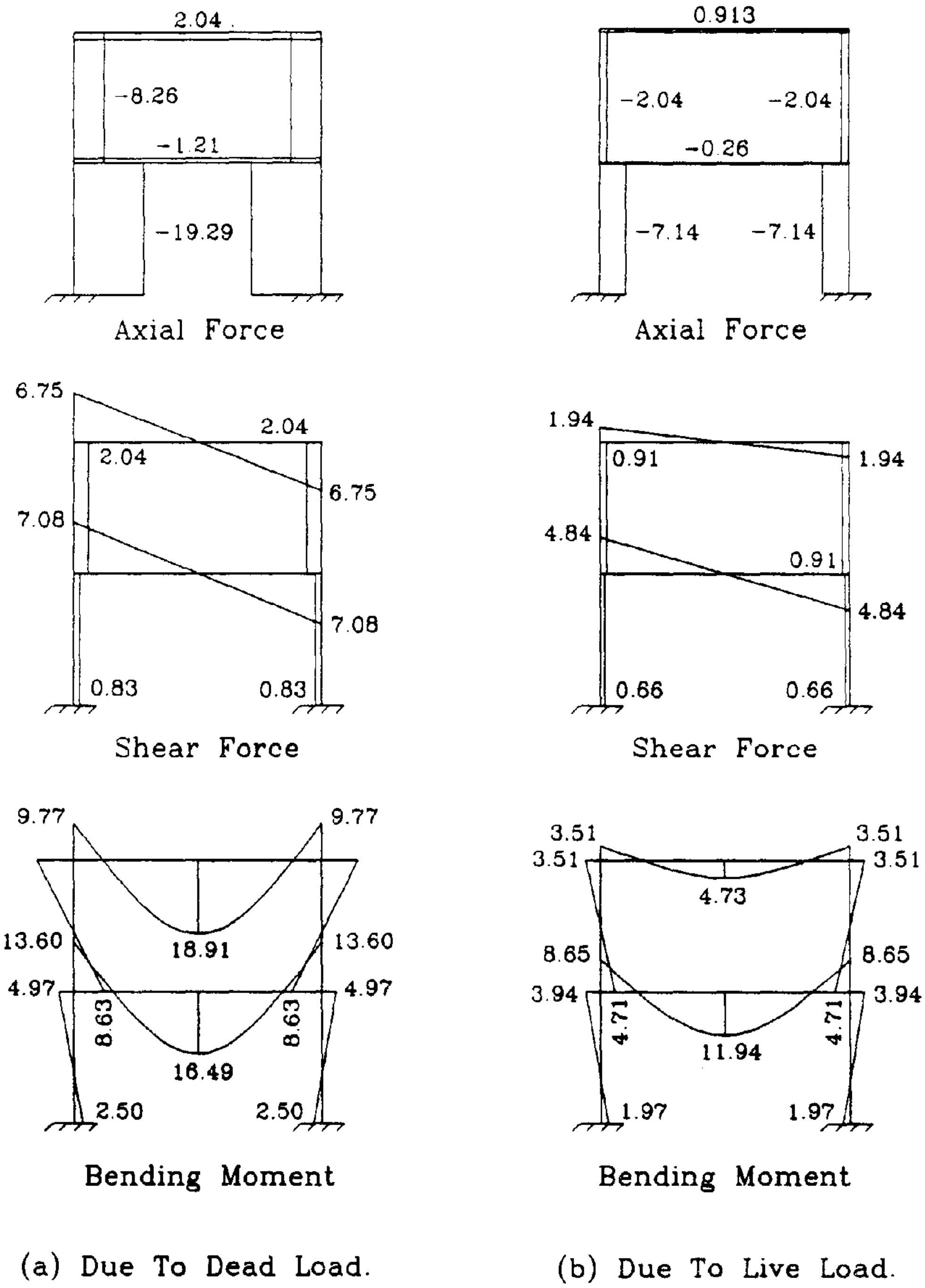

Figure A.4: Stress Resultants on The Main Frame.

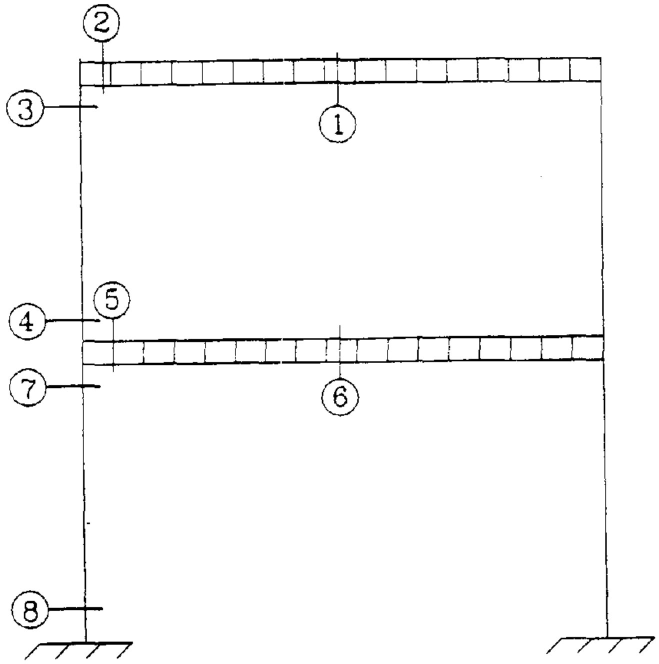

Figure A.5: Main Frame Critical Sections.

Table A.2: Design Loads

Section	Moment			Shear			Normal		
	D.L.	L.L.	Ult.	D.L.	L.L.	Ult.	D.L.	L.L.	Ult.
1	18.91	4.73	34.5	—	—	—	—	—	—
2	9.77	3.51	19.65	6.75	1.94	12.75	—	—	—
3	9.77	3.51	19.60	2.04	0.91	4.41	8.26	2.04	15.53
4	8.63	4.71	20.10	2.04	0.91	4.41	8.26	2.04	15.53
5	13.61	8.65	33.80	7.08	4.84	18.14	—	—	—
6	16.49	11.94	43.40	—	—	—	—	—	—
7	5.00	3.94	13.70	0.83	0.66	2.28	19.29	7.14	39.14
8	2.50	1.97	6.80	0.83	0.66	2.28	19.29	7.14	39.14

A.6.1 Bottom Story Column:

A typical column cross section is shown in figure A.6.

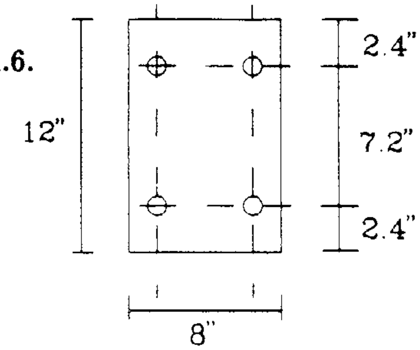

Figure A.6: Typical Column Cross Section.

Strong axis;

P_u = 39.14 kips

M_2 = 13.70 k.ft

M_1 = 6.80 k.ft

$I_{cr_{beam}} = 5602\ in^4$

$I_{cg} = \frac{8\times12^3}{12} = 1152\ in^4$

l_u = 108"

$\psi_A = \frac{\sum EI_{col}/l_u}{\sum EI_b/l_n} = \frac{2\times1152\times17}{5602\times9} = 0.78$

For a fixed base assume that $\psi_B = 1.0$

K = 1.4 (conservatively estimated)

r = 0.3 h = 3.6

$\frac{Kl_u}{r} = 42 > 22$

C_m = 1.0 (unbraced column)

$M_{D.L}$ = 7.0 k'

$M_{L.L}$ = 6.7 k'

$\beta_d = \frac{7}{7+6.7} = 0.78$

$EI = \frac{1152\times3600}{2.5\times1.511} = 1100\times10^3\ kips.in^2$

$P_{cr} = \frac{\pi^2\times1100}{1.4\times l_u} \times 10^3 = 475$ kips

Weak axis;

$I_g = \frac{12\times8^3}{12} = 512\ in^4$

$EI_g = \frac{512\times3600}{2.5\times1.511} = 488\times10^3\ in^2$

$P_{cr} = \frac{\pi^2\times488\times10^3}{1.4\times108^2} = 184$ kips

Magnification factor

$\delta \quad = \frac{1}{1-\frac{39.14}{0.7\times 475}} = 1.13$

M $\quad = 1.13 \times 13.7 = 15.53$ k'

$A_{s_{min}} \quad = 0.01$ b.d $= 0.768\ in^2$

Use $A_s = A'_s = 2\#6\ (0.44\ in^2)$

<u>Check;</u>

e = $\frac{15.53}{39.14}$ = 0.4' = 4.76" e'= 4.76 + 3.6 = 8.36"

$P_n \quad = 27.2\text{ a} - 3.009 \qquad (1)$

$8.36\ P_n = 27.2\text{ a }(9.6 - \text{a}/2) + 233.22 \qquad (2)$

From equations 1 and 2;

a $\quad$ = 5.77"

$P_n \quad = 108$ kips

<u>Design for shear;</u>

$V_c \quad = b_w \cdot d \cdot (1.9\sqrt{f'_c} + 2500\ \rho_\omega . \frac{V_u \cdot d}{M_m}) \qquad$ (ACI eqn. 11.6)

$M_m \quad = M_u - N_u \cdot \frac{4h-d}{8} \qquad$ (ACI eqn. 11.7)

$M_u \quad = 13.7$ k'

$N_u \quad = 39.14$ kips

$V_u \quad = 2.28$ kips

$M_u \quad = 13.7 - 39.14\ (\frac{4\times 12 - 9.4}{12\times 8}) = -2.04$

For members under axial compression N_u use the equation;

$V_c \quad = 3.5\sqrt{f'_c}\ b_w \cdot \text{d} \cdot \sqrt{1 + \frac{N_u}{500 \cdot A_g}} \qquad$ (ACI eqn. 11.8)

$V_c \quad = 3.5\sqrt{4000} \times 8 \times 9.6 \times \sqrt{1 + \frac{39140}{500\times 8\times 12}}$

$V_c \quad = 22.9 \text{ kips} > \frac{V_u}{\phi}$

$V_n \quad > 0.5\ \phi V_c$ (no shear reinforcement is required)

According to ACI code section 7.10.5.1, use minimum shear reinforcement of ♯3 bars at maximum spacing S given by;

S $\not>$ 16 × 0.75 $\not>$ 12"

S $\not>$ 48 × 0.375 $\not>$ 18"

S $\not>$ least dimension of the member $\not>$ 8" (governs)

Use ♯3 bars at 8" spacing all over the column length.

A.6.2 Top Story Column

$\frac{kl_u}{r}$ $= 66 > 22$

β_d $= 0.6$

EI $= \frac{3610 \times 512}{2.5 \times 1.6} = 462 \times 10^3$

P_{cr} $= \frac{\pi^2 \times 462 \times 10^3}{(1.4 \times 108)^2}$

$= 199$ kips

ϕ $= 0.70$

P_u $= 12.75$

δ $= \frac{1}{1 - \frac{12.75}{0.7 \times 199}} = 1.10$

P_b $= 106$ kips > 12.75 (tension failure)

M_u $= 20.1$ k'

V_u $= 4.41$ kips

P $= 12.75$ kips

M_c $= 1.1 \times 20.1 = 22.11$

e $= \frac{22.11}{12.75} \times 12 = 20.8$"

e' $= 20.8 + 3.6 = 24.41$"

$\frac{e'}{d}$ $= 2.543$"

$$P_u = 0.7 \times 0.85 \times 8 \times 9.6 \times -\rho + 1 - 2.543$$
$$+ \sqrt{1.543^2 + 2\rho(10.76 \times 0.75 + 2.543)}$$

$$= 182.78 \times (-\rho - 1.543 + \sqrt{2.38 + 21.23 \times \rho})$$

For $\rho \;\; = 0.0115 \rightarrow P_u = 11.96$ kips

Use 4♯7 $\rho = 0.0125 \rightarrow P_u = 13$ kips

For shear reinforcement, use ♯3 at 8" spacing.

A.6.3 Bottom Story Girder

M = 33.8 k'

b = 8"

From equilibrium (figure A.7); $\quad 0.85 \times 4000 \times a \times 8 = A_s \times 40{,}000 \qquad (1)$

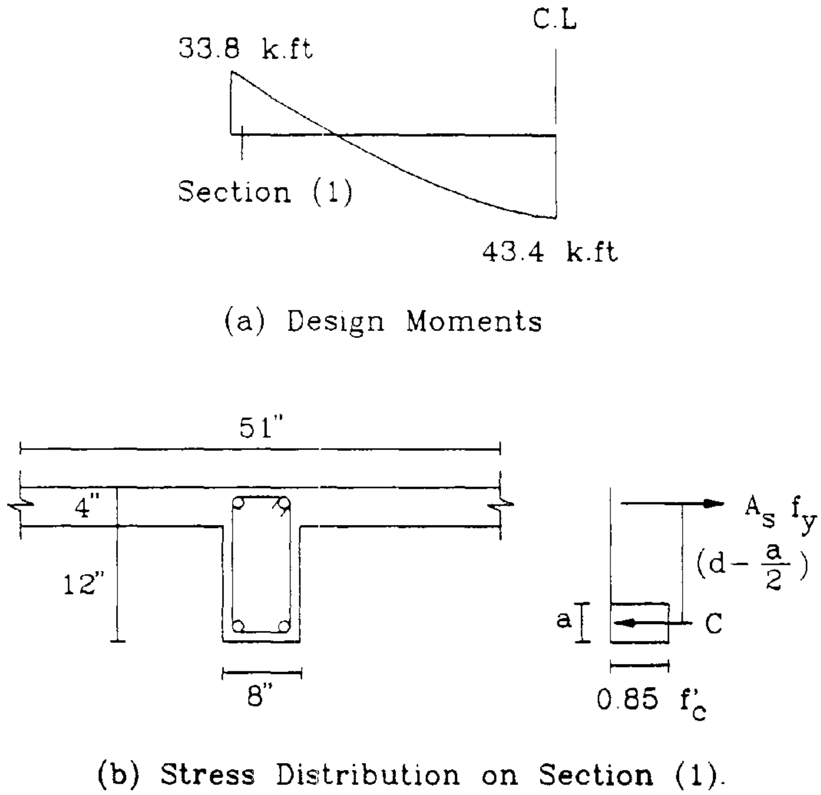

(a) Design Moments

(b) Stress Distribution on Section (1).

Figure A.7: Design of The Negative Moment Section of The Bottom Story Longitudinal Beam.

$A_s \times 40,000 \times (13.6 - \frac{a}{2}) = 33.8 \times 12,000$ (2)

From equations (1) and (2);

$A_s = 0.79\ in^2 = 2\sharp 6$

Development length $L_d = 30$ dia. $= 22.5"$.

Mid. section:

$A_s \times 40 \times (13.6 - \frac{4}{2}) = \frac{43.4 \times 12}{0.9}$

$A_s \quad = 1.125\ in^2 \rightarrow 2\sharp 7\ (A_s = 1.2\ in^2)$

Shear design:

$V_u \quad = 18.17$ kips

$\phi \times V_c = 0.85 \times 2\sqrt{4000} \times 13.6 \times 8 = 11.7$ kips

$A_v \quad = (\frac{V_U - \phi V_c}{\phi f_y})(\frac{S}{d})$

$\quad = (\frac{18.17 - 11.7}{0.85 \times 40})(\frac{6}{13.6}) = 0.084 \rightarrow$ stirrup $\sharp 3$

Maximum spacing of the stirrups is given by:

S $\quad \not> \frac{d}{2} \not> \frac{13.6}{2} \not> 6.8"$ (governs)

S $\quad \not> \frac{A_v \times f_y}{50 \times b_w} \not> \frac{0.22 \times 40,000}{50 \times 8} \not> 22"$

Use $\sharp 3$ stirrups at 6" spacing.

The design of the top and transverse beams was carried out in a similar fashion.

NATIONAL CENTER FOR EARTHQUAKE ENGINEERING RESEARCH
LIST OF TECHNICAL REPORTS

The National Center for Earthquake Engineering Research (NCEER) publishes technical reports on a variety of subjects related to earthquake engineering written by authors funded through NCEER. These reports are available from both NCEER's Publications Department and the National Technical Information Service (NTIS). Requests for reports should be directed to the Publications Department, National Center for Earthquake Engineering Research, State University of New York at Buffalo, Red Jacket Quadrangle, Buffalo, New York 14261. Reports can also be requested through NTIS, 5285 Port Royal Road, Springfield, Virginia 22161. NTIS accession numbers are shown in parenthesis, if available.

NCEER-87-0001 "First-Year Program in Research, Education and Technology Transfer," 3/5/87, (PB88-134275/AS).

NCEER-87-0002 "Experimental Evaluation of Instantaneous Optimal Algorithms for Structural Control," by R.C. Lin, T.T. Soong and A.M. Reinhorn, 4/20/87, (PB88-134341/AS).

NCEER-87-0003 "Experimentation Using the Earthquake Simulation Facilities at University at Buffalo," by A.M. Reinhorn and R.L. Ketter, to be published.

NCEER-87-0004 "The System Characteristics and Performance of a Shaking Table," by J.S. Hwang, K.C. Chang and G.C. Lee, 6/1/87, (PB88-134259/AS). This report is available only through NTIS (see address given above).

NCEER-87-0005 "A Finite Element Formulation for Nonlinear Viscoplastic Material Using a Q Model," by O. Gyebi and G. Dasgupta, 11/2/87, (PB88-213764/AS).

NCEER-87-0006 "Symbolic Manipulation Program (SMP) - Algebraic Codes for Two and Three Dimensional Finite Element Formulations," by X. Lee and G. Dasgupta, 11/9/87, (PB88-219522/AS).

NCEER-87-0007 "Instantaneous Optimal Control Laws for Tall Buildings Under Seismic Excitations," by J.N. Yang, A. Akbarpour and P. Ghaemmaghami, 6/10/87, (PB88-134333/AS).

NCEER-87-0008 "IDARC: Inelastic Damage Analysis of Reinforced Concrete Frame - Shear-Wall Structures," by Y.J. Park, A.M. Reinhorn and S.K. Kunnath, 7/20/87, (PB88-134325/AS).

NCEER-87-0009 "Liquefaction Potential for New York State: A Preliminary Report on Sites in Manhattan and Buffalo," by M. Budhu, V. Vijayakumar, R.F. Giese and L. Baumgras, 8/31/87, (PB88-163704/AS). This report is available only through NTIS (see address given above).

NCEER-87-0010 "Vertical and Torsional Vibration of Foundations in Inhomogeneous Media," by A.S. Veletsos and K.W. Dotson, 6/1/87, (PB88-134291/AS).

NCEER-87-0011 "Seismic Probabilistic Risk Assessment and Seismic Margins Studies for Nuclear Power Plants," by Howard H.M. Hwang, 6/15/87, (PB88-134267/AS).

NCEER-87-0012 "Parametric Studies of Frequency Response of Secondary Systems Under Ground-Acceleration Excitations," by Y. Yong and Y.K. Lin, 6/10/87, (PB88-134309/AS).

NCEER-87-0013 "Frequency Response of Secondary Systems Under Seismic Excitation," by J.A. HoLung, J. Cai and Y.K. Lin, 7/31/87, (PB88-134317/AS).

NCEER-87-0014 "Modelling Earthquake Ground Motions in Seismically Active Regions Using Parametric Time Series Methods," by G.W. Ellis and A.S. Cakmak, 8/25/87, (PB88-134283/AS).

NCEER-87-0015 "Detection and Assessment of Seismic Structural Damage," by E. DiPasquale and A.S. Cakmak, 8/25/87, (PB88-163712/AS).

NCEER-87-0016 "Pipeline Experiment at Parkfield, California," by J. Isenberg and E. Richardson, 9/15/87, (PB88-163720/AS). This report is available only through NTIS (see address given above).

NCEER-87-0017 "Digital Simulation of Seismic Ground Motion," by M. Shinozuka, G. Deodatis and T. Harada, 8/31/87, (PB88-155197/AS). This report is available only through NTIS (see address given above).

NCEER-87-0018 "Practical Considerations for Structural Control: System Uncertainty, System Time Delay and Truncation of Small Control Forces," J.N. Yang and A. Akbarpour, 8/10/87, (PB88-163738/AS).

NCEER-87-0019 "Modal Analysis of Nonclassically Damped Structural Systems Using Canonical Transformation," by J.N. Yang, S. Sarkani and F.X. Long, 9/27/87, (PB88-187851/AS).

NCEER-87-0020 "A Nonstationary Solution in Random Vibration Theory," by J.R. Red-Horse and P.D. Spanos, 11/3/87, (PB88-163746/AS).

NCEER-87-0021 "Horizontal Impedances for Radially Inhomogeneous Viscoelastic Soil Layers," by A.S. Veletsos and K.W. Dotson, 10/15/87, (PB88-150859/AS).

NCEER-87-0022 "Seismic Damage Assessment of Reinforced Concrete Members," by Y.S. Chung, C. Meyer and M. Shinozuka, 10/9/87, (PB88-150867/AS). This report is available only through NTIS (see address given above).

NCEER-87-0023 "Active Structural Control in Civil Engineering," by T.T. Soong, 11/11/87, (PB88-187778/AS).

NCEER-87-0024 "Vertical and Torsional Impedances for Radially Inhomogeneous Viscoelastic Soil Layers," by K.W. Dotson and A.S. Veletsos, 12/87, (PB88-187786/AS).

NCEER-87-0025 "Proceedings from the Symposium on Seismic Hazards, Ground Motions, Soil-Liquefaction and Engineering Practice in Eastern North America," October 20-22, 1987, edited by K.H. Jacob, 12/87, (PB88-188115/AS).

NCEER-87-0026 "Report on the Whittier-Narrows, California, Earthquake of October 1, 1987," by J. Pantelic and A. Reinhorn, 11/87, (PB88-187752/AS). This report is available only through NTIS (see address given above).

NCEER-87-0027 "Design of a Modular Program for Transient Nonlinear Analysis of Large 3-D Building Structures," by S. Srivastav and J.F. Abel, 12/30/87, (PB88-187950/AS).

NCEER-87-0028 "Second-Year Program in Research, Education and Technology Transfer," 3/8/88, (PB88-219480/AS).

NCEER-88-0001 "Workshop on Seismic Computer Analysis and Design of Buildings With Interactive Graphics," by W. McGuire, J.F. Abel and C.H. Conley, 1/18/88, (PB88-187760/AS).

NCEER-88-0002 "Optimal Control of Nonlinear Flexible Structures," by J.N. Yang, F.X. Long and D. Wong, 1/22/88, (PB88-213772/AS).

NCEER-88-0003 "Substructuring Techniques in the Time Domain for Primary-Secondary Structural Systems," by G.D. Manolis and G. Juhn, 2/10/88, (PB88-213780/AS).

NCEER-88-0004 "Iterative Seismic Analysis of Primary-Secondary Systems," by A. Singhal, L.D. Lutes and P.D. Spanos, 2/23/88, (PB88-213798/AS).

NCEER-88-0005 "Stochastic Finite Element Expansion for Random Media," by P.D. Spanos and R. Ghanem, 3/14/88, (PB88-213806/AS).

NCEER-88-0006 "Combining Structural Optimization and Structural Control," by F.Y. Cheng and C.P. Pantelides, 1/10/88, (PB88-213814/AS).

NCEER-88-0007 "Seismic Performance Assessment of Code-Designed Structures," by H.H-M. Hwang, J-W. Jaw and H-J. Shau, 3/20/88, (PB88-219423/AS).

NCEER-88-0008 "Reliability Analysis of Code-Designed Structures Under Natural Hazards," by H.H-M. Hwang, H. Ushiba and M. Shinozuka, 2/29/88, (PB88-229471/AS).

NCEER-88-0009 "Seismic Fragility Analysis of Shear Wall Structures," by J-W Jaw and H.H-M. Hwang, 4/30/88, (PB89-102867/AS).

NCEER-88-0010 "Base Isolation of a Multi-Story Building Under a Harmonic Ground Motion - A Comparison of Performances of Various Systems," by F-G Fan, G. Ahmadi and I.G. Tadjbakhsh, 5/18/88, (PB89-122238/AS).

NCEER-88-0011 "Seismic Floor Response Spectra for a Combined System by Green's Functions," by F.M. Lavelle, L.A. Bergman and P.D. Spanos, 5/1/88, (PB89-102875/AS).

NCEER-88-0012 "A New Solution Technique for Randomly Excited Hysteretic Structures," by G.Q. Cai and Y.K. Lin, 5/16/88, (PB89-102883/AS).

NCEER-88-0013 "A Study of Radiation Damping and Soil-Structure Interaction Effects in the Centrifuge," by K. Weissman, supervised by J.H. Prevost, 5/24/88, (PB89-144703/AS).

NCEER-88-0014 "Parameter Identification and Implementation of a Kinematic Plasticity Model for Frictional Soils," by J.H. Prevost and D.V. Griffiths, to be published.

NCEER-88-0015 "Two- and Three- Dimensional Dynamic Finite Element Analyses of the Long Valley Dam," by D.V. Griffiths and J.H. Prevost, 6/17/88, (PB89-144711/AS).

NCEER-88-0016 "Damage Assessment of Reinforced Concrete Structures in Eastern United States," by A.M. Reinhorn, M.J. Seidel, S.K. Kunnath and Y.J. Park, 6/15/88, (PB89-122220/AS).

NCEER-88-0017 "Dynamic Compliance of Vertically Loaded Strip Foundations in Multilayered Viscoelastic Soils," by S. Ahmad and A.S.M. Israil, 6/17/88, (PB89-102891/AS).

NCEER-88-0018 "An Experimental Study of Seismic Structural Response With Added Viscoelastic Dampers," by R.C. Lin, Z. Liang, T.T. Soong and R.H. Zhang, 6/30/88, (PB89-122212/AS). This report is available only through NTIS (see address given above).

NCEER-88-0019 "Experimental Investigation of Primary - Secondary System Interaction," by G.D. Manolis, G. Juhn and A.M. Reinhorn, 5/27/88, (PB89-122204/AS).

NCEER-88-0020 "A Response Spectrum Approach For Analysis of Nonclassically Damped Structures," by J.N. Yang, S. Sarkani and F.X. Long, 4/22/88, (PB89-102909/AS).

NCEER-88-0021 "Seismic Interaction of Structures and Soils: Stochastic Approach," by A.S. Veletsos and A.M. Prasad, 7/21/88, (PB89-122196/AS).

NCEER-88-0022 "Identification of the Serviceability Limit State and Detection of Seismic Structural Damage," by E. DiPasquale and A.S. Cakmak, 6/15/88, (PB89-122188/AS). This report is available only through NTIS (see address given above).

NCEER-88-0023 "Multi-Hazard Risk Analysis: Case of a Simple Offshore Structure," by B.K. Bhartia and E.H. Vanmarcke, 7/21/88, (PB89-145213/AS).

NCEER-88-0024 "Automated Seismic Design of Reinforced Concrete Buildings," by Y.S. Chung, C. Meyer and M. Shinozuka, 7/5/88, (PB89-122170/AS). This report is available only through NTIS (see address given above).

NCEER-88-0025 "Experimental Study of Active Control of MDOF Structures Under Seismic Excitations," by L.L. Chung, R.C. Lin, T.T. Soong and A.M. Reinhorn, 7/10/88, (PB89-122600/AS).

NCEER-88-0026 "Earthquake Simulation Tests of a Low-Rise Metal Structure," by J.S. Hwang, K.C. Chang, G.C. Lee and R.L. Ketter, 8/1/88, (PB89-102917/AS).

NCEER-88-0027 "Systems Study of Urban Response and Reconstruction Due to Catastrophic Earthquakes," by F. Kozin and H.K. Zhou, 9/22/88, (PB90-162348/AS).

NCEER-88-0028 "Seismic Fragility Analysis of Plane Frame Structures," by H.H-M. Hwang and Y.K. Low, 7/31/88, (PB89-131445/AS).

NCEER-88-0029 "Response Analysis of Stochastic Structures," by A. Kardara, C. Bucher and M. Shinozuka, 9/22/88, (PB89-174429/AS).

NCEER-88-0030 "Nonnormal Accelerations Due to Yielding in a Primary Structure," by D.C.K. Chen and L.D. Lutes, 9/19/88, (PB89-131437/AS).

NCEER-88-0031 "Design Approaches for Soil-Structure Interaction," by A.S. Veletsos, A.M. Prasad and Y. Tang, 12/30/88, (PB89-174437/AS). This report is available only through NTIS (see address given above).

NCEER-88-0032 "A Re-evaluation of Design Spectra for Seismic Damage Control," by C.J. Turkstra and A.G. Tallin, 11/7/88, (PB89-145221/AS).

NCEER-88-0033 "The Behavior and Design of Noncontact Lap Splices Subjected to Repeated Inelastic Tensile Loading," by V.E. Sagan, P. Gergely and R.N. White, 12/8/88, (PB89-163737/AS).

NCEER-88-0034 "Seismic Response of Pile Foundations," by S.M. Mamoon, P.K. Banerjee and S. Ahmad, 11/1/88, (PB89-145239/AS).

NCEER-88-0035 "Modeling of R/C Building Structures With Flexible Floor Diaphragms (IDARC2)," by A.M. Reinhorn, S.K. Kunnath and N. Panahshahi, 9/7/88, (PB89-207153/AS).

NCEER-88-0036 "Solution of the Dam-Reservoir Interaction Problem Using a Combination of FEM, BEM with Particular Integrals, Modal Analysis, and Substructuring," by C-S. Tsai, G.C. Lee and R.L. Ketter, 12/31/88, (PB89-207146/AS).

NCEER-88-0037 "Optimal Placement of Actuators for Structural Control," by F.Y. Cheng and C.P. Pantelides, 8/15/88, (PB89-162846/AS).

NCEER-88-0038 "Teflon Bearings in Aseismic Base Isolation: Experimental Studies and Mathematical Modeling," by A. Mokha, M.C. Constantinou and A.M. Reinhorn, 12/5/88, (PB89-218457/AS). This report is available only through NTIS (see address given above).

NCEER-88-0039 "Seismic Behavior of Flat Slab High-Rise Buildings in the New York City Area," by P. Weidlinger and M. Ettouney, 10/15/88, (PB90-145681/AS).

NCEER-88-0040 "Evaluation of the Earthquake Resistance of Existing Buildings in New York City," by P. Weidlinger and M. Ettouney, 10/15/88, to be published.

NCEER-88-0041 "Small-Scale Modeling Techniques for Reinforced Concrete Structures Subjected to Seismic Loads," by W. Kim, A. El-Attar and R.N. White, 11/22/88, (PB89-189625/AS).

NCEER-88-0042 "Modeling Strong Ground Motion from Multiple Event Earthquakes," by G.W. Ellis and A.S. Cakmak, 10/15/88, (PB89-174445/AS).

NCEER-88-0043 "Nonstationary Models of Seismic Ground Acceleration," by M. Grigoriu, S.E. Ruiz and E. Rosenblueth, 7/15/88, (PB89-189617/AS).

NCEER-88-0044 "SARCF User's Guide: Seismic Analysis of Reinforced Concrete Frames," by Y.S. Chung, C. Meyer and M. Shinozuka, 11/9/88, (PB89-174452/AS).

NCEER-88-0045 "First Expert Panel Meeting on Disaster Research and Planning," edited by J. Pantelic and J. Stoyle, 9/15/88, (PB89-174460/AS).

NCEER-88-0046 "Preliminary Studies of the Effect of Degrading Infill Walls on the Nonlinear Seismic Response of Steel Frames," by C.Z. Chrysostomou, P. Gergely and J.F. Abel, 12/19/88, (PB89-208383/AS).

NCEER-88-0047 "Reinforced Concrete Frame Component Testing Facility - Design, Construction, Instrumentation and Operation," by S.P. Pessiki, C. Conley, T. Bond, P. Gergely and R.N. White, 12/16/88, (PB89-174478/AS).

NCEER-89-0001 "Effects of Protective Cushion and Soil Compliancy on the Response of Equipment Within a Seismically Excited Building," by J.A. HoLung, 2/16/89, (PB89-207179/AS).

NCEER-89-0002 "Statistical Evaluation of Response Modification Factors for Reinforced Concrete Structures," by H.H-M. Hwang and J-W. Jaw, 2/17/89, (PB89-207187/AS).

NCEER-89-0003 "Hysteretic Columns Under Random Excitation," by G-Q. Cai and Y.K. Lin, 1/9/89, (PB89-196513/AS).

NCEER-89-0004 "Experimental Study of 'Elephant Foot Bulge' Instability of Thin-Walled Metal Tanks," by Z-H. Jia and R.L. Ketter, 2/22/89, (PB89-207195/AS).

NCEER-89-0005 "Experiment on Performance of Buried Pipelines Across San Andreas Fault," by J. Isenberg, E. Richardson and T.D. O'Rourke, 3/10/89, (PB89-218440/AS).

NCEER-89-0006 "A Knowledge-Based Approach to Structural Design of Earthquake-Resistant Buildings," by M. Subramani, P. Gergely, C.H. Conley, J.F. Abel and A.H. Zaghw, 1/15/89, (PB89-218465/AS).

NCEER-89-0007 "Liquefaction Hazards and Their Effects on Buried Pipelines," by T.D. O'Rourke and P.A. Lane, 2/1/89, (PB89-218481).

NCEER-89-0008 "Fundamentals of System Identification in Structural Dynamics," by H. Imai, C-B. Yun, O. Maruyama and M. Shinozuka, 1/26/89, (PB89-207211/AS).

NCEER-89-0009 "Effects of the 1985 Michoacan Earthquake on Water Systems and Other Buried Lifelines in Mexico," by A.G. Ayala and M.J. O'Rourke, 3/8/89, (PB89-207229/AS).

NCEER-89-R010 "NCEER Bibliography of Earthquake Education Materials," by K.E.K. Ross, Second Revision, 9/1/89, (PB90-125352/AS).

NCEER-89-0011 "Inelastic Three-Dimensional Response Analysis of Reinforced Concrete Building Structures (IDARC-3D), Part I - Modeling," by S.K. Kunnath and A.M. Reinhorn, 4/17/89, (PB90-114612/AS).

NCEER-89-0012 "Recommended Modifications to ATC-14," by C.D. Poland and J.O. Malley, 4/12/89, (PB90-108648/AS).

NCEER-89-0013 "Repair and Strengthening of Beam-to-Column Connections Subjected to Earthquake Loading," by M. Corazao and A.J. Durrani, 2/28/89, (PB90-109885/AS).

NCEER-89-0014 "Program EXKAL2 for Identification of Structural Dynamic Systems," by O. Maruyama, C-B. Yun, M. Hoshiya and M. Shinozuka, 5/19/89, (PB90-109877/AS).

NCEER-89-0015 "Response of Frames With Bolted Semi-Rigid Connections, Part I - Experimental Study and Analytical Predictions," by P.J. DiCorso, A.M. Reinhorn, J.R. Dickerson, J.B. Radziminski and W.L. Harper, 6/1/89, to be published.

NCEER-89-0016 "ARMA Monte Carlo Simulation in Probabilistic Structural Analysis," by P.D. Spanos and M.P. Mignolet, 7/10/89, (PB90-109893/AS).

NCEER-89-P017 "Preliminary Proceedings from the Conference on Disaster Preparedness - The Place of Earthquake Education in Our Schools," Edited by K.E.K. Ross, 6/23/89.

NCEER-89-0017 "Proceedings from the Conference on Disaster Preparedness - The Place of Earthquake Education in Our Schools," Edited by K.E.K. Ross, 12/31/89, (PB90-207895). This report is available only through NTIS (see address given above).

NCEER-89-0018 "Multidimensional Models of Hysteretic Material Behavior for Vibration Analysis of Shape Memory Energy Absorbing Devices, by E.J. Graesser and F.A. Cozzarelli, 6/7/89, (PB90-164146/AS).

NCEER-89-0019 "Nonlinear Dynamic Analysis of Three-Dimensional Base Isolated Structures (3D-BASIS)," by S. Nagarajaiah, A.M. Reinhorn and M.C. Constantinou, 8/3/89, (PB90-161936/AS). This report is available only through NTIS (see address given above).

NCEER-89-0020 "Structural Control Considering Time-Rate of Control Forces and Control Rate Constraints," by F.Y. Cheng and C.P. Pantelides, 8/3/89, (PB90-120445/AS).

NCEER-89-0021 "Subsurface Conditions of Memphis and Shelby County," by K.W. Ng, T-S. Chang and H-H.M. Hwang, 7/26/89, (PB90-120437/AS).

NCEER-89-0022 "Seismic Wave Propagation Effects on Straight Jointed Buried Pipelines," by K. Elhmadi and M.J. O'Rourke, 8/24/89, (PB90-162322/AS).

NCEER-89-0023 "Workshop on Serviceability Analysis of Water Delivery Systems," edited by M. Grigoriu, 3/6/89, (PB90-127424/AS).

NCEER-89-0024 "Shaking Table Study of a 1/5 Scale Steel Frame Composed of Tapered Members," by K.C. Chang, J.S. Hwang and G.C. Lee, 9/18/89, (PB90-160169/AS).

NCEER-89-0025 "DYNA1D: A Computer Program for Nonlinear Seismic Site Response Analysis - Technical Documentation," by Jean H. Prevost, 9/14/89, (PB90-161944/AS). This report is available only through NTIS (see address given above).

NCEER-89-0026 "1:4 Scale Model Studies of Active Tendon Systems and Active Mass Dampers for Aseismic Protection," by A.M. Reinhorn, T.T. Soong, R.C. Lin, Y.P. Yang, Y. Fukao, H. Abe and M. Nakai, 9/15/89, (PB90-173246/AS).

NCEER-89-0027 "Scattering of Waves by Inclusions in a Nonhomogeneous Elastic Half Space Solved by Boundary Element Methods," by P.K. Hadley, A. Askar and A.S. Cakmak, 6/15/89, (PB90-145699/AS).

NCEER-89-0028 "Statistical Evaluation of Deflection Amplification Factors for Reinforced Concrete Structures," by H.H.M. Hwang, J-W. Jaw and A.L. Ch'ng, 8/31/89, (PB90-164633/AS).

NCEER-89-0029 "Bedrock Accelerations in Memphis Area Due to Large New Madrid Earthquakes," by H.H.M. Hwang, C.H.S. Chen and G. Yu, 11/7/89, (PB90-162330/AS).

NCEER-89-0030 "Seismic Behavior and Response Sensitivity of Secondary Structural Systems," by Y.Q. Chen and T.T. Soong, 10/23/89, (PB90-164658/AS).

NCEER-89-0031 "Random Vibration and Reliability Analysis of Primary-Secondary Structural Systems," by Y. Ibrahim, M. Grigoriu and T.T. Soong, 11/10/89, (PB90-161951/AS).

NCEER-89-0032 "Proceedings from the Second U.S. - Japan Workshop on Liquefaction, Large Ground Deformation and Their Effects on Lifelines, September 26-29, 1989," Edited by T.D. O'Rourke and M. Hamada, 12/1/89, (PB90-209388/AS).

NCEER-89-0033 "Deterministic Model for Seismic Damage Evaluation of Reinforced Concrete Structures," by J.M. Bracci, A.M. Reinhorn, J.B. Mander and S.K. Kunnath, 9/27/89.

NCEER-89-0034 "On the Relation Between Local and Global Damage Indices," by E. DiPasquale and A.S. Cakmak, 8/15/89, (PB90-173865).

NCEER-89-0035 "Cyclic Undrained Behavior of Nonplastic and Low Plasticity Silts," by A.J. Walker and H.E. Stewart, 7/26/89, (PB90-183518/AS).

NCEER-89-0036 "Liquefaction Potential of Surficial Deposits in the City of Buffalo, New York," by M. Budhu, R. Giese and L. Baumgrass, 1/17/89, (PB90-208455/AS).

NCEER-89-0037 "A Determinstic Assessment of Effects of Ground Motion Incoherence," by A.S. Veletsos and Y. Tang, 7/15/89, (PB90-164294/AS).

NCEER-89-0038 "Workshop on Ground Motion Parameters for Seismic Hazard Mapping," July 17-18, 1989, edited by R.V. Whitman, 12/1/89, (PB90-173923/AS).

NCEER-89-0039 "Seismic Effects on Elevated Transit Lines of the New York City Transit Authority," by C.J. Costantino, C.A. Miller and E. Heymsfield, 12/26/89, (PB90-207887/AS).

NCEER-89-0040 "Centrifugal Modeling of Dynamic Soil-Structure Interaction," by K. Weissman, Supervised by J.H. Prevost, 5/10/89, (PB90-207879/AS).

NCEER-89-0041 "Linearized Identification of Buildings With Cores for Seismic Vulnerability Assessment," by I-K. Ho and A.E. Aktan, 11/1/89, (PB90-251943/AS).

NCEER-90-0001 "Geotechnical and Lifeline Aspects of the October 17, 1989 Loma Prieta Earthquake in San Francisco," by T.D. O'Rourke, H.E. Stewart, F.T. Blackburn and T.S. Dickerman, 1/90, (PB90-208596/AS).

NCEER-90-0002 "Nonnormal Secondary Response Due to Yielding in a Primary Structure," by D.C.K. Chen and L.D. Lutes, 2/28/90, (PB90-251976/AS).

NCEER-90-0003 "Earthquake Education Materials for Grades K-12," by K.E.K. Ross, 4/16/90, (PB91-113415/AS).

NCEER-90-0004 "Catalog of Strong Motion Stations in Eastern North America," by R.W. Busby, 4/3/90, (PB90-251984)/AS.

NCEER-90-0005 "NCEER Strong-Motion Data Base: A User Manuel for the GeoBase Release (Version 1.0 for the Sun3)," by P. Friberg and K. Jacob, 3/31/90 (PB90-258062/AS).

NCEER-90-0006 "Seismic Hazard Along a Crude Oil Pipeline in the Event of an 1811-1812 Type New Madrid Earthquake," by H.H.M. Hwang and C-H.S. Chen, 4/16/90(PB90-258054).

NCEER-90-0007 "Site-Specific Response Spectra for Memphis Sheahan Pumping Station," by H.H.M. Hwang and C.S. Lee, 5/15/90, (PB91-108811/AS).

NCEER-90-0008 "Pilot Study on Seismic Vulnerability of Crude Oil Transmission Systems," by T. Ariman, R. Dobry, M. Grigoriu, F. Kozin, M. O'Rourke, T. O'Rourke and M. Shinozuka, 5/25/90, (PB91-108837/AS).

NCEER-90-0009 "A Program to Generate Site Dependent Time Histories: EQGEN," by G.W. Ellis, M. Srinivasan and A.S. Cakmak, 1/30/90, (PB91-108829/AS).

NCEER-90-0010 "Active Isolation for Seismic Protection of Operating Rooms," by M.E. Talbott, Supervised by M. Shinozuka, 6/8/9, (PB91-110205/AS).

NCEER-90-0011 "Program LINEARID for Identification of Linear Structural Dynamic Systems," by C-B. Yun and M. Shinozuka, 6/25/90, (PB91-110312/AS).

NCEER-90-0012 "Two-Dimensional Two-Phase Elasto-Plastic Seismic Response of Earth Dams," by A.N. Yiagos, Supervised by J.H. Prevost, 6/20/90, (PB91-110197/AS).

NCEER-90-0013 "Secondary Systems in Base-Isolated Structures: Experimental Investigation, Stochastic Response and Stochastic Sensitivity," by G.D. Manolis, G. Juhn, M.C. Constantinou and A.M. Reinhorn, 7/1/90, (PB91-110320/AS).

NCEER-90-0014 "Seismic Behavior of Lightly-Reinforced Concrete Column and Beam-Column Joint Details," by S.P. Pessiki, C.H. Conley, P. Gergely and R.N. White, 8/22/90, (PB91-108795/AS).

NCEER-90-0015 "Two Hybrid Control Systems for Building Structures Under Strong Earthquakes," by J.N. Yang and A. Danielians, 6/29/90, (PB91-125393/AS).

NCEER-90-0016 "Instantaneous Optimal Control with Acceleration and Velocity Feedback," by J.N. Yang and Z. Li, 6/29/90, (PB91-125401/AS).

NCEER-90-0017 "Reconnaissance Report on the Northern Iran Earthquake of June 21, 1990," by M. Mehrain, 10/4/90, (PB91-125377/AS).

NCEER-90-0018 "Evaluation of Liquefaction Potential in Memphis and Shelby County," by T.S. Chang, P.S. Tang, C.S. Lee and H. Hwang, 8/10/90, (PB91-125427/AS).

NCEER-90-0019 "Experimental and Analytical Study of a Combined Sliding Disc Bearing and Helical Steel Spring Isolation System," by M.C. Constantinou, A.S. Mokha and A.M. Reinhorn, 10/4/90, (PB91-125385/AS).

NCEER-90-0020 "Experimental Study and Analytical Prediction of Earthquake Response of a Sliding Isolation System with a Spherical Surface," by A.S. Mokha, M.C. Constantinou and A.M. Reinhorn, 10/11/90, (PB91-125419/AS).

NCEER-90-0021 "Dynamic Interaction Factors for Floating Pile Groups," by G. Gazetas, K. Fan, A. Kaynia and E. Kausel, 9/10/90, (PB91-170381/AS).

NCEER-90-0022 "Evaluation of Seismic Damage Indices for Reinforced Concrete Structures," by S. Rodriguez-Gomez and A.S. Cakmak, 9/30/90, PB91-171322/AS).

NCEER-90-0023 "Study of Site Response at a Selected Memphis Site," by H. Desai, S. Ahmad, E.S. Gazetas and M.R. Oh, 10/11/90, (PB91-196857/AS).

NCEER-90-0024 "A User's Guide to Strongmo: Version 1.0 of NCEER's Strong-Motion Data Access Tool for PCs and Terminals," by P.A. Friberg and C.A.T. Susch, 11/15/90, (PB91-171272/AS).

NCEER-90-0025 "A Three-Dimensional Analytical Study of Spatial Variability of Seismic Ground Motions," by L-L. Hong and A.H.-S. Ang, 10/30/90, (PB91-170399/AS).

NCEER-90-0026 "MUMOID User's Guide - A Program for the Identification of Modal Parameters," by S. Rodriguez-Gomez and E. DiPasquale, 9/30/90, (PB91-171298/AS).

NCEER-90-0027 "SARCF-II User's Guide - Seismic Analysis of Reinforced Concrete Frames," by S. Rodriguez-Gomez, Y.S. Chung and C. Meyer, 9/30/90, (PB91-171280/AS).

NCEER-90-0028 "Viscous Dampers: Testing, Modeling and Application in Vibration and Seismic Isolation," by N. Makris and M.C. Constantinou, 12/20/90 (PB91-190561/AS).

NCEER-90-0029 "Soil Effects on Earthquake Ground Motions in the Memphis Area," by H. Hwang, C.S. Lee, K.W. Ng and T.S. Chang, 8/2/90, (PB91-190751/AS).

NCEER-91-0001 "Proceedings from the Third Japan-U.S. Workshop on Earthquake Resistant Design of Lifeline Facilities and Countermeasures for Soil Liquefaction, December 17-19, 1990," edited by T.D. O'Rourke and M. Hamada, 2/1/91, (PB91-179259/AS).

NCEER-91-0002 "Physical Space Solutions of Non-Proportionally Damped Systems," by M. Tong, Z. Liang and G.C. Lee, 1/15/91, (PB91-179242/AS).

NCEER-91-0003 "Seismic Response of Single Piles and Pile Groups," by K. Fan and G. Gazetas, 1/10/91.

NCEER-91-0004 "Damping of Structures: Part 1 - Theory of Complex Damping," by Z. Liang and G. Lee, 10/10/91.

NCEER-91-0005 "3D-BASIS - Nonlinear Dynamic Analysis of Three Dimensional Base Isolated Structures: Part II," by S. Nagarajaiah, A.M. Reinhorn and M.C. Constantinou, 2/28/91, (PB91-190553/AS).

NCEER-91-0006 "A Multidimensional Hysteretic Model for Plasticity Deforming Metals in Energy Absorbing Devices," by E.J. Graesser and F.A. Cozzarelli, 4/9/91.

NCEER-91-0007 "A Framework for Customizable Knowledge-Based Expert Systems with an Application to a KBES for Evaluating the Seismic Resistance of Existing Buildings," by E.G. Ibarra-Anaya and S.J. Fenves, 4/9/91, (PB91-210930/AS).

NCEER-91-0008 "Nonlinear Analysis of Steel Frames with Semi-Rigid Connections Using the Capacity Spectrum Method," by G.G. Deierlein, S-H. Hsieh, Y-J. Shen and J.F. Abel, 7/2/91, (PB92-113828/AS).

NCEER-91-0009 "Earthquake Education Materials for Grades K-12," by K.E.K. Ross, 4/30/91, (PB91-212142/AS).

NCEER-91-0010 "Phase Wave Velocities and Displacement Phase Differences in a Harmonically Oscillating Pile," by N. Makris and G. Gazetas, 7/8/91, (PB92-108356/AS).

NCEER-91-0011 "Dynamic Characteristics of a Full-Sized Five-Story Steel Structure and a 2/5 Model," by K.C. Chang, G.C. Yao, G.C. Lee, D.S. Hao and Y.C. Yeh," to be published.

NCEER-91-0012 "Seismic Response of a 2/5 Scale Steel Structure with Added Viscoelastic Dampers," by K.C. Chang, T.T. Soong, S-T. Oh and M.L. Lai, 5/17/91 (PB92-110816/AS).

NCEER-91-0013 "Earthquake Response of Retaining Walls; Full-Scale Testing and Computational Modeling," by S. Alampalli and A-W.M. Elgamal, 6/20/91, to be published.

NCEER-91-0014 "3D-BASIS-M: Nonlinear Dynamic Analysis of Multiple Building Base Isolated Structures," by P.C. Tsopelas, S. Nagarajaiah, M.C. Constantinou and A.M. Reinhorn, 5/28/91, (PB92-113885/AS).

NCEER-91-0015 "Evaluation of SEAOC Design Requirements for Sliding Isolated Structures," by D. Theodossiou and M.C. Constantinou, 6/10/91, (PB92-114602/AS).

NCEER-91-0016 "Closed-Loop Modal Testing of a 27-Story Reinforced Concrete Flat Plate-Core Building," by H.R. Somaprasad, T. Toksoy, H. Yoshiyuki and A.E. Aktan, 7/15/91, (PB92-129980/AS).

NCEER-91-0017 "Shake Table Test of a 1/6 Scale Two-Story Lightly Reinforced Concrete Building," by A.G. El-Attar, R.N. White and P. Gergely, 2/28/91.